ESD-TR-68-157, Vol. I

MODELS FOR ANALYSIS OF THE CAPABILITIES OF GROUND BASED SENSORS IN DETERMINING THE MASS OF ORBITING BODIES

23 June 1967

ESSXS

SPACE DEFENSE SYSTEMS PROGRAM OFFICE
ELECTRONIC SYSTEMS DIVISION
AIR FORCE SYSTEMS COMMAND
UNITED STATES AIR FORCE
L. G. Hanscom Field, Bedford, Massachusetts

(Prepared under Contract No. F19628-67-C0041 by Westinghouse Defense and Space Center, Surface Division, Baltimore, Maryland)

LEGAL NOTICE

When U. S. Government drawings, specifications or other data are used for any purpose other than a definitely related government procurement operation, the government thereby incurs no responsibility nor any obligation whatsoever; and the fact that the government may have formulated, furnished, or in any way supplied the said drawings, specifications, or other data is not to be regarded by implication or otherwise as in any manner licensing the holder or any other person or conveying any rights or permission to manufacture, use, or sell any patented invention that may in any way be related thereto.

OTHER NOTICES

Do not return this copy. Retain or destroy.

MODELS

for

ANALYSIS OF THE CAPABILITIES OF GROUND BASED SENSORS IN DETERMINING THE MASS OF ORBITING BODIES

Prepared by

WESTINGHOUSE DEFENSE AND SPACE CENTER
SURFACE DIVISION
Baltimore, Maryland

June 23, 1967

for

SPACE DEFENSE SYSTEMS PROGRAM OFFICE
ELECTRONICS SYSTEMS DIVISION
U.S. AIR FORCE SYSTEMS COMMAND
L.G. Hanscom Field, Bedford, Massachusetts

FOREWORD

This report is submitted by the Surface Division, Westinghouse Defense and Space Center, Baltimore, Maryland to the Space Defense Systems Program Office, Electronics Systems Division, U.S. Air Force Systems Command, L.G. Hanscom Field, Bedford, Massachusetts. It covers work performed under Task I, Part 1 of Contract F19628-67-C0041 over the period 13 September 1966 to 24 April 1967. It is Technical Report Number 1 of six required technical reports.

A. **AVAILABILITY**

U. S. Government agencies may obtain copies of this report directly from the Defense Documentation Center. Other qualified DDC users will request through Headquarters (ESTI), Electronics Systems Division, U.S. Air Force Systems Command, L.G. Hanscom Field, Bedford, Massachusetts.

B. REPRODUCTION

This report may be reproduced to satisfy needs of U. S. Government Agencies. No other reproduction is authorized except with permission of Headquarters (ESTI), Electronics Systems Division, U.S. Air Force Systems Command, L.G. Hanscom Field, Bedford, Massachusetts.

C. LEGAL NOTICE

When U. S. Government drawings, specifications, or other data are used for any purpose other than a definitely related Government procurement operation, the Government incurs no responsibility nor any obligation whatsoever, and the fact that the Government may have formulated, furnished, or in any way supplied the said drawings, specifications, or other data, is not to be regarded by implication or otherwise, or in any manner licensing the holder or any other person or corporation, or conveying any rights or permission to manufacture, use, or sell any patented invention that may in any way be related thereto.

D. DISPOSITION

Do not return this copy. Retain or destroy.

E. APPROVAL

This technical report has been reviewed and approved 6 June 1967.

Bernard J. Filliatreault
Contracting Officer
Space Defense/Command
Systems Program Office

TABLE OF CONTENTS

TABLE OF CONTENTS (Con't)

TABLE OF CONTENTS (Con't)

ABSTRACT

This report contains a description of the models to be used in analyzing the capabilities of ground-based sensors in determining the mass of orbiting bodies, a description of the model coefficients, and the justification for their selection. Relations are derived for computing sensitivity coefficients and their coupling to mass variance.

SECTION I

INTRODUCTION

This document is Technical Report Number 1, the first in a series of three theoretical reports prepared under Air Force Contract F19628-67-C0041. It is concerned with the mathematical models and relationships necessary to perform a detailed maximum-likelihood/minimum-variance error analysis of the capability of ground-based sensors in determining the mass of a satellite. It is specialized to account for the following restrictions:

1) The sensors observe the satellite without error.

2) The satellite is a sphere of 5-meter diameter.

3) All the physical characteristics of the satellite except mass are known without error.

4) All the error in the computer mass results from errors and uncertainties in the knowledge of the orbit-perturbing forces.

Technical Report Number 3 will be a companion document, extending the theoretical development to remove the restrictions of perfect sensor observations and perfect knowledge of the non-mass body characteristics. In addition, the body shapes will be generalized from the sphere of this report to include also one of a pair of tumbling cylindrical objects of length 10 meters and diameters 2 and 5 meters, respectively.

The theoretical basis for mass determination rests in the fact that the mass of a man-made satellite drops out of the gravitationally induced motion of the satellite and appears only in the effects produced by the non-conservative force fields. For the sort of satellites specified in

the contract, solar radiation pressure and atmospheric drag are the only two non-conservative phenomena whose effects are reasonably observable. Hence the problem is to separate the gravitationally induced motion from the net motion and then use the proper solar pressure and atmospheric drag models to extract mass-parameter values for the satellites tracked.

This contract is not concerned with the processing of real tracking data. Rather it is a study to ascertain how accurately mass parameters can be typically determined in the way just described and what are the critical error sources in such a determination.

In choosing the mathematical models upon which to base the necessary orbital calculations, one finds oneself deeply involved with questions of practical computation. A central-force gravity law, for example, leads to expressions for the state of the orbit which are closed-form functions of eccentric anomaly and hence are easily computable. Unfortunately, this solution is far too inaccurate a representation of the real world to be used as is in orbit or vehicle-parameter determination.

More exact models of satellite dynamics do not lead to closed-form solutions. Not only must the trajectories that evolve from the direct use of these more accurate models be determined by numerical integration, but also the state and mass-parameter estimates and the associated sensitivity matrices must be determined by numerical integration.

To handle this problem, the use and extensions of techniques contained in NASA's MINIVAR family of orbit-determination computer programs will be made in this contract.

In what follows in this first Technical Report, the basic theory of two-body mechanics will be presented, the means for correcting this model for various pertubation effects will be discussed, and methods for computing the effects of variations in the model coefficients will be developed so as to avoid the need for numerous integrations. Finally, the models themselves will be discussed.

SECTION II

TWO-BODY MECHANICS

A two-body or Keplerian earth orbit leads to an essentially closed-form expression for the state of the orbit as a function of the state at any prior time.

In particular, if

$$\underline{r} = \begin{bmatrix} x \\ y \\ z \end{bmatrix}$$

is the column vector of satellite position in the geocentric inertial coordinate system (X, Y, Z) depicted in Figure 1, then the central-force-law acceleration is

$$d^2\underline{r}/dt^2 = -\mu\underline{r}/r^3, \qquad (2.1)$$

where μ is the gravitational constant of the earth. Given initial conditions at some time t_o for position and velocity, $\underline{r}_o$ and

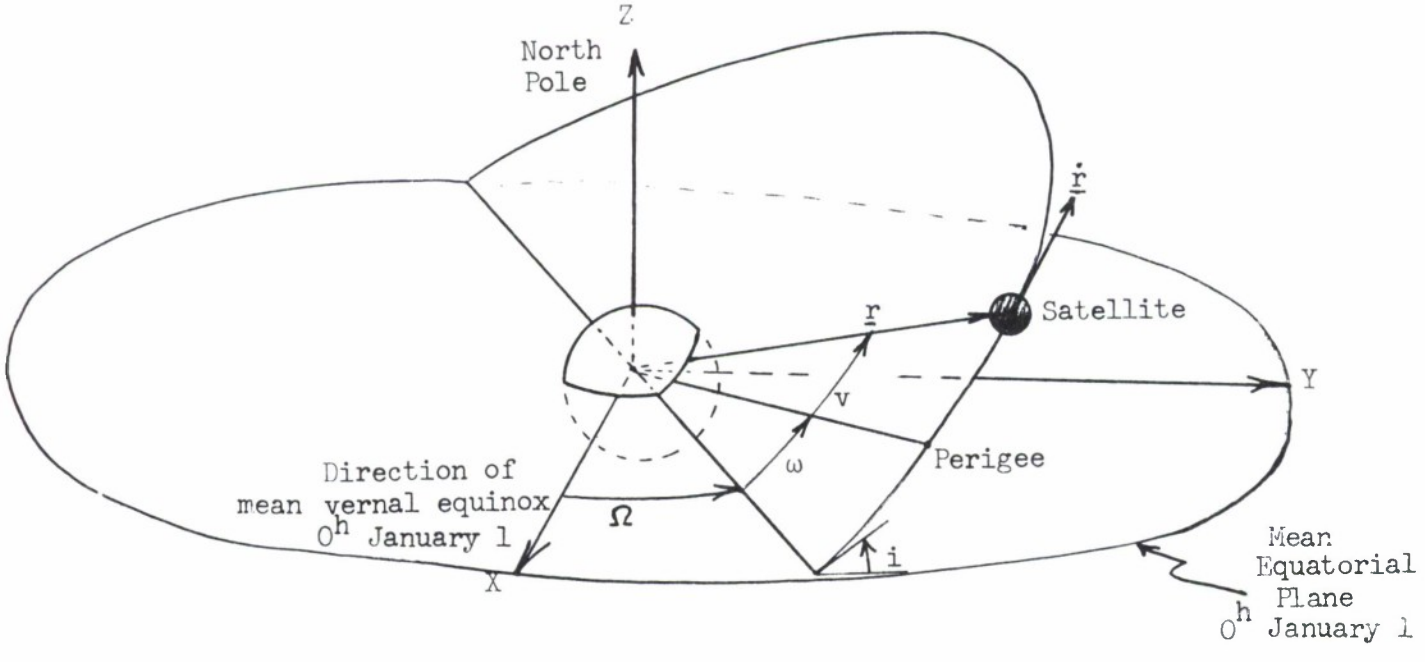

Figure 1. Geocentric Inertial Coordinates

$\dot{\underline{r}}_o = (d\underline{r}/dt)_o$, respectively, one can write the position and velocity at any later time t as [1, 2, 3, 4]*

$$\underline{r} = \underline{r}_o f(\Delta E) + \dot{\underline{r}}_o g(\Delta E),$$

$$d\underline{r}/dt = \underline{r}_o f_t(\Delta E) + \dot{\underline{r}}_o g_t(\Delta E), \qquad (2.2)$$

where

$$f(\Delta E) = 1 - (a/r_o)(1 - \cos \Delta E),$$

$$g(\Delta E) = r_o(a/\mu)^{(1/2)} \sin \Delta E + (ad_o/\mu)(1 - \cos \Delta E),$$

$$f_t(\Delta E) = -(a/r)(1/r_o)(\mu/a)^{(1/2)} \sin \Delta E,$$

$$g_t(\Delta E) = 1 - (a/r)(1 - \cos \Delta E),$$

and

$a = \mu r_o/(2\mu - r_o\dot{r}_o^2)$, the semi-major axis

$d_o = \underline{r}_o \cdot \dot{\underline{r}}_o$,

$\Delta E = E - E_o$, the change in the eccentric anomaly from time t_o,

$r/a = (1 - \cos \Delta E) + (r_o/a) \cos \Delta E + d_o(\mu a)^{-(1/2)} \sin \Delta E.$

Kepler's equation provides the means for finding ΔE, given E_o, the time step Δt, and the eccentricity e:

$$n \Delta t = \Delta E - e (\sin E - \sin E_o),$$

or, after some elementary substitutions,

$$n\Delta t = \Delta E + (d_o/\sqrt{\mu a})(1 - \cos \Delta E) + (r_o/a - 1) \sin \Delta E, \qquad (2.4)$$

where

$\Delta t = t - t_o$

n = the mean motion, $(\mu/a^3)^{(1/2)}$.

*Superscript numerals denote entries in the References Section of this report.

The solving of (2.4) for ΔE completes the two-body solution.

For notational simplicity, the equations (2.2) can be expressed in state-variable form:

$$\underline{x} = \underline{x}(\underline{x}_o, \Delta E), \tag{2.5}$$

where

$$\underline{x} = \begin{bmatrix} x_1 \\ \vdots \\ x_6 \end{bmatrix} ; \; x_1 = x, \; x_2 = y, \; x_3 = z, \; x_4 = \dot{x}, \; x_5 = \dot{y}, \; x_6 = \dot{z}.$$

$$\underline{x}_o = \begin{bmatrix} x_{o1} \\ \vdots \\ x_{o6} \end{bmatrix} ; \; x_{o1} = x_o, \text{ etc.}$$

Hence a small change $\Delta \underline{x}$ in the state caused by a variational change $\Delta \underline{x}_o$ in the initial conditions is, to first-order accuracy,

$$\Delta \underline{x} = \Phi(t, t_o) \; \Delta \underline{x}_o, \tag{2.6}$$

where

$$\Phi(t, t_o) = \left[\partial x_i / \partial x_{oj} \right] .$$

The 36 elements of the transition matrix $\Phi(t, t_o)$ are derived in Appendix IV. They are evaluated on the nominal two-body orbit calculated from (2.2).

SECTION III

PERTURBATIONS TO TWO-BODY MOTION

Although the means has just been developed for accounting for variations in initial conditions, two-body assumptions are still inadequate. The closed-form solutions presented above will, however, be useful in the more sophisticated computations which can be made.

A. GENERAL EQUATIONS OF MOTION

In general,

$$d\underline{x}/dt = \underline{f}(\underline{x}, t) + \underline{F}(\underline{x}, \underline{\xi}, \underline{u}, t), \tag{3.1}$$

$$d\underline{\xi}/dt = \underline{G}(\underline{x}, \underline{\xi}, \underline{u}, t), \tag{3.2}$$

where $\underline{x}$ is as defined for equation (2.5), $\underline{\xi}$ is a six-dimensional state vector describing rigid-body rotation, having the Euler angles of the satellite as its first three elements and their time derivatives as its remaining three, and $\underline{u}$ is a vector containing all the model parameters about which there exists modeled uncertainty.

The vector $\underline{f}(\underline{x}, t)$ describes the two-body accelerations, while the non-Keplerian perturbations enter with $\underline{F}(\underline{x}, \underline{\xi}, \underline{u}, t)$, which contains also all the dynamic biases and uncertainties:

$$\underline{f}(\underline{x}, t) = \text{column } (x_4, x_5, x_6, -\mu x_1/r^3, -\mu x_2/r^3, -\mu x_3/r^3)$$

$$\underline{F}(\underline{x}, \underline{\xi}, \underline{u}, t) = \text{column } (0, 0, 0, F_3, F_4, F_5). \tag{3.3}$$

The rotational states $\underline{\xi}$ arise for aspherical satellites to describe the cross sectional area presented to the drag media and to account for the

dynamic coupling between rotational and translational energy.

B. EQUATIONS FOR SPHERICAL SATELLITES

For the purposes of this Task I effort, only spherical satellites are to be considered. To a high degree of accuracy, then, $\underline{\xi}$ may be dropped from (3.1) and (3.3), and equation (3.2) can be discarded.

Only the following need therefore be considered:

$$d\underline{x}/dt = \underline{f}(\underline{x}, t) + \underline{F}(\underline{x}, \underline{u}, t), \tag{3.4}$$

The non-Keplerian perturbations contained in $\underline{F}(\underline{x}, \underline{u}, t)$ will consist of 1) an atmospheric drag acceleration

$$\ddot{\underline{r}}_{drag} = \left[u_1(t) + u_2\right] \underline{\beta}(\underline{x}, t), \tag{3.5}$$

where

$u_2 = (A/m)C_D$, the ballistic coefficient, constant but unknown,

$u_1(t)$ = a stationary random error in the ballistic coefficient with autocorrelation function $\sigma^2_{drag}\, e^{-|\tau/\tau_d|}$, due to atmospheric density uncertainties,

$$\underline{\beta}(\underline{x}, t) = \begin{bmatrix} \beta_1 \\ \beta_2 \\ \beta_3 \end{bmatrix} = -\frac{1}{2}\rho \sqrt{(x_4 + \omega_e x_2)^2 + (x_5 - \omega_e x_1)^2 + x_6^2} \begin{bmatrix} x_4 + \omega_e x_2 \\ x_5 - \omega_e x_1 \\ x_6 \end{bmatrix}$$

where, in turn,

ρ = mean atmospheric density at $\underline{x}$ and t,

ω_e = rotation rate of the earth;

2) a solar pressure acceleration (see Appendix I)

$$\ddot{\underline{r}}_{solar} = u_3 \, \underline{\gamma}(\underline{x}, t) \tag{3.6}$$

where, for the spherical satellites in this Task I effort,

$u_3 = (1+4k_d/9)\,(I_{nom}/c)$(A/m), a solar "ballistic" coefficient, constant but unknown,

and

$$\underline{\gamma}(\underline{x}, t) = \begin{bmatrix} \gamma_1 \\ \gamma_2 \\ \gamma_3 \end{bmatrix} = (R_{es}/r_{es})^2(p_1\hat{i}_r + p_2\hat{i}_{ss}),$$

where

k_d = diffuse reflectivity of satellite,

I_{nom} = solar irradiance at nominal earth-sun distance R_{es},

R_{es} = nominal earth-sun distance,

r_{es} = actual earth-sun distance,

c = speed of light

$\hat{i}_r$ = unit vector from center of earth to center of satellite,

$\hat{i}_{ss}$ = unit vector from center of sun to satellite,

$$p_1 = \begin{cases} \lambda q\,(a_1 + a_2)\cos\alpha & , \quad |\alpha| \le \pi/2 - B_\lambda \\ \lambda q\, a_r & , \quad \pi/2 - B_\lambda \le |\alpha| \le \pi/2 + B_\lambda \\ 0 & , \quad \pi/2 + B_\lambda \le |\alpha| < \pi \end{cases}$$

$$p_2 = \begin{cases} (1 + \lambda q a_2) & , \quad |\alpha| \le \pi/2 - B_\lambda \\ (1 + \lambda q a_{ss}) & , \quad \pi/2 - B_\lambda \le |\alpha| \le \pi/2 + B_\lambda \\ 0 & , \quad \pi/2 + B_\lambda \le |\alpha| \le \pi \end{cases}$$

$\cos\alpha = -(\hat{i}_r \cdot \hat{i}_{ss})$, $0 \le \alpha \le \pi$,

$\sin\alpha = +(1-\cos^2\alpha)^{(1/2)}$

q = earth albedo,

λ = ratio of earth radius to distance between satellite and earth center,

$B_\lambda = \cos^{-1}\lambda$,

$a_1 = -(.0417 + .5431\lambda)/3$

$a_2 = \{.0444 - 3.17(\lambda - .77)^3 + .0045\,(\lambda - .77)\sin[14.3(\lambda - .77)\pi]\}/3$

$a_{ss} = a_2[1 + s - se^{s\tau y} - e^{-\tau y}(2 + sy)]/2$

$a_r = \{a_{ss} + a_1/2\,[s + 1 - s(1 + sy)^d]\}\cos\alpha$

$$+ \left\{ \frac{\lambda^2[(1/\lambda - \sin\alpha)^3 + (\lambda - \sin\alpha)^3]}{(1+\lambda^2 - 2\lambda\sin\alpha)^{3/2}} - \frac{(1-\lambda^2)^{3/2}}{\lambda} \right\} \frac{\sin\alpha}{6} ,$$

$\tau = -4 + 9.3\lambda$

$y = (\alpha - \pi/2)/B_\lambda$

$s = \begin{cases} -1 , & y \ge 0, \\ 1 , & y < 0, \end{cases}$

$d = 3.7 + 59(\lambda - .77)^2;$

3) an acceleration due to solar and lunar attraction

$$\ddot{\underline{r}}_{\text{sun, moon}} = \mu_{\text{sun}}\left[\frac{\hat{i}_{se}}{R_{es}^2} - \frac{\hat{i}_{ss}}{R_{ss}^2}\right] + \mu_{\text{moon}}\left[\frac{\hat{i}_{me}}{R_{em}^2} - \frac{\hat{i}_{ms}}{R_{ms}^2}\right] \tag{3.7}$$

where

$\mu_{\text{sun}}, \mu_{\text{moon}}$ = gravitational constants for sun and moon,

$\hat{i}_{se}, \hat{i}_{me}$ = sun-to-earth and moon-to-earth unit vectors,

R_{es}, R_{em} = sun-to-earth and moon-to-earth distances,

$\hat{i}_{ss}, \hat{i}_{ms}$ = sun-to-satellite and moon-to-satellite unit vectors,

R_{ss}, R_{ms} = sun-to-satellite and moon-to-satellite distances;

4) and, finally, a geopotential acceleration due to the oblateness (more generally, the asphericity) of the earth (see Appendix III):

$$\underline{F}_o(\underline{x}) = T \sum_{n=2}^{N} \cdot \sum_{m=0}^{n} (C_{nm}\,\text{grad}\, U_n^m + S_{nm}\,\text{grad}\, V_n^m), \tag{3.8}$$

where T = the rotation transformation that takes the earth-fixed geocentric coordinate system (X^1, Y^1, Z^1), defined as the right-hand system with X^1 at Greenwich and Z^1 being the north-directed polar axis at time t, into the inertial geocentric coordinate system (X, Y, Z) defined in Figure 1,

C_{nm}, S_{nm} = the geopotential coefficients from (n, m) equal to (2, 2) upto (N, N) whose published values have constant but unknown biases on them,

$$\text{grad} = \text{column}\left(\frac{\partial}{\partial x_1}, \frac{\partial}{\partial y_1}, \frac{\partial}{\partial z_1}\right),$$

$$\begin{Bmatrix} U_n^m \\ V_n^m \end{Bmatrix} = (\mu/r)\,(R/r)^n\, P_n^m(\sin\beta) \begin{Bmatrix} \cos m\lambda \\ \sin m\lambda \end{Bmatrix},$$

where

μ = earth's gravitational constant,

r = the geocentric distance to the satellite at time t,

R = earth's mean equatorial radius,

$P_n^m(\sin\beta)$ = associated Legendre polynomials,

β, λ = satellite latitude and longitude, respectively, at time t.

Hence

$$\underline{F}(\underline{x}, \underline{u}, t) = \begin{bmatrix} 0 \\ \hline \underline{a}_{drag} \end{bmatrix} + \begin{bmatrix} 0 \\ \hline \underline{a}_{solar} \end{bmatrix} + \begin{bmatrix} 0 \\ \hline \underline{a}_{sun,\ moon} \end{bmatrix} + \begin{bmatrix} 0 \\ \hline \underline{F}_o \end{bmatrix}. \qquad (3.9)$$

C. ENCKE INTEGRATION

Given the initial condition $\underline{x}(t_o)$ and the actual values of the parameters that appear in (3.9), equation (3.4) can be integrated numerically to yield the satellite trajectory $\underline{x}(t)$. Since in the class of orbits

germane to this contract the earth's central-force field is the strongly dominant effect, an Encke integration of (3.4) will generally be the most accurate approach for a given integration step size and arithmetic precision.[1]

The Encke method that will be used computes small perturbations about the two-body orbit defined by equations (2.2) and (2.5). Call the two body orbit $\underline{x}^o(t)$, or, more exactly,

$$\underline{x}^o(t) = \underline{x}^o\left[t, \underline{x}(t_o)\right].$$

It satisfies the equation

$$d\underline{x}^o/dt = \underline{f}(\underline{x}^o, t), \tag{3.10}$$

$$\underline{x}(t_o) = \text{given}.$$

If we define

$$\Delta\underline{x}(t) = \Delta\underline{x}\left[t, \underline{x}(t_o)\right] = \underline{x}(t) - \underline{x}^o\left[t, \underline{x}(t_o)\right]$$

and subtract (3.10) from (3.4), we find

$$d(\Delta\underline{x})/dt = \underline{f}(\underline{x}, t) - \underline{f}(\underline{x}^o, t) + \underline{F}(\underline{x}, \underline{u}, t),$$

$$\Delta\underline{x}(t_o) = 0. \tag{3.11}$$

The integration of this equation by an appropriate starting technique, such as the Range-Kutta-Gill, and an appropriate long-term technique, such as an Adams interpolation method, completes the Encke orbit computation.

Reference 4 presents the Runge-Kutta-Gill and Adams methods that will be used, except that it associates the Adams method with a Cowell integrator. The CPCEI Detail Specifications, Part II, for the present contract will describe the same Adams method in the context used here.

D. RECTIFICATION

If we continue assuming that $\underline{x}(t_o)$ and the actual parameter values are known exactly, care must nontheless be taken that the magnitude of $\Delta\underline{x}(t)$ does not exceed certain assignable bounds, or the Encke integrator will lose its accuracy. If it does, say at time t_r, then the integration must be stopped and the generated value

$$\underline{x}(t_r) = \underline{x}^o \left[t_r, \underline{x}(t_o)\right] + \Delta\underline{x} \left[t_r, \underline{x}(t_o)\right]$$

used as a new initial condition. A new two-body trajectory is generated from (2.2) and (2.5),

$$\underline{x}^o(t) = \underline{x}^o \left[t, \underline{x}(t_r)\right] ,$$

a new $\Delta\underline{x}(t)$ defined,

$$\Delta\underline{x}(t) = \Delta\underline{x} \left[t, \underline{x}(t_r)\right] = \underline{x}(t) - \underline{x}^o \left[t, x(t_r)\right] ,$$

and the process continued. The technique is known as rectification, and proceeds in one dimension as shown in Figure 2, below. The times $t_{r_1}, t_{r_2}, \ldots$, are the rectification times.

The generation of an orbit under the assumption of perfect knowledge is carried out in the Reference Mode of MINIVAR[3,4] in the manner discussed in this section.

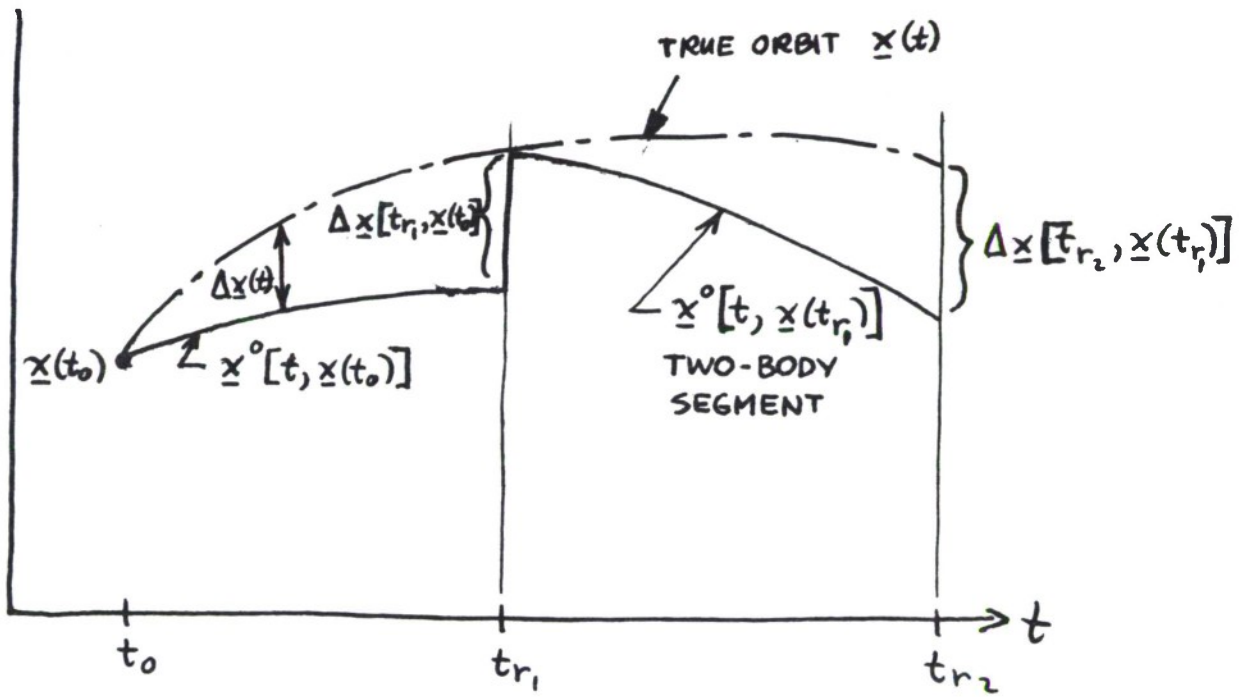

Figure 2. Actual Orbit as It Would Be Represented in an Encke Integration

SECTION IV

ESTIMATION AND PREDICTION

The assumptions of the previous section, i.e., that the initial conditions and the model parameters are completely known, led to an Encke integration which, in reality, only God can perform. Rather, a ground-based observer has incomplete knowledge of the initial conditions and model parameters and often can see only some nonlinear combination of some of the satellite states. Even that which can be seen is masked in uncertainty because of fluctuating measurement noise and fixed, but unknown, measurement biases.

A. PROBLEM FORMULATION

Consider the equations

$$d(\Delta\underline{x})/dt = \underline{f}(\underline{x}, t) - \underline{f}(\underline{x}^{\circ}, t) + \underline{F}(\underline{x}, \underline{u}, t), \tag{4.1}$$

$$\Delta\underline{z} = \underline{h}(\underline{x}, \underline{\eta}, \underline{b}, t) - \underline{h}(\underline{x}^{\circ}, 0, 0, t), \tag{4.2}$$

where $\Delta\underline{x}(t)$ is the Encke variation from the two-body orbit $\underline{x}^{\circ}(t)$ discussed in Section III, and the vector

$$\underline{z} = \underline{h}(\underline{x}, \underline{\eta}, \underline{b}, t) \tag{4.3}$$

defines the observations $\underline{z}(t)$ on the orbit, where

$\underline{\eta}(t)$ = zero-mean Gaussian white noise,

$\underline{b}$ = constant but unknown biases,

$\Delta\underline{z}(t) = \underline{z} - \underline{z}^{\circ}$, the difference between the actual noisy observation and the noise-free observation of the two-body motion.

For the special case of perfect sensors to be considered in this Task I report, $\underline{z}(t)$ is always $\underline{h}(\underline{x}, 0, 0, t)$, which we will shorten to

$$\underline{z} = \underline{h}(\underline{x}). \tag{4.3'}$$

In addition to the physically meaningful equations (4.1) and (4.2), additional equations can be written which describe how the unknown parameters and biases within $\underline{F}(\underline{x}, \underline{u}, t)$ change with time. Three of these will be modeled and estimated from received sensor data: the three "ballistic" coefficients u_1, u_2, and u_3 in expressions (3.5) and (3.6), which have the dynamics

$$\begin{aligned} du_1/dt &= -(1/\tau_d)\, u_1 + w_1(t), \\ du_2/dt &= 0, \\ du_3/dt &= 0, \end{aligned} \tag{4.4}$$

where $w_1(t)$ is a zero-mean, Gaussian white-noise process with power $(2/\tau_d)\sigma^2_{drag}$ per-unit-double-bandwidth in rad./sec.; i.e., it has covariance

$$\text{Cov}\left[w_1(t), w_1(t')\right] = (2/\tau_d)\sigma^2_{drag}\,\delta(t-t'), \tag{4.5}$$

where $\delta(t)$ is the Dirac delta function, and where in general, for random vectors $\underline{a}(t)$, $\underline{b}(t)$,

$$\text{Cov}\left[\underline{a}(t), \underline{b}(t)\right] = E\left[\underline{a}(t)\,\underline{b}(t)\right] - E\left[\underline{a}(t)\right] E\left[\underline{b}^T(t)\right],$$

where $E(\ )$ denotes mathematical expectation and $(\ )^T$ denotes matrix transpose.

Additional uncertain parameters are contained in the oblateness contribution $\underline{F}_o$ to $\underline{F}(\underline{x}, \underline{u}, t)$. These are the geopotential coefficients

$$\underline{J} = \text{column } (C_{20}, C_{30}, \cdots \; ; C_{22}; C_{31}, \cdots, C_{33}; \cdots \; ; S_{22}; S_{31}, \cdots, S_{33}; \cdots),$$

which are constant but have unknown biases on their published values. These errors will be modeled, but sensor data will not be used to correct the published values.

For simplicity of notation, the vector $\underline{v}_1$ will be used to denote those biases and parameters which will be actively estimated, and $\underline{v}_2$ will be used to account for those that will be modeled, but not actively estimated. If $\underline{y}$ is defined as the vector which contains all variables that are to be actively estimated, then it is the 9-vector

$$\underline{y} = \begin{bmatrix} \Delta\underline{x} \\ \text{----} \\ \underline{v}_1 \end{bmatrix} , \tag{4.6}$$

where

$$\underline{v}_1 = \begin{bmatrix} u_1 \\ u_2 \\ u_3 \end{bmatrix} .$$

Now, for any random vectors $\underline{a}(t)$ and $\underline{b}(t)$ we will define

$\hat{\underline{a}}(n/k) = \hat{\underline{a}}(t_n/t_k)$, the minimum - variance estimate of the vector $\underline{a}$ at time $t = t_n$ based upon data upto and including time $t = t_k$,

$P_{ab}(n/k) = \text{Cov}\left[\underline{a}(n) - \hat{\underline{a}}(n/k), \underline{b}(n) - \hat{\underline{b}}(n/k)\right]$, the covariance matrix on the estimation errors between $\underline{a}$ and $\underline{b}$,

and the short-form notation.

$$\text{Cov}\left[\underline{a}(t), \underline{a}(t)\right] = \text{Cov}\left[\underline{a}(t)\right] .$$

In this notation, the problem of minimum - variance estimation on the vector $\underline{y}$ is simply the problem of choosing a filter for the data sequence $\{\Delta\underline{z}(n)\}$ such that

$$\sum_{i=1}^{9} \alpha_i^2 \sigma_{y_i}^2(n/n) = \text{trace}\left\{AP_{yy}(n/n)A\right\} = \text{min.}, \tag{4.7}$$

where*

$$\sigma_{y_i}^2(n/n) = \text{Cov}\left[y_i(n) - \hat{y}_i(n/n)\right] ,$$

α_i = a pre-assigned weight given to an error in the estimate of the ith variable y_i,

$$A = \begin{bmatrix} \alpha_1 & & \\ & \ddots & \\ & & \alpha_9 \end{bmatrix},$$

trace ( ) = the sum of the diagonal elements of its argument matrix.

To derive the filter as the sequential processor implemented in MINIVAR,[3,4] a regression formula will be applied to incorporate into the estimate each new data point as it arrives:

$$\hat{\underline{y}}(n/n) = \hat{\underline{y}}(n/n-1) + R_y(n)\left[\Delta\underline{z}(n) - \Delta\hat{\underline{z}}(n/n-1)\right] , \tag{4.8}$$

where

$\underset{y}{B}(n)$ is a 9 x (dim z) gain matrix which has yet to be determined,*

$\Delta\underline{z}(n/n-1) = \underline{h}\left[\hat{\underline{x}}(n/n-1)\right] - \underline{h}\left[\underline{x}^{o}(n)\right]$ in the notation of (4.3').

The computation of the one-step extrapolation $\hat{\underline{y}}(n/n-1)$ is straightforward, given state and parameter initial conditions (or prior in-step estimates) $\hat{\underline{y}}(n-1/n-1)$. From equations (4.4), since $w_1(t)$ has an expected value of zero,

$$\hat{u}_1(n/n-1) = \hat{u}_1(n-1/n-1)\, e^{-(t_n - t_{n-1})/\tau_d},$$

$$\hat{u}_2(n/n-1) = \hat{u}_2(n-1/n-1)$$

$$\hat{u}_3(n/n-1) = \hat{u}_3(n-1/n-1) \qquad (4.9)$$

The rest of the $\hat{\underline{y}}(n/n-1)$ vector is computed directly from (4.1) by numerically integrating up to time $t = t_n$ after the appropriate notational changes have been made:

$$d(\Delta\hat{\underline{x}})/dt = \underline{f}(\underline{x}^{o} + \Delta\hat{\underline{x}},\, t) - \underline{f}(\underline{x}^{o},\, t) + \underline{F}(\underline{x}^{o} + \Delta\hat{\underline{x}},\, \hat{\underline{u}},\, t)$$

$$\Delta\hat{\underline{x}}\,\Big|_{\substack{\text{initial}\\ \text{cond.}}} = \Delta\hat{\underline{x}}\,(n-1/n-1), \qquad (4.10)$$

where $\Delta\hat{\underline{x}}$ and $\hat{\underline{u}}$ are short-form notation for $\Delta\hat{\underline{x}}(t/t_{n-1})$ and $\hat{\underline{u}}(t/t_{n-1})$, respectively.

Hence $\underset{y}{B}(n)$ in (4.8) is the only computation for which the machinery does not yet exist. The remainder of the section will describe how it is computed by linearization techniques. Note, however, that up to this point in the discussion no linearizing assumptions have been made, since so far $B_y(n)$ could just as easily have been a function of $\underline{y}$ as not.

*The notation dim z is the dimension of the vector $\underline{z}$.

B. MINIMUM-VARIANCE DERIVATION

1. Basic Principles

By their very mode of operation, ground-based sensors deal with sampled-data information which can become rather sparse after normal pre-processing and conditioning is performed. Hence, only at discrete points in time need we have the ideal curves (or their equations) to which the data is to be fit.

This section will generate the sampled-data expressions for $\underline{y}(t)$ which describe the ideal orbital motion. They will not be integrated to yield the best estimate itself, since equation (4.10) has already been developed to do that. Rather these sampled-data expressions will be used for the received data.

Because of the inherent theoretical problems in obtaining B(n), the equations of motion must be linearized around a nominal trajectory, and Gaussian probability distributions will be assumed for all the random variables. Then some rather well-developed theory [6,7,11] and available computer programs [4,5] apply after some modification.

2. The Linearized Equations of Motion

Consider equations (4.1) and (4.10):

$$d(\Delta\underline{x})/dt = \underline{f}(\underline{x},t)-\underline{f}(\underline{x}^{\circ},t)+\underline{F}(\underline{x},\underline{u},t),$$

$$d(\Delta\hat{\underline{x}})/dt = \underline{f}(\hat{\underline{x}},t)-\underline{f}(\underline{x}^{\circ},t)+\underline{F}(\hat{\underline{x}},\hat{\underline{u}},t)$$

where again $\Delta\hat{\underline{x}}$ and $\hat{\underline{u}}$ are $\Delta\hat{\underline{x}}(t/t_{n-1})$ and $\hat{\underline{u}}(t/t_{n-1})$ respectively, and $\underline{x}(t) = \underline{x}^{\circ}(t)+\Delta\underline{x}(t)$ and $\hat{\underline{x}}(t/t_{n-1}) = \underline{x}^{\circ}(t) + \Delta\hat{\underline{x}}(t/t_{n-1})$.

Note that if $\underline{x}$ and $\hat{\underline{x}}$ are both sufficiently close to $\underline{x}^{\circ}$ and hence to each other, then the $\underline{f}$ terms can be replaced with the first-order

terms in the Taylor's series expansions around $\underline{x}^o$:

$$d\,(\Delta\underline{x})/dt \approx \left(\frac{\partial \underline{f}}{\partial \underline{x}}\right)_o \Delta\underline{x} + \underline{F}(\underline{x},\underline{u},t), \tag{4.11}$$

$$d\,(\Delta\hat{\underline{x}})/dt \approx \left(\frac{\partial \underline{f}}{\partial \underline{x}}\right)_o \Delta\hat{\underline{x}} + \underline{F}(\hat{\underline{x}},\hat{\underline{u}},t). \tag{4.12}$$

Now $\underline{F}(\underline{x},\underline{u},t)$ can be expanded in a Taylor's series around the best estimates $\hat{\underline{x}}\,(t/t_{n-1})$ and $\hat{\underline{u}}\,(t/t_{n-1})$: to first order,

$$\underline{F}\,(\underline{x},\underline{u},t) \approx \underline{F}\,(\hat{\underline{x}},\hat{\underline{u}},t) + \left(\frac{\partial \hat{\underline{F}}}{\partial \underline{x}}\right)(\Delta\underline{x}-\Delta\hat{\underline{x}}) + \left(\frac{\partial \hat{\underline{F}}}{\partial \underline{u}}\right)(\underline{u}-\hat{\underline{u}}) \tag{4.13}$$

where $\left(\frac{\partial \hat{\underline{F}}}{\partial \underline{x}}\right)$ is $\frac{\partial \underline{F}}{\partial \underline{x}}$ evaluated at $\hat{\underline{x}}(t/t_n),\hat{\underline{u}}(t/t_n)$.

Moreover, we can define the error vector

$\underline{e}_a\,(t/t_k) = \underline{a}\,(t) - \hat{\underline{a}}\,(t/t_k)$ for any vector $\underline{a}\,(t)$. In the special cases where t assumes discrete values, t_n, the notation will be simplified to $\underline{e}_a\,(n/k)$.

Clearly, then, equation (4.12) can be subtracted from (4.11), after (4.13) is substituted in, to yield the error propagation equation

$$\dot{\underline{e}}_x\,(t/t_{n-1}) \approx \left[\left(\frac{\partial \underline{f}}{\partial \underline{x}}\right)_o + \left(\frac{\partial \hat{\underline{F}}}{\partial \underline{x}}\right)\right] \underline{e}_x\,(t/t_{n-1}) + \left(\frac{\partial \hat{\underline{F}}}{\partial \underline{u}}\right) \underline{e}_u\,(t/t_{n-1}) . \tag{4.14}$$

In the coefficient matrix $\left(\frac{\partial \underline{f}}{\partial \underline{x}}\right)_o + \left(\frac{\partial \hat{\underline{F}}}{\partial \underline{x}}\right)$ the non-Keplenian accelerations appear in the lower three rows. However, the components of $\underline{F}$ are smaller than those in $\underline{f}$ by at least two orders of magnitude even for the lowest-altitude satellites.[5] Since the components of the lower half of $\underline{f}$ attenuate as $1/r^2$ and those of $\underline{F}$ attenuate at least as fast in the altitude range of interest, it is clear (see the slopes of the curves in Figure 3) that the column inequalities

$$|\partial F_i/\partial x_j| \ll |\partial f_i/\partial x_j| \ , \ j = 1,2,3, \text{ all } i,$$

hold in a component-by component sense when averaged over a complete orbit. Because $\underline{F}$ contains velocity terms (x_3, x_4, x_5) whereas $\underline{f}$ does not, the column inequalities will fail to hold for $j = 4, 5, 6$. Still, the velocity contributions (damping terms) are very small, and a part of these <u>are</u> included in (4.14) via the term

$$\frac{\partial \hat{\underline{F}}}{\partial \underline{u}} \ \underline{e}_u \ (t/t_{n-1}).$$

Since, in addition, $\underline{x}^o(t)$ is forced by the rectification process described in Section III to remain close to the best approximation to the actual, decaying orbit, we can expect $\left(\frac{\partial \underline{f}}{\partial \underline{x}}\right)_o$ to provide sufficiently accurate long-term behavior in (4.14) to allow $\left(\frac{\partial \underline{F}}{\partial \underline{x}}\right)$ to be dropped.

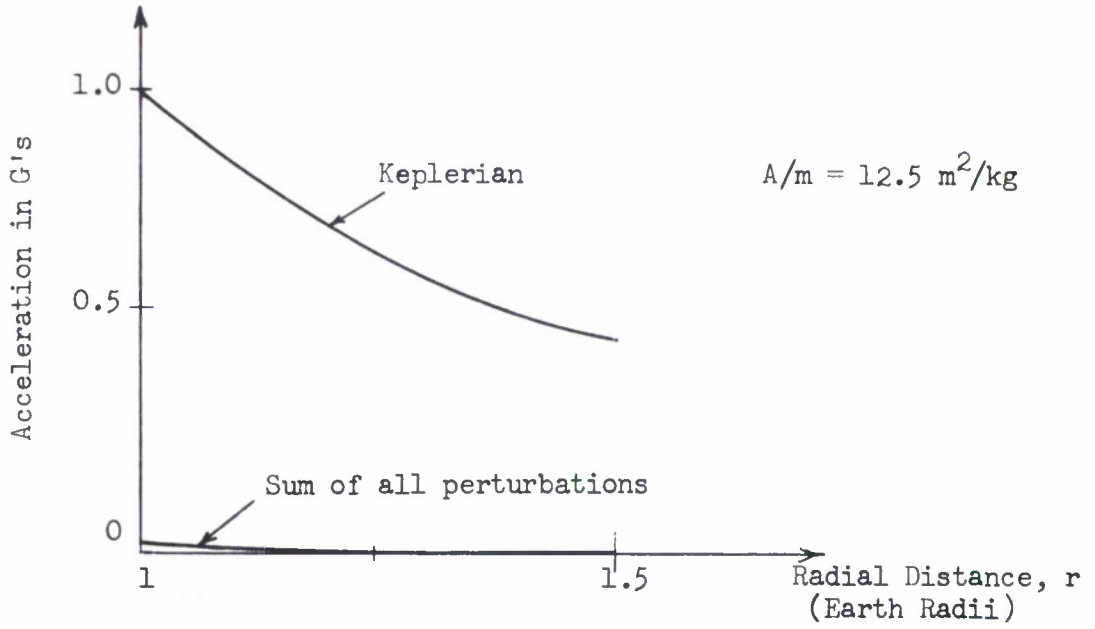

FIGURE 3. Relative Magnitudes of Keplerian versus Pertubative Accelerations

All such terms, except one, will in fact be dropped. The one that will be kept is the oblateness contribution. This is because in

$$\underline{F}(\underline{x}, \underline{u}, t) = \begin{bmatrix} 0 \\ \hline \ddot{\underline{r}}_{\text{drag}} \end{bmatrix} + \begin{bmatrix} 0 \\ \hline \ddot{\underline{r}}_{\text{solar}} \end{bmatrix} + \begin{bmatrix} 0 \\ \hline \ddot{\underline{r}}_{\text{sun, moon}} \end{bmatrix} + \begin{bmatrix} 0 \\ \hline \underline{F}_o \end{bmatrix},$$

the oblateness-acceleration 3-vector $\underline{F}_o$ is a function of the geopotential coefficients $\underline{J}$, which correspond to all but the first three entries in the vector $\underline{e}_u$ that appears in (4.14). However, the satellite does not sense the $\underline{J}$ vector; rather it senses the oblateness force, which happens to be modeled often as an expansion (3.8) having coefficients $\underline{J}$. There are only three components of force, but (in our case) 113 components in $\underline{J}$. Hence, to account for these modeled but not actively estimated parameters, it is economical to let the 3-vector

$$\underline{v}_2(t) = \underline{F}_o(\underline{x}, \underline{J}) - \underline{F}_o(\hat{\underline{x}}, \hat{\underline{J}})$$

denote the change in the force due to deviations in position and in J from their best estimates. Again employing the first-order terms in a Taylor's series expansion about $\hat{x}$, $\hat{J}$, we find

$$\begin{aligned} \underline{v}_2(t) &\approx \left(\frac{\partial \underline{F}_o}{\partial \underline{x}}\right)^{\wedge} \left[\Delta\underline{x}(t) - \Delta\hat{\underline{x}}(t/t_{n-1})\right] + \left(\frac{\partial \underline{F}_o}{\partial \underline{J}}\right)^{\wedge} \Delta\underline{J}, \\ &= \left(\frac{\partial \underline{F}_o}{\partial \underline{r}}\right)^{\wedge} \left[\Delta\underline{r}(t) - \Delta\hat{\underline{r}}(t/t_{n-1})\right] + \left(\frac{\partial \underline{F}_o}{\partial \underline{J}}\right)^{\wedge} \Delta\underline{J}, \end{aligned} \tag{4.15}$$

where $\underline{r}$ and $\Delta\underline{r}$ are the first three components (the position components) of $\underline{x}$ and $\Delta\underline{x}$, respectively. Obviously, since $\hat{\underline{v}}_2(t/t_{n-1}) \equiv 0$, then

$$\underline{e}_{v_2}(t/t_{n-1}) = \underline{v}_2(t). \tag{4.16}$$

Identifying the first three components of $\underline{e}_u$ in (4.14) as $\underline{e}_{v_1}$ and the rest as $\underline{e}_{v_2}$, we find that after throwing away all of $(\frac{\partial \hat{\underline{F}}}{\partial \underline{x}})$ except the oblateness part and using (4.4),

$$\begin{bmatrix} \dot{\underline{e}}_x(t/t_{n-1}) \\ \hline \dot{\underline{e}}_{v_1}(t/t_{n-1}) \end{bmatrix} \approx \left[\begin{array}{c|c} (\frac{\partial \underline{f}}{\partial \underline{x}})_o & (\frac{\partial \hat{\underline{F}}}{\partial \underline{v}_1}) \\ \hline 0 & \begin{matrix} -1/t_d & & \\ & 0 & \\ & & 0 \end{matrix} \end{array}\right] \begin{bmatrix} \underline{e}_x(t/t_{n-1}) \\ \hline \underline{e}_{v_1}(t/t_{n-1}) \end{bmatrix} + \begin{bmatrix} 0 \\ 0 \\ 0 \\ \hline \underline{e}_{v_2}(t/t_{n-1}) \\ \hline 0 \\ 0 \\ 0 \end{bmatrix} + \begin{bmatrix} 0 \\ \vdots \\ 0 \\ \hline w_1(t) \\ 0 \\ 0 \end{bmatrix} . \quad (4.17)$$

Even though $\underline{e}_{v_2}$ is a function of $\underline{e}_x$, the equation can still be integrated formally in the following way. Write only the first part of (4.17):

$$\dot{\underline{e}}_y(t/t_{n-1}) = A(t)\ \underline{e}_y(t/t_{n-1}), \quad (4.18)$$

where

$$\underline{e}_y = \begin{bmatrix} \underline{e}_x \\ \hline \underline{e}_{v_1} \end{bmatrix},$$

$$A(t) = \left[\begin{array}{c|c} (\frac{\partial \underline{f}}{\partial \underline{x}})_o & (\frac{\partial \hat{\underline{F}}}{\partial \underline{v}_1}) \\ \hline 0 & \begin{matrix} -1/t_d & & \\ & 0 & \\ & & 0 \end{matrix} \end{array}\right] .$$

Find the transition matrix $\Phi_y(t, s)$ for (4.18). This can be done either by noting that

$$\Phi_y(t, s) = \frac{\partial \underline{y}(t)}{\partial \underline{y}(s)} = \left[\begin{array}{c|c} \dfrac{\partial \underline{x}(t)}{\partial \underline{x}(s)} & \dfrac{\partial \underline{x}(t)}{\partial \underline{v}_1(s)} \\ \hline \dfrac{\partial \underline{v}_1(t)}{\partial \underline{x}(s)} & \dfrac{\partial \underline{v}_1(t)}{\partial \underline{v}_1(s)} \end{array}\right] \tag{4.19}$$

or by writing the Volterra series solution for (4.18),

$$\Phi_y(t, s) = I + \int_s^t A(\alpha)d\alpha + \int_s^t \int_s^{\alpha} A(\alpha)A(\alpha_1)d\alpha_1 d\alpha +$$

$$\int_s^t \int_s^{\alpha} \int_s^{\alpha_1} A(\alpha)A(\alpha_1)A(\alpha_2)d\alpha_2 d\alpha_1 d\alpha + \ldots,$$

and picking out the developing infinite series.

If we take the first approach to finding Φ_y, we write

$$\underline{x}(t) = \underline{x}\left[\underline{v}_1(t), \underline{v}_2(t), \underline{x}(s), t, s\right] ,$$

$$\underline{v}_1(t) = \begin{bmatrix} e^{-(t-s)/\tilde{\tau}_d} & & \\ & 1 & \\ & & 1 \end{bmatrix} \underline{v}_1(s) + \begin{bmatrix} 1 \\ 0 \\ 0 \end{bmatrix} \int_s^t e^{-(t-\alpha)/\tilde{\tau}_d} w_1(\alpha)d\alpha,$$

and we abreviate equation (3.4) to

$$\dot{\underline{x}}(t) = \underline{f}(\underline{x},t) + \underline{F}(\underline{x}, \underline{u}, t) = \underline{W}\left[\underline{x}(t), \underline{v}_1(t), \underline{v}_2(t), t\right]. \tag{4.20}$$

Applying the chain rule to (4.20), we obtain

$$\frac{\partial \dot{\underline{x}}(t)}{\partial \underline{x}(s)} = \frac{\partial \underline{W}(t)}{\partial \underline{x}(t)} \frac{\partial \underline{x}(t)}{\partial \underline{x}(s)} + \cancelto{0}{\frac{\partial \underline{W}(t)}{\partial \underline{x}(s)}}, \tag{4.21a}$$

$$\frac{\partial \dot{\underline{x}}(t)}{\partial \underline{v}_1(s)} = \frac{\partial \underline{W}(t)}{\partial \underline{x}(t)} \frac{\partial \underline{x}(t)}{\partial \underline{v}_1(s)} + \frac{\partial \underline{W}(t)}{\partial \underline{v}_1(s)}, \tag{4.21b}$$

$$\frac{\partial \underline{v}_1(t)}{\partial \underline{x}(s)} = 0, \tag{4.21c}$$

$$\frac{\partial \underline{v}_1(t)}{\partial \underline{v}_1(s)} = \begin{bmatrix} e^{-(t-s)/\tau_d} & & \\ & 1 & \\ & & 1 \end{bmatrix}, \tag{4.21d}$$

where $\underline{W}(t) = \underline{W}\left[\underline{x}(t), \underline{v}_1(t), \underline{v}_2(t), t\right]$. Again, to first-order accuracy,

$$\frac{\partial \underline{W}}{\partial \underline{x}} = \left(\frac{\partial \underline{f}}{\partial \underline{x}}\right)_o + \left(\frac{\partial \hat{\underline{F}}}{\partial \underline{x}}\right) \approx \left(\frac{\partial \underline{f}}{\partial \underline{x}}\right)_o .$$

Hence (4.21a) is a homogeneous equation in $\frac{\partial \underline{x}(t)}{\partial \underline{x}(s)}$ with approximately the two-body coefficient matrix $\left(\frac{\partial \underline{f}}{\partial \underline{x}}\right)_o$, so that

$$\frac{\partial \underline{x}(t)}{\partial \underline{x}(s)} \approx \underline{\Phi}(t, s). \tag{4.22}$$

On the other hand, (4.21b) becomes

$$\frac{\partial \dot{\underline{x}}(t)}{\partial \underline{v}_1(s)} \approx \left(\frac{\partial \underline{f}}{\partial \underline{x}}\right)_o \frac{\partial \underline{x}(t)}{\partial \underline{v}_1(s)} + \left(\frac{\partial \hat{\underline{W}}(t)}{\partial \underline{v}_1(t)}\right) \left(\frac{\partial \underline{v}_1(t)}{\partial \underline{v}_1(s)}\right)$$

Integrating $\frac{\partial \dot{\underline{x}}(t)}{\partial \underline{v}_1(s)}$ with respect to time t, we have

$$\frac{\partial \underline{x}(t)}{\partial \underline{v}_1(s)} \approx \Phi(t, s) \frac{\partial \underline{x}(s)}{\partial \underline{v}_1(s)} + \int_s^t \Phi(t, u) \left(\frac{\partial \hat{\underline{W}}(u)}{\partial \underline{v}_1(u)}\right) \left(\frac{\partial \underline{v}_1(u)}{\partial \underline{v}_1(s)}\right) du. \qquad (4.23)$$

Since by definition

$$\Phi_y(s, s) \equiv I,$$

the initial condition on (4.23) is $\frac{\partial \underline{x}(s)}{\partial \underline{v}_1(s)} = 0$ for all s. Moreover, from (3.4) and (3.5), we obtain the 6 x 3 matrix

$$\frac{\partial \underline{W}(t)}{\partial \underline{v}_1(t)} = \left[\begin{array}{c|c|c} 0 & 0 & 0 \\ \hline \underline{\beta}(t) & \underline{\beta}(t) & \underline{\gamma}(t) \end{array}\right],$$

which in conjunction with (4.21d), provides the final form for (4.23):

$$\frac{\partial \underline{x}(t)}{\partial \underline{v}_1(s)} = \frac{\partial \underline{x}}{\partial \underline{v}_1}(t, s) \approx \int_s^t \Phi(t, \alpha) \left[\begin{array}{c|c|c} 0 & 0 & 0 \\ \hline \hat{\underline{\beta}}(\alpha) e^{-(\alpha - s)/\tau_d} & \hat{\underline{\beta}}(\alpha) & \hat{\underline{\gamma}}(\alpha) \end{array}\right] d\alpha, \qquad (4.24)$$

where the notation $\hat{\underline{\beta}}(\alpha)$ and $\hat{\underline{\gamma}}(\alpha)$ indicates evaluation around $\hat{\underline{x}}(\alpha/s)$.

Equations (4.21c), (4.21d), (4.22), and (4.24) define the transition matrix $\Phi_y(t, s)$ in (4.19):

$$\Phi_y(n, n-1) = \left[\begin{array}{c|c} \Phi(n, n-1) & \frac{\partial \underline{x}}{\partial \underline{v}_1}(n, n-1) \\ \hline 0 & \begin{array}{cc} e^{-T_n/\tau_d} & \\ & 1 \\ & & 1 \end{array} \end{array}\right]$$

where $T_n = t_n - t_{n-1}$. The formal solution to (4.17) can now be written as the Volterra equation

$$\underline{e}_y(t/t_{n-1}) \approx \Phi_y(t, t_{n-1})\underline{e}_y(t_{n-1}/t_{n-1}) + \int_{t_{n-1}}^{t} \Phi_y(t, s) \left[\begin{array}{c} 0 \\ 0 \\ 0 \\ \hline \underline{e}_{v_2}(s/t_{n-1}) \\ \hline 0 \\ 0 \\ 0 \end{array}\right] ds$$

$$+ \int_{t_{n-1}}^{t} \Phi_y(t, s) \left[\begin{array}{c} 0 \\ \vdots \\ 0 \\ \hline \underline{w}_1(s) \\ 0 \\ 0 \end{array}\right] \qquad (4.25)$$

which in general cannot be solved in closed form because the middle term is a function of $\underline{e}_y$. However, that term is extremely small compared to the rest of the expression. Hence it is not unreasonable to approximate that term by rectangular integration: that is, to take $\underline{e}_{v_2}(s/t_{n-1})$ to be constant between time points t_n and t_{n-1}, where these instants may be data points, or rectification points called by the Encke integrator (see Section III), or rectification points called by a test on the constancy of $\underline{e}_{v_2}(s/t_{n-1})$.

The approach will be to take $\underline{e}_{v_2}(s/t_{n-1}) = \underline{e}_v(t_{n-1}/t_{n-1})$ for $t_{n-1} \leq t \leq t_n$ to produce the staircase approximation suggested in one dimension by Figure 4, below. Of course, we cannot test the error itself to ascertain that it is near enough to being constant, but we can test to see if its covariance has changed significantly with reference to the covariance of that to which it contributes: i.e., the $\underline{e}_y(t/t_{n-1})$ in equation (4.25). This will be made clear shortly.

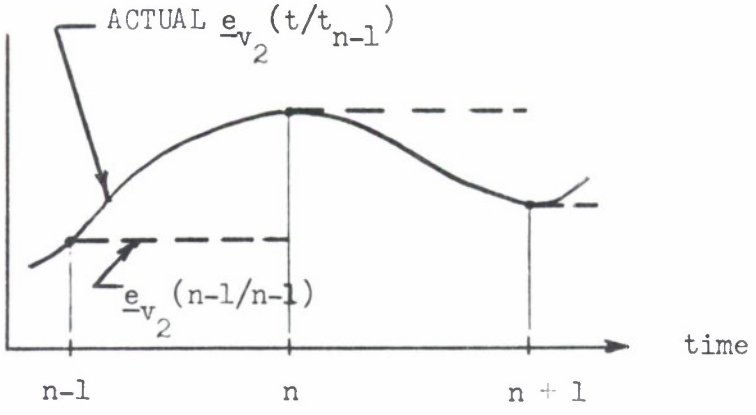

FIGURE 4. STAIRCASE APPROXIMATION TO $\underline{e}_{v_2}(t/t_{n-1})$.

A final linearization is still to be performed on the observation equations. In particular, using the notation developed in this perfect-sensor case for (4.2) and (4.8), we see that the residual term in (4.8) upon which $B_y(n)$ operates is

$$\Delta\underline{z}(n) - \Delta\hat{\underline{z}}(n/n-1) = \underline{h}\left[\underline{x}(n)\right] - \cancel{\underline{h}\left[\underline{x}^{\circ}(n)\right]} - \underline{h}\left[\hat{\underline{x}}(n/n-1)\right] + \cancel{\underline{h}\left[\underline{x}^{\circ}(n)\right]} \ ,$$

which, after a first-order expansion around $\hat{\underline{x}}(n/n-1)$, can be written as

$$\Delta\underline{z}(n) - \Delta\hat{\underline{z}}(n/n-1) \approx \left(\frac{\partial\hat{\underline{h}}}{\partial\underline{x}}\right)\left[\underline{x}(n) - \hat{\underline{x}}(n/n-1)\right]$$

$$= H(n)\left[\Delta\underline{x}(n) - \Delta\hat{\underline{x}}(n/n-1)\right] \ , \qquad (4.26)$$

where $H(n) = \left(\frac{\partial \hat{\underline{h}}}{\partial \underline{x}}\right)$ is the partial derivative evaluated at $\hat{\underline{x}}(n/n-1)$.

3. Prediction Covariance Computations

Evaluate equation (4.25) at time $t = t_n$.

Call

$$\frac{\partial \underline{y}}{\partial \underline{v}_2}(n, n-1) = \int_{t_{n-1}}^{t_n} \Phi_y(t_n, s)\, ds \begin{bmatrix} 0 & 0 & 0 \\ 0 & 0 & 0 \\ 0 & 0 & 0 \\ 1 & 0 & 0 \\ 0 & 1 & 0 \\ 0 & 0 & 1 \\ 0 & 0 & 0 \\ 0 & 0 & 0 \\ 0 & 0 & 0 \end{bmatrix}, \tag{4.27}$$

and assume the staircase approximation

$$\underline{e}_{v_2}(s/t_{n-1}) = \underline{e}_{v_2}(n-1/n-1). \tag{4.28}$$

Define the 9-vector

$$\underline{\omega}(n-1) = \int_{t_{n-1}}^{t_n} \Phi_y(t_n, s) \begin{bmatrix} 0 \\ \vdots \\ 0 \\ \hline w_1(s) \\ 0 \\ 0 \end{bmatrix} ds,$$

$$= \int_{t_{n-1}}^{t_n} \begin{bmatrix} \frac{\partial \underline{x}}{\partial u_1}(t_n, s) \\ \hline e^{-(t_n - s)/\tau_d} \\ 0 \\ 0 \end{bmatrix} w_1(s)\, ds, \tag{4.29}$$

and its covariance matrix

$$\text{Cov}\ \underline{\omega}(n) = Q_{yy}(n) = \left[\begin{array}{c|c|c|c} Q_{11}(n) & \underline{q}(n) & 0 & 0 \\ \hline \underline{q}^T(n) & \sigma^2(n) & & \\ \hline 0 & & 0 & \\ \hline 0 & & & 0 \end{array}\right] , \qquad (4.30)$$

where, from (4.29) and (4.5), it can be computed that

$$Q_{11}(n\text{-}1) = (2/\tau_d)\sigma^2_{drag}\left[\int_{t_{n-1}}^{t_n} \frac{\partial \underline{x}}{\partial u_1}(t_n,s)\left\{\frac{\partial \underline{x}}{\partial u_1}(t_n,s)\right\}^T ds\right],$$

$$\underline{q}(n\text{-}1) = (2/\tau_d)\sigma^2_{drag}\left[\int_{t_{n-1}}^{t_n} \frac{\partial \underline{x}}{\partial u_1}(t_n,s)e^{-(t_n-s)/\tau_d} ds\right],$$

$$\sigma^2(n\text{-}1) = (1-e^{-2(t_n-t_{n-1})/\tau_d})\sigma^2_{drag} .$$

Then (4.25) can be rewritten as

$$\underline{e}_y(n/n\text{-}1) = \Phi_y(n, n\text{-}1)\,\underline{e}_y(n\text{-}1/n\text{-}1) + \frac{\partial \underline{y}}{\partial \underline{v}_2}(n, n\text{-}1)\,\underline{e}_{v_2}(n\text{-}1/n\text{-}1)$$

$$+ \underline{\omega}(n\text{-}1), \qquad (4.31)$$

and its covariance $P_{yy}(n/n-1)$ becomes, after we note that $\underline{\omega}(n-1)$ is uncorrelated with $\underline{\omega}(n-2)$, and hence is uncorrelated with everything else on the right,

$$P_{yy}(n/n-1) = \Phi_y(n, n-1)P_{yy}(n-1/n-1)\Phi_y^T(n, n-1)$$
$$+ \Phi_y(n, n-1)P_{yv_2}(n-1/n-1)\frac{\partial \underline{y}}{\partial \underline{v}_2}^T(n, n-1)$$
$$+ \frac{\partial \underline{y}}{\partial \underline{v}_2}(n, n-1)P_{yv_2}^T(n-1/n-1)\Phi_y^T(n, n-1)$$
$$+ \frac{\partial \underline{y}}{\partial \underline{v}_2}(n, n-1)P_{v_2v_2}(n-1/n-1)\frac{\partial \underline{y}}{\partial \underline{v}_2}^T(n, n-1) + Q_{yy}(n-1) \qquad (4.32)$$

A recursion can be developed once the in-step covariance matrices $P_{yy}(n/n)$, $P_{yv_2}(n/n)$, and $P_{v_2v_2}(n/n)$ are defined in terms of covariance matrices with argument $(n/n-1)$. However, since these in-step covariances are functions of $B_y(n)$, that gain matrix will now be developed explicitly.

4. Computation of Optimal Gain $B_y(n)$

We begin by applying the linearization (4.26) to (4.8) and subtracting $\underline{y}(n)$ from both sides of the resultant equation. We find

$$\underline{e}_y(n/n) = \underline{e}_y(n/n-1) - B_y(n)H(n)\underline{e}_x(n/n-1). \qquad (4.33)$$

If we define the (dim z) x 9 observation matrix

$$H_y(n) = \left[H(n) \vdots 0\right], \qquad (4.34)$$

then (4.33) becomes

$$\underline{e}_y(n/n) = (I - B_y H_y)\underline{e}_y(n/n-1), \tag{4.35}$$

where the argument (n) has been dropped from B_y and H_y.

Clearly, then,

$$P_{yy}(n/n) = (I-B_y H_y)\, P_{yy}(n/n-1)\, (I-B_y H_y)^T, \tag{4.36}$$

and its total differential, given that B_y is the only variable that can be manipulated, is just

$$\begin{aligned} dP_{yy}(n/n) = {} & dB_y \left\{\left[H_y P_{yy}(n/n-1)H_y^T\right] B_y^T - H_y P_{yy}(n/n-1)\right\} \\ & + dB_y \left\{\left[H_y P_{yy}(n/n-1)H_y^T\right] B_y^T - H_y P_{yy}(n/n-1)\right\}^T \end{aligned} \tag{4.37}$$

Now, to achieve the minimum required by (4.7), the total differential of the terms on the left of that expression must be zero:

$$d\left[\text{trace}\left\{AP_{yy}(n/n)A\right\}\right] = \text{trace}\left\{AdP_{yy}(n/n)A\right\} = 0. \tag{4.38}$$

It is a property of the trace that

$$\text{trace}\{XY\} = \text{trace}\{YX\},$$

$$\text{trace}\{X+Y\} = \text{trace } X + \text{trace } Y,$$

$$\text{trace } X = \text{trace } X^T,$$

for any square matrices X and Y. Therefore (4.37) and (4.38) combine to yield

$$\text{trace}\left\{A^2\left(B_y\left[H_y P_{yy}(n/n-1)H_y^T\right] - P_{yy}(n/n-1)H_y^T\right) dB_y\right\} = 0.$$

Since this must hold for all differentials dB_y,

$$A^2 \left(B_y \left[H_y P_{yy}(n/n-1) H_y^T \right] - P_{yy}(n/n-1) H_y^T \right) = 0 \qquad (4.39)$$

is the condition for an optimum. When A is any nonsingular matrix, the optimal $B_y(n)$ is defined to be

$$B_y(n) = P_{yy}(n/n-1)\, H_y^T(n) \left[H_y(n) P_{yy}(n/n-1) H_y^T(n) \right]^{-1}, \qquad (4.40)$$

which is the usual Kalman gain matrix.[6,7]

In the event that we are interested only in estimating the mass parameters, we can set all the α_i in A to zero excep for α_8 and α_9. Then only the last two rows in $B_y(n)$ are defined by (4.39), the others being arbitrary. These last two rows are the same as the last two rows in the usual Kalman matrix given by (4.40). The remaining rows we can set to anything. Let us set them to the usual Kalman values defined by (4.40). Hence, independent of the weights A, the Kalman gain (4.40) is always optimal. Note that if we had generalized A to be non-diagonal, the result would have been the same.

In terms of the partition

$$P_{yy}(n/k) = \left[\begin{array}{c|c} P_{xx}(n/k) & P_{xv_1}(n/k) \\ \hline P_{xv_1}^T(n/k) & P_{v_1v_1}(n/k) \end{array}\right],$$

equation (4.40) becomes

$$B_y(n) = \left[\begin{array}{c} B_x(n) \\ \hline B_{v_1}(n) \end{array}\right] = \left[\begin{array}{c} P_{xx}(n/n-1) \\ \hline P_{xv_1}^T(n/n-1) \end{array}\right] H^T(n) \left[H(n) P_{xx}(n/n-1) H^T(n) \right]^{-1} \qquad (4.40')$$

where $B_x(n)$ is the 6 x (dim z) gain for the satellite state estimates and $B_{v_1}(n)$ is the 3 x (dim z) gain for the mass parameters $\underline{v}_1$.

5. In-Step Covariance Computations

Inserting (4.40) in (4.36), we can show that

$$P_{yy}(n/n) = (I-B_y H_y)^2 P_{yy}(n/n-1) = (I-B_y H_y)\ P_{yy}(n/n-1). \tag{4.41}$$

Moreover, we can post-multiply equation (4.35) by $\underline{e}_{v_2}^T(n/n)$, use (4.15) and (4.16), and take the expectation:

$$P_{yv_2}(n/n) = (I-B_y H_y)\ P_{yy}(n/n-1)\ \frac{\hat{\partial \underline{F}_o}}{\partial \underline{y}}^T(n)$$

$$+ (I-B_y H_y)\ P_{yJ}(n/n-1)\ \frac{\hat{\partial \underline{F}_o}}{\partial \underline{J}}^T(n), \tag{4.42}$$

where the argument (n) on the partial derivatives indicate evaluation at the point $\hat{\underline{x}}(n/n)$, and

$$\frac{\partial \underline{F}_o}{\partial \underline{y}} = \left[\begin{array}{c|c|c} \frac{\partial \underline{F}_o}{\partial \underline{r}} & 000 & 000 \\ & 000 & 000 \\ & 000 & 000 \end{array}\right] .$$

The matrix $P_{yJ}(n/n-1)$ is found by multiplying (4.31) by $(\Delta J)^T$ and taking the expectation:

$$P_{yJ}(n/n-1) = \left[\Phi_y(n, n-1) + \frac{\partial \underline{y}}{\partial \underline{v}_2}(n, n-1)\,\frac{\hat{\partial \underline{F}}_o}{\partial \underline{y}}(n-1)\right] P_{yJ}(n-1/n-1)$$

$$+ \frac{\partial \underline{y}}{\partial \underline{v}_2}(n, n-1)\,\frac{\hat{\partial \underline{F}}_o}{\partial \underline{J}}(n-1)\,P_{JJ}, \tag{4.43}$$

where $P_{JJ} = \mathrm{Cov}\,(\Delta \underline{J})$. The in-step matrix $P_{yJ}(n-1/n-1)$ obtains by multiplying (4.35) by $(\Delta \underline{J})^T$ and taking the expectation:

$$P_{yJ}(n/n) = (I - B_y H_y)\,P_{yJ}(n/n-1). \tag{4.44}$$

This completes the detail for (4.42). To summarize what we have done so far,

$$P_{yy}(n/n) = D(n) P_{yy}(n/n-1), \tag{4.45}$$

$$P_{yJ}(n/n) = D(n)\,P_{yJ}(n/n-1), \tag{4.46}$$

$$P_{yv_2}(n/n) = P_{yy}(n/n)\,\frac{\partial \underline{F}_o}{\partial \underline{y}}^T(n) + P_{yJ}(n/n)\,\frac{\partial \underline{F}_o}{\partial \underline{J}}^T(n), \tag{4.47}$$

where

$$D(n) = \left[\begin{array}{c|c} I - B_x(n)H(n) & 0 \\ \hline -B_{v_1}(n)H(n) & I \end{array}\right]. \tag{4.48}$$

and where $P_{yJ}(n/n-1)$ is given by (4.43).

To compute $P_{v_2 v_2}(n/n)$ from (4.15) is now theoretically straightforward:

$$P_{v_2 v_2}(n/n) = \frac{\partial \hat{F}_{-o}}{\partial \underline{r}}(n) P_{rr}(n/n) \frac{\partial \hat{F}_{-o}}{\partial \underline{r}}^T(n) + \frac{\partial \hat{F}_{-o}}{\partial \underline{J}}(n) P_{JJ} \frac{\partial \hat{F}_{-o}}{\partial \underline{J}}^T(n) + \Pi(n/n) + \Pi^T(n/n), \tag{4.49}$$

where

$$\Pi(n/n) = \frac{\partial \hat{F}_{-o}}{\partial \underline{r}}(n)\ P_{rJ}(n/n)\ \frac{\partial \hat{F}_{-o}}{\partial \underline{J}}^T(n),$$

and P_{rr} and P_{rJ} are the submatrices defined by

$$P_{xx}(n/n) = \left[\begin{array}{c|c} P_{rr}(n/n) & P_{r\dot{r}}(n/n) \\ \hline P_{r\dot{r}}^T(n/n) & P_{\dot{r}\dot{r}}(n/n) \end{array}\right],$$

$$P_{yJ}(n/n) = \left[\begin{array}{c} P_{rJ}(n/n) \\ \hline P_{\dot{r}J}(n/n) \\ \hline P_{v_1 J}(n/n) \end{array}\right],$$

the latter being given by (4.46).

So far, the updating of P_{yy} has been described only for the case of closely spaced data points, t_{n-1} and t_n; for widely spaced points, the assumption of constant $\underline{e}_{v_2}(s/t_{n-1})$ in equation (4.25) is not valid. This problem is easily circumvented; there is no need to wait until data point t_n to perform the covariance matrix update. Rather, when (according to some criterion) the assumption of constant $\underline{e}_{v_2}$ is in danger of

being violated, say at intermediate time $t_{n-1,1} = t_{n-1} + \Delta t$, a new in-step covariance matrix can be defined as

$$P_{yy}(t_{n-1,1}/t_{n-1,1}) = P_{yy}(t_{n-1,1}/n),$$

i.e., the filter gain $B_y(t_{n-1,1})$ that appears in equation (4.41) is set to zero. The update procedure for the extrapolated covariance matrix can now proceed normally from $t_{n-1,1}$, either to the next data point, t_n, or another non-data update point, $t_{n-1,2}$.

Calculate $P_{v_2v_2}(n-1/n-1)$ from (4.49); compute $P_{yy}(t_{n-1,1}/n-1)$ from (4.32), retaining the sum of the first and last terms, which involve $P_{yy}(n-1/n-1)$ and $Q_{yy}(n-1)$. Compute now, the matrices $P_{yv_2}(t_{n-1,1}/t_{n-1,1})$ and $P_{v_2v_2}(t_{n-1,1}/t_{n-1,1})$ to be used in the next update. Before updating, recompute $P_{yy}(t_{n-1,1}/n-1)$ using the same first and last terms as before. In place of $P_{yv_2}(n-1/n-1)$ and $P_{v_2v_2}(n-1/n-1)$, use $P_{yv_2}(t_{n-1,1}/t_{n-1,1})$ and $P_{v_2v_2}(t_{n-1,1}/t_{n-1,1})$, respectively.

The changes in the P_{yv_2} and $P_{v_2v_2}$ matrices are indicative of the errors implicit in the constant $\underline{e}_{v_2}$ assumption; the difference between the $P_{yy}(t_{n-1,1}/n-1)$ matrices using the old and new P_{yv_2} and $P_{v_2v_2}$ illustrate the order of magnitude of the maximum errors in P_{yy} that result from the assumption under test. Thus, for the elements p_{ij} of the extrapolated P_{yy}, and p'_{ij} of the recomputed P_{yy}, find

$$E_{yy} = \max_{i,j} \frac{|p_{ij} - p'_{ij}|}{|p_{ij}| + |p'_{ij}|}$$

Then, if $E_{yy} > b$, for some upper bound, b, reduce the Δt used to advance to the next non-data update point, if any. If $E_{yy} < a$, for some lower bound, a, increase Δt.

C. SUMMARY OF FILTERING PROCEDURE

1. Start with an initial estimate

$$\hat{\underline{y}}\ (0/0) = \begin{bmatrix} \Delta\hat{\underline{x}}(0/0) \\ \hline \hat{\underline{v}}_1(0/0) \end{bmatrix}$$

of the satellite states $\Delta\underline{x}$ and the mass parameters $\underline{v}_1$.

2. Use the mass-parameter model (4.9) to compute the extrapolations

$$\hat{\underline{v}}_1\ (t/0) = \begin{bmatrix} e^{-(t-t_o)/\tau_d} & & \\ & 1 & \\ & & 1 \end{bmatrix} \hat{\underline{v}}_1\ (0/0).$$

3. Employ these extrapolations in the Encke equation

[equation (4.10)]

$$d(\Delta\hat{\underline{x}})dt = \underline{f}(\underline{x}^o+\Delta\hat{\underline{x}},t)-\underline{f}(\underline{x}^o,t) + \underline{F}(\underline{x}^o+\Delta\hat{\underline{x}},\ \hat{\underline{v}}_1(t/0),\ \hat{J}),$$

and integrate from the initial condition $\Delta\hat{\underline{x}}(0/0)$ to obtain $\Delta\hat{\underline{x}}(1/0)$. Also evaluate $\hat{\underline{v}}_1(t/0)$ at $t = t_1$ to obtain $\hat{\underline{v}}_1(1/0)$.

4. Guess at the covariances on the initial estimates:

$P_{yy}(0/0)$, $P_{yv_2}(0/0)$, $P_{yJ}(0/0)$.

5. Use these matrices to compute [from (4.49)]

$$P_{v_2v_2}(0/0) = \frac{\partial\hat{\underline{F}}_o}{\partial\underline{r}}(0)P_{rr}(0/0)\frac{\partial\hat{\underline{F}}_o}{\partial\underline{r}}^T(0) + \frac{\partial\hat{\underline{F}}_o}{\partial\underline{J}}(0)\ P_{JJ}\ \frac{\partial\hat{\underline{F}}_o}{\partial\underline{J}}^T(0) + \mathbf{\Pi}(0/0) + \mathbf{\Pi}^T(0/0),$$

where

$$\mathbf{\Pi}(0/0) = \frac{\partial \hat{\underline{F}}_o}{\partial \underline{r}}(0) P_{rJ}(0/0) \frac{\partial \hat{\underline{F}}_o}{\partial \underline{J}}^T(0).$$

6. Then evaluate (4.32):

$$P_{yy}(1/0) = \Phi_y(1,0)\, P_{yy}(0/0)\, \Phi_y^T(1,0) + \Delta(1/0) + \Delta^T(1/0) + \frac{\partial \underline{y}}{\partial \underline{v}_2}(1,0)\, P_{v_2 v_2}(0/0) \frac{\partial \underline{y}}{\partial \underline{v}_2}^T(1,0) + Q_{yy}(0),$$

where

$$\Delta(1/0) = \Phi_y(1,0)\, P_{y v_2}(0/0) \frac{\partial \underline{y}}{\partial \underline{v}_2}^T(1,0).$$

Also evalute (4.43):

$$P_{yJ}(1/0) = \left[\Phi_y(1,0) + \frac{\partial \underline{y}}{\partial \underline{v}_2}(1,0) \frac{\partial \hat{\underline{F}}_o}{\partial \underline{y}}(0)\right] P_{yJ}(0/0) + \frac{\partial \underline{y}}{\partial \underline{v}_2}(1,0) \frac{\partial \hat{\underline{F}}_o}{\partial \underline{J}}(0) P_{JJ}.$$

7. Then use the first of these in (4.40′):

$$B_y(1) = \left[\begin{array}{c} B_x(1) \\ \hline B_{v_1}(1) \end{array}\right] = \left[\begin{array}{c} P_{xx}(1/0) \\ \hline P_{x v_1}^T(1/0) \end{array}\right] H^T(1) \left[H(1)\, P_{xx}(1/0) H^T(1)\right]^{-1}.$$

8. Use $B_y(1)$ in (4.45):

$$P_{yy}(1/1) = D(1)\, P_{yy}(1/0),$$

and (4.46):

$$P_{yJ}(1/1) = D(1)P_{yJ}(1/0),$$

where

$$D(1) = \left[\begin{array}{c|c} I-B_x(1)H(1) & 0 \\ \hline -B_{v_1}(1)H(1) & I \end{array}\right]$$

9. From $P_{yy}(1/1)$ compute $P_{yv_1}(1/1)$ using (4.47),

$$P_{yv_2}(1/1) = P_{yy}(1/1)\ \frac{\partial \hat{F}_o}{\partial \underline{y}}^T(1) + D(1)P_{yJ}(1/0)\ \frac{\partial \hat{F}_o}{\partial \underline{J}}^T(1),$$

and compute $P_{v_2v_2}(1/1)$ from step 5 with "0"s replaced by "1"s.

10. Use $B_y(1)$ and $y(1/0)$, together with a measurement $\underline{z}(1)$, to compute $\hat{\underline{y}}(1/1)$ from (4.8):

$$\hat{\underline{y}}(1/1) = \hat{\underline{y}}(1/0) + B(1)\left[\ \underline{Z}(1)-\underline{h}\left[\underline{x}(1/0)\right]\right] \quad .$$

11. Return to step 1 and re-do the process with "0" subscripts and arguments replaced with "1"s and "1"s replaced with "2"s. Skip steps 4 and 5. Repeat for t_2, t_3, ...,t_n, t_{n+1},....

The above holds for two data times t_n and t_{n+1} sufficiently close. If the test on the constancy of $\underline{e}_{v_2}(t/tn)$ requires an update point at $t_n+\Delta t < t_{n+1}$, the same process as the above is followed, except that

(a) $t_n+\Delta t$ replaces t_{n+1} in the program;

(b) step 7 is replaced with a step that sets $B_y(1) = 0$.

D. SENSITIVITY COEFFICIENTS

One of the major aims of this study is to determine the quantitative effects of an error source on the estimates of the ballistic coefficients u_2 and u_3. These effects are computed classically by assuming that the error contributions from each source are small. In addition, it is assumed that the functional relationships between the error-source parameters, say $\underline{\alpha}$ = column (α_1, α_2,...), and the ballistic-coefficient estimates are known to be, say,

$$\hat{u}_2 = g_2(\underline{\alpha}),$$
$$\hat{u}_3 = g_3(\underline{\alpha}). \qquad (4.50)$$

Then a Taylor's series expansion in the errors can be performed and truncated at the first-order terms to yield

$$\Delta u_2 = (\text{grad } g_2)^T \Delta \underline{\alpha},$$
$$\Delta u_3 = (\text{grad } g_3)^T \Delta \underline{\alpha}, \qquad (4.51)$$

where the gradients are taken with respect to $\underline{\alpha}$ and evaluated around the nominal values of the parameters. The biases in the ballistic coefficients are

$$E(\Delta u_2) = (\text{grad } g_2)^T E(\Delta \underline{\alpha}),$$
$$E(\Delta u_3) = (\text{grad } g_3)^T E(\Delta \underline{\alpha}).$$

The variances are

$$\sigma^2_{u_2} = (\text{grad } g_2)^T E(\Delta \underline{\alpha} \Delta \underline{\alpha}^T)(\text{grad } g_2) - E^2(\Delta u_2),$$

$$\sigma^2_{u_3} = (\text{grad } g_3)^T E(\Delta \underline{\alpha} \Delta \underline{\alpha}^T)(\text{grad } g_3) - E^2(\Delta u_3),$$

or

$$\sigma_{u_2}^2 = (\text{grad } g_2)^T \text{ Cov } (\Delta \underline{\alpha}) (\text{grad } g_2),$$

$$\sigma_{u_3}^2 = (\text{grad } g_3)^T \text{ Cov } (\Delta \underline{\alpha}) (\text{grad } g_3). \qquad (4.52)$$

In terms of these second-order statistics, the gradient vectors define completely the importance of each error-source parameter in the ballistic-coefficient error build-up. The elements of these gradient vectors are often called "sensitivity coefficients."

Unfortunately, in a maximum-likelihood or minimum-variance estimation procedure of the sort required here, the functions g_2 and g_3 in (4.50) cannot be written as closed-form expressions of the error-source parameters $\underline{\alpha}$. Hence the gradients cannot be obtained analytically.

1. Modeled Parameters

In the minimum-variance estimation equations developed in parts A and B of this section, certain parameters have variance-covariance values associated with them. It is said that the errors in these parameters are thereby "modeled." The stochastic component of drag, u_1, and the geopotential perturbation acceleration $\underline{v}_2$ are the only two modeled error sources considered in this perfect-sensor phase of the study. Call these modeled error parameters β_1, β_2, ..., and the variances $\sigma_{\beta_1}^2$, $\sigma_{\beta_2}^2$, ...

Then the minimum-variance equations yield implicitly the in-step estimation errors

$$\Delta u_2 = G_2 \left(\sigma_{\beta_1}, \sigma_{\beta_2}, \ldots \right),$$

$$\Delta u_3 = G_3 \left(\sigma_{\beta_1}, \sigma_{\beta_2}, \ldots \right).$$

To ascertain the importance of reducing the ignorance in one modeled parameter relative to another, assuming small reduction in such ignorance, we need to find for all i

$$\partial \sigma_{u_2}^2 / \partial \sigma_{\beta_i} \approx \Delta \sigma_{u_2}^2 / \Delta \sigma_{\beta_i}$$

$$\partial \sigma_{u_3}^2 / \partial \sigma_{\beta_i} \approx \Delta \sigma_{u_2}^2 / \Delta \beta_i$$

where Δ indicates a (small) change in the variable that follows it.

Each of these partials is a form of sensitivity coefficient which is really the desired end product of the study. The manner of computing it consists simply of making a run with all the σ_{β_i} reduced by the amount $\Delta \sigma_{\beta_i}$.

2. Unmodeled Parameters

The minimum-variance expressions contain a few parameters which may have incorrect values, but for which no reasonable variance-covariance information exists. Such parameters, having so-called "unmodeled" errors, are typified by the correlation time constant τ_d in the stochastic drag expression (4.4), or the geomagnetic index a_p that enters the nominal

atmospheric-density calculations. Call these unmodeled parameters γ_1, γ_2, ..., and their (unknown) variances $\sigma^2_{\gamma_1}$, $\sigma^2_{\gamma_2}$, ...

Now the estimation errors will not directly reflect any improvement in our knowledge of the error-source parameter values. However the estimates themselves are implicit functions of the parameters: from (4.50),

$$\hat{u}_2 = g_2 (\beta_1, \beta_2, \ldots; \quad \gamma_1, \quad \gamma_2, \ldots),$$

$$\hat{u}_3 = g_3 (\beta_1, \beta_2, \ldots; \quad \gamma_1, \quad \gamma_2, \ldots).$$

Hence by changing each γ_i while holding the other parameters at their nominal values, each sensitivity coefficient in grad g_2 and grad g_3 can be determined numerically. Put into (4.52), these coefficients lead at once to the pinpointing of the dominant error sources.

E. MINIMUM-VARIANCE VERSUS MAXIMUM LIKELIHOOD

Although the contract specifies analysis of the errors in the maximum-likelihood estimation of mass, the approach contained herein is based upon minimum-variance estimation. As is shown in detail in Appendix V, the theoretical details may be different, but the practical solution to the problem is essentially the same in both cases. Computationally, the problems that arise in one approach arise also in the other.

SECTION V

ENVIRONMENTAL MODELS

A. SOLAR RADIATION PRESSURE

The model is discussed in Appendix I. It will become important at altitudes of about 500 km or higher, and will be the sole mass-determining force at altitudes in excess of 1000 km.

B. ELECTROMAGNETIC DRAG

A detailed analysis of the three types of significant electromagnetic drag is carried out in Appendix II based upon the CIRA 1965[21] tables for ion and neutral-particle densities.

Of the three types of electromagnetic drag, two are distinguishable from atmospheric drag because they are latitude-longitude dependent and have a velocity dependence different from atmospheric drag. These consist of

(1) Electromotive drag, where the charged vehicle interacts with the earth's magnetic field;

(2) Induced drag, where the potential induced in the moving satellite (conductor) by the earth's magnetic field sets up a current through the ionized atmosphere which produces a back-EMF retardation.

Under the worst-case conditions (the largest satellite, highest charged-particle densities, and strongest magnetic field), these effects are at least two orders of magnitude smaller than atmospheric drag.

The remaining type of electromagnetic drag is indistinguishable from atmospheric drag to the ground-based observer. It is known as coulomb drag, and results because the charged satellite electrostatically attracts to it ionized particles that it would not otherwise hit. The ensuing increase in the effective area-to-mass ratio may reach 10 per cent or more. It will be accounted for by making off-line corrections to the estimate of ballistic coefficient u_2.

C. GEOPOTENTIAL MODEL

The earth's geopotential model is discussed in Appendix III.

D. SOLAR-LUNAR GRAVITATION

The solar-lunar gravitational accelerations on the satellite will be computed from the assumption that the sun and the moon are point masses. Computational details will be as specified for the MINIVAR computer program,[3,4] and presented in equation (3.7) of this report. The respective distances and gravitational constants will be assumed exact.

E. ATMOSPHERIC DRAG

Atmospheric drag can be computed interchangeably from the expression of Appendix II or from the usual velocity-squared law given in (3.5). Both require an accurate upper-atmosphere model. The Jacchia 1965 model, published in Reference 8 and described briefly below, will be used here, in conjunction with expression (3.5) of this report. RMS values σ_{drag} and correlation times τ_d for equation (3.5) will be chosen in concert with the contracting agency. Suggested values are given in Reference 7.

The following summary of the Jacchia 1965 model was extracted, with minor corrections, from Reference 28:

> Jacchia's 1965 atmospheric model (Reference 8) begins at a boundary altitude of 120 kilometers where the following assumptions are made:
>
> 1) $T_{120} = 355^{\circ}K$
>
> $n(N_2) = 4.0 \times 10^{11}$ molecules/cm^3
>
> $n(O_2) = 7.5 \times 10^{10}$ " "

$n(O) = 7.6 \times 10^{10}$ molecules/cm^3

$n(He) = 3.4 \times 10^{7}$ " "

Below the altitude, Z = 500 kilometers, n(H) = 0.

At 500 kilometers, the boundary condition for hydrogen is:

$$LOG_{10}[n(H)] = 73.13 - 39.40\ LOG_{10}(T_{500}) + 5.5[LOG_{10}(T_{500})]^2$$

Where:

T_{500} = temperature in degrees Kelvin at 500 kilometers.

n = number density of individual constituents of the atmosphere; nitrogen(N_2), oxygen(O_2), free oxygen(O), helium(He) and hydrogen(H).

Using the boundary conditions as a starting point for the concentrations n_i of each consitituent i, the following diffusion equation is integrated to find the concentrations as a function of altitude Z.

2) $$\frac{dn_i}{n_i} = \frac{-dZ}{H_i} - \frac{dT}{T}(1 + \alpha)$$

Where:

T = temperature in degrees Kelvin

α = thermal diffusion factor

- 0.38 for helium
- 0.0 for other consitutuents

m_i = mass of each constituents.

$m(N_2) = 4.6515 \times 10^{-23}$ grams/molecule

$m(O_2) = 5.3129 \times 10^{-23}$ grams/molecule

$m(O) = 2.6565 \times 10^{-23}$ grams/atom

$m(He) = 0.6648 \times 10^{-23}$ grams/atom

$m(H) = 0.1674 \times 10^{-23}$ grams/atom

$k = 1.38054 \times 10^{-16}$ ergs/$^\circ$K (Boltzmann's constant)

$R = 6.35677 \times 10^{8}$ cm. (radius of the earth)

$g = 980.665 \left(1 + \frac{Z}{R}\right)^{-2}$ cm./sec.^{2} (acceleration due to gravity)

$H_i = \frac{kT}{m_i g}$ (scale height)

Equation 2) when integrated becomes:

$$3) \quad n_i = n_{120} \left[\frac{T_{120}}{T}\right]^{1 + \alpha} \exp\left[\frac{-m_i}{k} \int_{120}^{Z} g \frac{dZ}{T}\right]$$

Simpson's rule of order 2 with a step size of .1 km is used for numerical integration.

The following sequence of operations determine the temperature T at the desired altitude Z

$$4) \quad T = T_\infty - (T_\infty - T_{120}) \exp\left[-S(Z - 120)\right]$$

Where:

T_∞ = exospheric temperature $^\circ$K

T_{120} = temperature at 120 km.

Z = altitude in km.

$$S = 0.0291 \exp\left(\frac{-X^2}{2}\right)$$

$$X = \frac{T_\infty - 800.0}{750.0 + 1.722 \times 10^{-4} (T_\infty - 800.0)^2}$$

Note: The expressions S and X are approximations to the profile derived by L. Jacchia by trial and error methods.

5) $\rho = \sum_i n_i m_i \quad gm/cm^3$

ρ = density as a function of altitude

The following procedure is used to determine the exospheric temperature, T_∞

1) $\bar{T}_o = 357^\circ K + 3.6\ \bar{F}_{10.7}$

Where:

$\bar{T}_o$ is the average nighttime minimum temperature

$\bar{F}_{10.7}$ is the smooth solar flux over 3 solar rotations

2) $T_o^1 = \bar{T}_o + 1.8^\circ\ (F_{10.7} - \bar{F}_{10.7})$

Where:

T_o^1 is the variation expected during a given solar rotation (27 days)

$F_{10.7}$ is the solar flux for the previous day.

3) $$T_o = T_o^1 + \left[0.37 + 0.14 \sin\left(2\pi \frac{d-151}{365}\right)\right] \bar{F}_{10.7} \sin\left(4\pi \frac{d-59}{365}\right)$$

Where:

T_o accounts for the semi-annual variation.

d is the number of days from January 1.

4) $$T = T_N \left[1.0 + \left(\frac{T_D - T_N}{T_N}\right) \cos^m\left(\frac{\tau}{2}\right)\right]$$

Where:

$$T_D = T_o \ (1.0 + R \cos^m \eta)$$

$$T_N = T_o \ (1.0 + R \sin^m \theta)$$

$$\eta = 0.5 \ |\phi - \delta_s|$$

$$\theta = 0.5 \ |\phi + \delta_s|$$

$$\delta_s = \text{TAN}^{-1}\left(\frac{Z_s}{\sqrt{X_s^2 + Y_s^2}}\right)$$

$$\phi = \text{TAN}^{-1}\left(\frac{Z_v}{\sqrt{X_v^2 + Y_v^2}}\right)$$

$$R = 0.28$$

$$m = 2.5$$

$$\tau = H + \beta + P \sin (H + \alpha)$$

$$H = \text{TAN}^{-1}\left(\frac{Y_v}{X_v}\right) - \text{TAN}^{-1}\left(\frac{Y_s}{X_s}\right)$$

$\beta = -45^{\circ}$

$P = 12^{\alpha}$

$\alpha = 45^{\circ}$

T accounts for the diurnal effect.

T_D is the daytime maxima.

T_N is the nighttime minima.

R is a factor for computing the maximum temperature as a function of the global minimum temperature.

ϕ is the geographic latitude of the vehicle.

δ_s is the declination of the sun.

X_v, Y_v, Z_v are the current coordinates of the vehicle in an earth-centered cartesian coordinate system.

X_s, Y_v, Z_s current coordinates of the sun

H is the hour angle of the sun

5) $T_\infty = T + 1.0^{\circ}\ a_p + 125^{\circ}\ [1.0 - \exp\ (-0.08\ a_p)]$

Where:

T_∞ is the exospheric temperature.

a_p is the 3 hour geomagnetic index (measured approximately 6 hours before the time in question.)

SECTION VI

REFERENCES

1. R. H. Battin, Astronomical Guidance, McGraw-Hill Publishing Co., New York, 1964.

2. "Interplanetary Trajectory Encke Method (ITEM) Program Manual," NASA Report X-640-63-71, NASA Goddard Space Flight Center, Greenbelt, Maryland, May 1963.

3. "Program Manual for Operational Minimum Variance Tracking and Orbit Prediction Program," (MINIVAR), prepared by Sperry Rand Systems Group, Sperry Gyroscope, Great Neck, New York, under contract No. NAS5-3509 for NASA Goddard Space Flight Center, Greenbelt, Maryland, January 1964.

4. "Sequential Position and Covariance Estimation (SPACE) Trajectory Program -- Analytical Manual," prepared by Sperry Rand Systems Group, Sperry Gyroscope Co., Great Neck, New York, under contract No. NAS5-3509 for NASA Goddard Space Flight Center, Greenbelt, Maryland, April 1965.

5. "Proposal for the Analysis of the Capabilities of Ground Based Sensors in Determining the Mass of Orbiting Bodies," prepared by the Surface Division, Westinghouse Defense and Space Center, Baltimore, Maryland for Proposal Request PR ES-6-496L-61117 for Electronics Systems Division, Air Force Systems Command, L.G. Hanscom Field, Bedford, Massachusetts, June 1966.

6. R. E. Kalman, "A New Approach to Linear Filtering and Prediction Problems," Trans. ASME (J. Basic Engr.), vol. 82, pp. 35-45, March 1960.

7. H. E. Rauch, "Optimum Estimation of Satellite Trajectories Including Random Fluctuations in Drag," AIAA J., vol. 3, n. 4, pp. 717-722, April 1965.

8. L. G. Jacchia, "Static Diffusion Models of the Upper Atmosphere with Empirical Temperature Profiles," Smithsonian Contributions to Astrophysics, vol. 8, no. 9, Smithsonian Institution, Washington, D. C., 1965.

9. Y-C. Ho, R. E. Kalman, and K. S. Narenda, "Controllability of Linear Dynamic Systems," Contributions to Ord. Differential Eqns., vol. 1, pp. 189-213, 1962.

10. R. A. Penrose, " A Generalized Inverse for Matrices," Proc. Cambridge Philosophical Society, vol. 51, pp. 406 - 413, 1955.

11. H. E. Rauch, F. Tung, and C. T. Striebel, "Maximum Likelihood Estimates of Linear Dynamic Systems," AIAA Journal, vol. 3, pp. 1445 - 1450, August 1965.

12. G. Joos and I.M. Freeman, Theoretical Physics, 3rd ed., Blackie and Sons Ltd., London, 1958

13. R. J. List, (ed.), Smithsonian Meteorological Tables, Smithsonian Institution, Washington, D. C. 1951.

14. Y. Kozai, "Effects of Solar Radiation Pressure on the Motion of an Artificial Satellite, "Research in Space Sciences, Special Report No. 56, Smithsonian Astrophysical Observatory, Cambridge, Massachusetts, January 1961.

15. H. R. Byers, "The Atmosphere up to 30 Kilometers," The Earth as a Planet, (G.P. Kuiper, ed.) University of Chicago Press, Chicago, 1954.

16. A.R. Harvey, "Incident Thermal Radiation Upon a Satellite," Air Arm Report AA-3055-62, Westinghouse Electric Corporation, Baltimore, Maryland, 1962.

17. I. L. Goldberg, "Radiation From Planet Earth," USASRDL Tech. Report 2231, U. S. Army Signal Research and Development Laboratory, Fort Monmouth, N.J., September 1961.

18. Fitz, Lukasik, et. al., "Albedo and Planet Radiation Intercepted by an Earth Satellite," AEDC-TDR-63-92, Vitro Laboratories, West Orange, N.J., May, 1963.

19. F.L. Beckner, "Some Notes on the exterior Forces Affecting Ballistic Missiles and Satellites," Military Physics Research Lab., Report MPRL-478, Univ. of Texas, Austin, Texas, March 1960. ASTIA Doc. No. AD-234370.

20. C. L. Brundin, "Effects of Charged Particles on the Motion of an Earth Satellite," AIAA Journal, vol. 1, no. 11, pp. 2529 - 2538, November 1963.

21. CIRA 1965 (Committee on Space Research International Reference Atmosphere 1965), North Holland Publishing Co., Amsterdam, 1965.

22. Y. Kozai, "New Determination of Zonal Harmonic Coefficients of the Earth's Gravitational Potential," Special Report No. 165, Smithsonian Astrophysical Observatory, Cambridge, Massachusetts, 1964.

23. E.M. Gaposchkin, "A Dynamical Solution for the Tesseral Harmonics of the Geopotential, and Statian Coordinates Using Baker-Nunn Data," Proc. 7th COSPAR International Space Science Symposium, Vienna, May 1966.

24. H. B. Wackernagel, "Spacetrack Earth Model 1966 (STEM 66), "HQ Ninth Aerospace Defense Division, Analysis Memorandum No. 66-3, Ent Air Force Base, Colorado, June 1966.

25. W. Köhnlein, "Corrections to Station Coordinates and to Nonzonal Harmonics from Baker-Nunn Observation," Proc. 7th COSPAR International Space Science Symposium, Vienna, May 1966.

26. P. Musen, "The Influence of Solar Radiation Pressure on the Motion of an Artificial Satellite," Journal Geophysical Research, vol. 65, no. 5, 1391 - 1396, May 1960.

27. R.N. DeWitt, "Derivations of Expressions Describing the Gravitational Field of the Earth," Tech. Memorandum K-35/62, U.S. Naval Weapons Lab., Dahlgrin, Virginia, November 1962.

28. C. V. McCarthy, "Modifications and Improvements in the NRTPOD Program," Working Paper WP-828, The MITRE Corporation, Bedford, Massachussetts, 24 October 1966.

29. A. J. Dennison, Jr., "Illumination of a Space Vehicle Surface Due to Sunlight Reflected From Earth", ARS Journal, pp. 635-637, April 1962.

30. R. E. Kalman, "New Methods and Results in Linear Prediction and Estimation Theory," RIAS Report 61-1, The Martin Company, Baltimore, Maryland 21212, 1961.

APPENDIX I

PERTURBATIONS ON SPHERICAL SATELLITES DUE TO SOLAR RADIATION PRESSURE

A. GENERAL

A photon flux of irradiance I_s directed along a unit vector $\hat{i}_{ss}$ from a distant radiating body (e. g., the sun) to a satellite will produce a pressure of

$$\underline{p} = (I_s/c)\,\hat{i}_{ss}, \tag{I.1}$$

where c is the speed of light. When $\underline{p}$ impinges upon a differential surface area $d\underline{A}$, the differential force due to the incident flux is

$$d\underline{F}_{in} = \hat{i}_{ss}\,(\underline{p} \cdot d\underline{A}) = \hat{i}_{ss}\,(I_s/c)\,(\hat{i}_{ss} \cdot d\underline{A}), \tag{I.2}$$

while the differential force due to the flux being reflected back from the surface is

$$d\underline{F}_{refl} = -\hat{i}_{refl}\,(I_r/c)\,(\hat{i}_{refl} \cdot d\underline{A}), \tag{I.3}$$

where $\hat{i}_{refl}$ is the unit vector in the direction of the reflected flux and I_r is the irradiance in that direction.

The net solar force due to direct solar radiation is the integral of (I.2) plus (I.3):

$$\underline{F}_d = (I_s/c) \int_{A_s} \left[\hat{i}_{ss}\,(\hat{i}_{ss} \cdot d\underline{A}) - \hat{i}_{refl}\,(I_r/I_s)\,(\hat{i}_{refl} \cdot d\underline{A})\right] \tag{I.4}$$

where A_s is the illuminated surface area of the satellite. For satellites with uniform reflectivity, equation (I.4) can be simplified to a form such that the acceleration magnitude due to direct solar pressure is

$$\ddot{r}_{direct} = F_d/m = K(I_s/c)\ (A/m), \qquad (I.5)$$

where K is a parameter dependent upon the shape of the satellite, its reflectivity coefficient, and its mode of reflection (diffuse on specular), A is the cross sectional area as seen by the radiation source, and m is the mass of the satellite.

The constant c is known very accurately, but I_s, which has a nominal value of 1.94 cal/(cm^2 - min),* may vary by as much as 1.5% due to solar activity.[13,17] Furthermore, the varying solar distance throughout the year causes the irradiation to change by as much as 3.5% from the mean. This latter phenomenon can be corrected for by expressing the solar constant as

$$I_s = (R_{es}/r_{es})^2 I_{nom} \qquad (I.6)$$

where R_{es} is the mean earth-sun distance, r_{es} is the actual earth-sun distance and I_{nom} is 1.94 cal/(cm^2-min). This leaves K(A/m), which can be considered a (partially) unknown parameter. The accuracy to which it can be determined is highly dependent upon the accuracy to which K can be determined by optical means.

For non-spherical satellites, the problem is considerably more complicated. This is principally a result of a different

---

* A calorie is referenced often as a gram-calorie.

cross-section area A being illuminated at each instant of time. This arises not only because of the earth's revolution about the sun, but also because of satellite tumbling. For the purposes of the present report, only spherical satellites will be considered.

B. DIRECT RADIATION FORCES ON A SPHERE

1. Specular Reflection

Consider a spherical satellite of radius R_s which reflects in a pure specular manner all light it does not absorb, having a uniform reflectivity coefficient k_s. The incident radiation pressure $\underline{p}$, having magnitude p and direction $\hat{i}_{ss}$, can be taken to approach the satellite in the coordinate triad $(\hat{i},\hat{j},\hat{k})$ shown in Figure 5 such that $\hat{i}_{ss} = -\hat{i}$. The angle ψ_n is defined as the angle that $\underline{p}$ makes with any differential element of surface area $d\underline{A}$, which has magnitude dA and outward normal $\hat{i}_A$. By the definition of specular reflection, the luminous flux leaving the surface element also makes an angle ψ_n with the normal in accordance with Snell's Law, and has an irradiance $I_r = k_s I_s$.

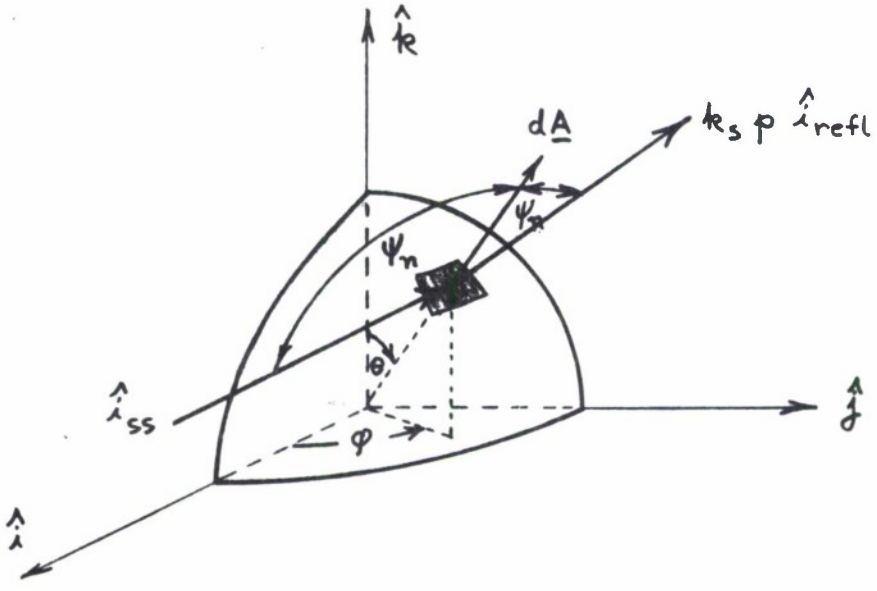

FIGURE 5. SPECULAR REFLECTION FROM A SPHERICAL SATELLITE

In spherical coordinates,

$$dA = R_s^2 \sin\theta \, d\theta \, d\phi,$$

$$\hat{i}_A = (\sin\theta \cos\phi)\,\hat{i} + (\sin\theta \sin\ )\,\hat{j} + (\cos\theta)\,\hat{k},$$

$$\hat{i}_{refl} = (2\sin^2\theta\cos^2\phi - 1)\,\hat{i} + 2(\sin^2\theta \sin\phi\cos\phi)\,\hat{j} + 2(\sin\theta\cos\theta\cos\phi)\,\hat{k}. \qquad (I.7)$$

The last unit vector can be computed by noting that $\hat{i}$, $\hat{i}_A$, and $\hat{i}_{refl}$ are necessarily co-planar and by working with the simple sketch in Figure 6, below.

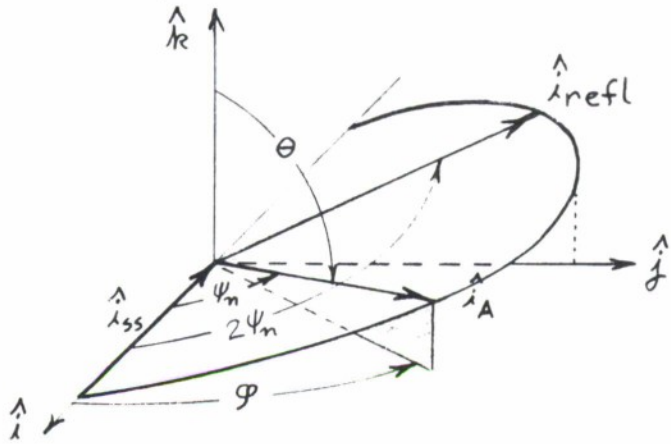

FIGURE 6. GEOMETRY FOR DIRECTION COSINES OF $\hat{i}_{refl}$.

Once the relations in (A.7) are used to obtain

$$\hat{i}_{refl} \cdot d\underline{A} = R_s^2 \sin^2\theta \cos\phi \, d\theta \, d\phi,$$

equation (I.4) can be evaluated over the illuminated surface, the hemisphere defined by $0 \le \theta \le \pi$ and $-(\pi/2) \le \phi \le (\pi/2)$, to yield

$$\underline{F}_d = -\hat{i}\,(I_s/c)\,R_s^2 \int_0^{\pi} \int_{-\pi/2}^{\pi/2} \left[\sin^2\theta\cos\phi - k_s(2\sin^4\theta\cos^3\phi - \sin^2\theta\cos\phi)\right] d\phi\, d\theta + \hat{j}\,\mathrm{Odd}(\phi) + \hat{k}\,\mathrm{Odd}(\theta),$$

where Odd (ϕ) is the integral of an odd function of ϕ , $\sin\phi \cdot \cos^2\phi$, over the range $-\pi/2$ to $\pi/2$, and Odd (θ) is the integral of a function of θ, $\sin^3\theta \cos\theta$, which is odd over the range 0 to π. Hence

$$\text{Odd } (\phi) = \text{Odd } (\theta) = 0,$$

and the net force is in the $-\hat{i}$ direction. Moreover, the factor multiplying k in the first integral is clearly odd over the interval $-\pi/2 \leq \phi \leq \pi/2$. Hence if $\underline{F}_d$ is divided by the mass m, and the final integration performed,

$$\boxed{\ddot{\underline{r}}_{direct} = \hat{i}_{ss} \, (I_s/c) \, (A/m),} \qquad \text{(I.8)}$$

where $A = \pi R_s^2$. Note that the constant K introduced in (I.5) is 1.0, independent of the reflectivity k_s for this pure specular case of a spherical satellite.

2. Diffuse Reflection

Consider a spherical satellite having uniform reflectivity k_d which reflects in a pure diffuse manner all light it does not absorb. The net differential forces $d\underline{F}_{refl}$ are normal to each incremental illuminated area dA, i.e., in the direction $\hat{i}_A$, and the reflection obeys Lambert's Law. The magnitude of $d\underline{F}_{refl}$ can be determined by centering a hemispherical "cake cover" of unity radius over dA, as suggested in Figure 7, below, and by noting that the total luminous flux (power) P passing through the cake cover is all that dA emits: it is k_d times the flux incident on dA. That is, if I (Ψ) is defined as the irradiance in the direction of $d\underline{S}$ due to reflection from dA,

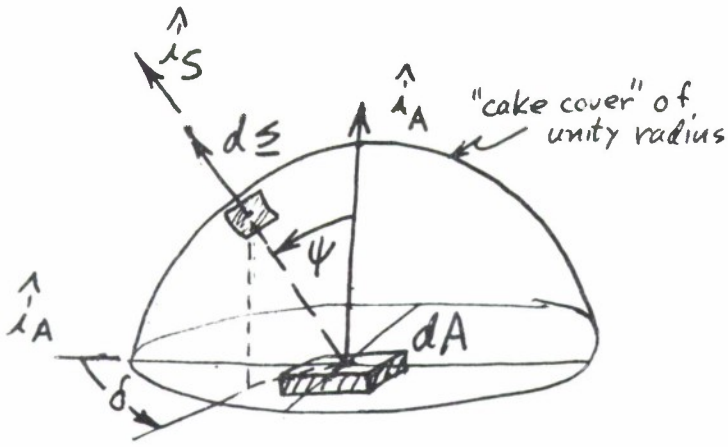

FIGURE 7. DETERMINATION OF NET PRESSURE NORMAL TO INCREMENTAL SURFACE AREA DUE TO DIFFUSE REFLECTION

$$P = k_d I_s (\hat{i}_{ss} \cdot d\underline{A}) = \int_{\text{cake cover}} I(\psi)\, dS. \qquad (I.9)$$

Denoting the irradiance normal to dA by I_A, Lambert's Law provides for diffuse reflection

$$I(\psi) = I_A \cos\psi . \qquad (I.10)$$

Putting this into the integral in (I.9), noting that $dS = (\sin\psi)\, d\psi\, d\delta$, and integrating over the range $0 \leq \delta \leq 2\pi$, we find that

$$I_A = -(1/\pi)\, k_d I_s (\hat{i}_{ss} \cdot d\underline{A}). \qquad (I.11)$$

The pressure on the cake cover due to the light reflected from dA is clearly

$$\underline{p}_{refl}(\psi) = (1/c)\, I(\psi)\, \hat{i}_S, \qquad (I.12)$$

of which only the component normal to dA produces a reaction force on dA:

$$d\underline{F}_{refl} = -\hat{i}_A (\hat{i}_A \cdot \int_{\text{cake cover}} \underline{p}_{refl}(\psi)\, dS).$$

From (I.10), (I.11), and (I.12), this becomes

$$d\underline{F}_{refl} = \hat{i}_A \, (2/3) \, (k_d I_s/c) \, (\hat{i}_{ss} \cdot d\underline{A}). \tag{I.13}$$

Hence, in (I.3),

$$I_r = (2/3) \, k_d I_s \, (\hat{i}_{ss} \cdot \hat{i}_A). \tag{I.14}$$

Using (I.7) and the convenience $\hat{i}_{ss} = -\hat{k}$, which is the unit vector in the minus vertical direction, (I.13) can be integrated over $0 \leq \Theta \leq \pi/2$ and $0 \leq \emptyset \leq 2\pi$ to provide

$$\underline{F}_{refl} = \hat{i}_{ss} \, (2/3) \, (k_d I_s/c) R_s^2 \int_0^{2\pi} \int_0^{\pi/2} \cos^2 \Theta \sin \Theta \, d\Theta \, d\emptyset$$

$$= \hat{i}_{ss} \, (4/9) \, (k_d I_s/c) \, \pi R_s^2 \tag{I.15}$$

Added to $\underline{F}_{in} = \underline{F}_d$, which is still valid, and then dividing by m,

$$\boxed{\ddot{\underline{r}}_{direct} = \hat{i}_{ss} \left[1 + k_d(4/9) \right] (I_s/c) \, (A/m),} \tag{I.16}$$

so that in this pure diffuse case the K introduced in (I.5) is dependent upon the reflectivity constant and assumes a maximum of 1.44.

C. SHADOW REGIONS

The above equations depend upon the direct solar radiation pressure, which is directly proportional to the free-space solar radiation pressure in full sunlight, some fraction thereof in the penumbra, and zero in the umbra.

In this section it will be shown that the penumbral region can be neglected and the umbral regions boundary can be expressed as the simple relationship

$$r \, |\sin \alpha| = R, \; (\pi/2) \leq \alpha \leq 3\pi/2$$

where r is the geocentric distance to the satellite, α is the geocentric angle between the sun and the satellite and R is the radius of the earth. The use of this approximation results in errors of less than 0.3 percent for orbits within 2000 miles of the earth.

Specifically, it suffices to assume that the sun and earth are perfect spheres and the satellite a point. The geometry then appears as in Figure 7, below,

R_{sun} = radius of the sun, 432×10^3 miles,

R = radius of the earth, 3.964×10^3 miles,

r_{es} = distance from sun to earth, having a mean R_{es} of 93×10^6 miles, a perihelion of 91.6×10^6 miles, and an aphelion of 94.7×10^6 miles,

r_c = radial height of the umbral cone measured from earth,

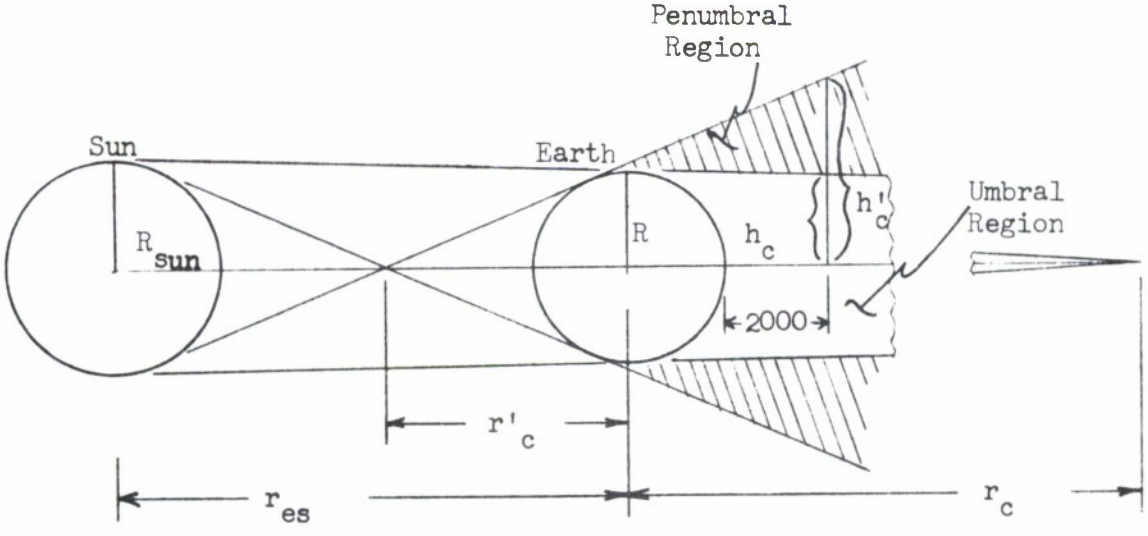

FIGURE 8

r_c' = radial distance to the apex of the penumbral cone as measured from earth.

By similar triangles,

$$r_c = R\, r_{es}/(R_{sun} - R)$$

$$= \text{a mean of } 860{,}000 \text{ miles and } 850{,}000 \leq r_c \leq 878{,}000 \text{ miles.}$$

Let the satellite be restricted to within 2000 miles of the earth. Consider the vertical line marked h_c in Figure 8 to cross the sun-earth line at a distance of 2000 miles from the earth's surface. The ratio of h_c to R is clearly

$$h_c/R = (r_c - R - 2000)/r_c$$

$$\geq 0.993.$$

Therefore, for all orbits within 2000 miles of the earth, the umbral region can be represented by boundaries parallel to the earth-sun line with an error of less than 0.7 percent.

For the penumbral region, similar calculations yield

$$r'_c \geq 845{,}000 \text{ miles,}$$

and

$$h'_c = (r'_c + R + 2000)/r'_c \leq 1.007.$$

Hence, for a satellite orbit in an earth-sun plane, the penumbra will be less than 0.7 percent larger than a cylindrical shadow.

The use of a cylindrical umbral region with no penumbral region at all involves the shrinking of the region of partial shadow and expanding the region of total shadow. Except in certain somewhat pathological cases, these changes will tend to cancel each other for

near-earth orbits. A rule-of-thumb estimate indicates that the maximum error in solar pressure due to the approximation will be on the order of 0.3 percent on any single pass, with the effect averaging to trivial proportions on multiple passes. In any event, the errors due to the assumption of only a cylindrical umbral region will be negligible in comparison with the uncertainties in solar intensity, in refraction of the shadow boundaries, and with similar ignorances of the physical situation.

To compute when the satellite is within these simplified boundaries is just a matter of analyzing the geometry of Figure 9: the satellite is in complete shadow if

$$|\sin \alpha| \leq R/r, \qquad (\pi/2) \leq \alpha \leq 3\pi/2, \tag{I.17}$$

and in full sunlight otherwise. An alternative expression avoids

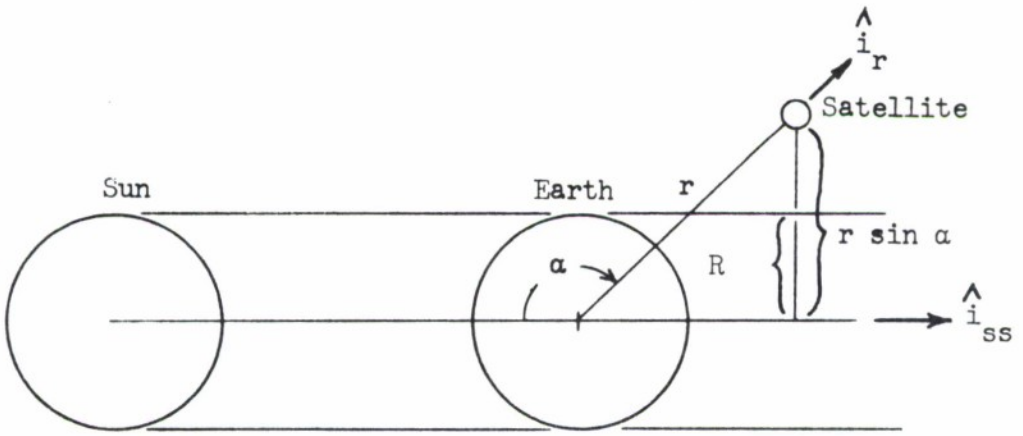

FIGURE 9

the computation of α from inverse trigonometric functions. Here (A.17) appears as

complete shadow: $|\sin \alpha| \leq R/r$ and $\cos \alpha \leq 0$,

full sunlight: otherwise. (I.17')

The cos α can be determined in terms of the ecliptic coordinates of the sun and the instantaneous orbital elements:

$$\cos \alpha = -\hat{i}_{ss} \cdot \hat{i}_r$$

$$= (\cos \lambda_e) \quad x/r$$

$$+(\sin \lambda_e)(\cos i_e) \quad y/r$$

$$+(\sin \lambda_e)(\sin i_e) \quad z/r$$

where λ_e = celestial longitude of the sun (measured in the ecliptic plane from the vernal equinox),

i_e = obliquity.

Sin α then follows from

$$\sin \alpha = (1 - \cos^2 \alpha)^{(1/2)} .$$

Musen[26] obtains expressions for the long-term effects of solar radiation pressure by neglecting shorter-term effects such as those due to the shadow. By examining long-term effects only, he is able to estimate such things as satellite lifetimes. However, these approximate methods are not applicable to observations on only a few periods.

D. REFLECTION AND RE-RADIATION

Terrestial radiation or "earth shine" pressure also exists. Of the total insolation, an average of 36 percent is reflected or back-scattered and 64 percent is absorbed and re-radiated thermally.[15] Reflection and back-scattering varies between 15 percent for a clear sky and 55 percent for an overcast sky. That which is absorbed and re-radiated as heat is primarily counter to the central-force acceleration of gravity and virtually uniform over the surface of the earth. Since this cannot exceed 10^{-4}g

for the satellite and orbit types specified under this contract, where g is the acceleration of gravity, it is doubtful that this radial component could ever be identifiable in a satellite orbit.

Hence thermal re-radiation will be neglected and only reflection and back-scattering will be examined. These two reflections have the alternative nomenclature "specular" (mirror-like) reflection and "diffuse" reflection. Of the two, diffuse reflection by far comprises the major form of "earth shine."

1. Earth Shine Theory

Consider a spherical earth illuminated by the sun. The fireball on the earth's surface can be neglected because of its small contribution to the total reflected irradiance at satellite altitudes (viz. pictures of the sunlit earth published by NASA which were taken by its Applications Technology Satellite (ATS)). Since the fireball is the manifestation of the specular part of the reflection, its negligibility permits the assumption that the earth is a perfect diffuse reflector.

Much of the analysis performed earlier in this appendix therefore applies. Instead of applying Lambert's Law to the satellite, however, we now apply it to the earth.

Examine Figure 10, below, where for convenience we have positioned the satellite along the $\hat{k}$ unit vector in the coordinate triad $(\hat{i}, \hat{j}, \hat{k})$, and the sun has been put along the $\hat{i}_{ss}$ unit vector in the $(\hat{i}, \hat{k})$ plane. We maintain the convention that the earth-sun angle α lies between 0 and π. The unit vector $\hat{i}_A$ is the outward normal from any infinitesimal

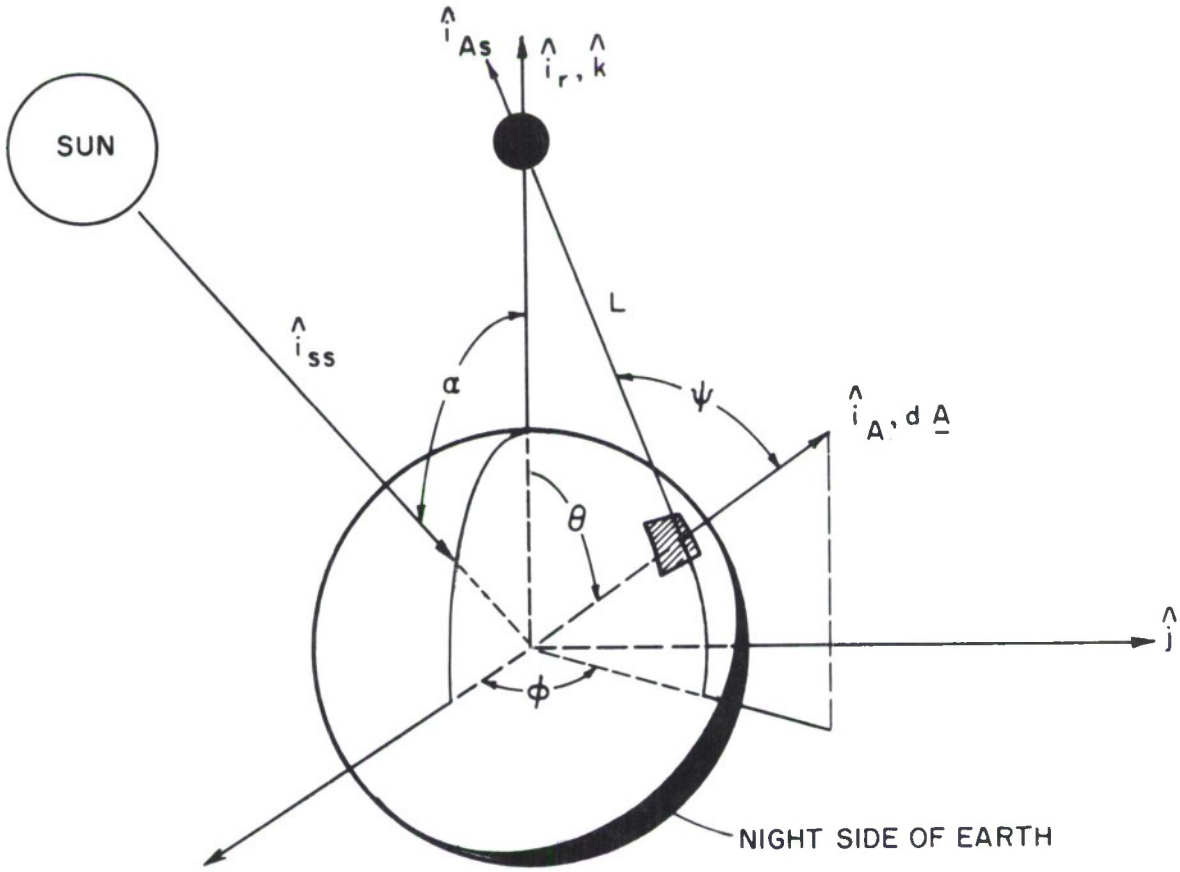

FIGURE 10. GEOMETRY FOR DIFFUSE EARTH SHINE

THIS PAGE INTENTIONALLY LEFT

BLANK

element of area dA on the earth's surface, L is distance between the element dA and the satellite, $\hat{i}_{As}$ is the element-to-satellite unit vector, and ψ is the interior angle between $\hat{i}_A$ and $\hat{i}_{As}$.

Clearly,

$$\hat{i}_r = \hat{k} ,$$
$$\hat{i}_{ss} = -(\sin \alpha)\, \hat{i} - (\cos \alpha)\hat{k},$$
$$\hat{i}_A = (\sin \Theta \cos \emptyset)\hat{i} + (\sin \Theta \sin \emptyset)\hat{j} + (\cos \Theta)\hat{k},$$
$$dA = R^2 \sin \Theta \, d\Theta \, d\emptyset. \qquad (I.19)$$

With I_A defined as the component of irradiance normal to dA at dA, we employ an equation much like (I.11):

$$I_A = -(1/\pi)\, qI_s\, (\hat{i}_{ss} \cdot d\underline{A}), \qquad (I.20)$$

where q = earth's albedo, or (diffuse) reflectivity coefficient. From Lambert's Law, the component in the $\hat{i}_{As}$ direction will be $I_A \cos \psi$. At the satellite, a distance L away, the irradiance $I(\psi)$ due to dA will therefore be

$$I(\psi) = (I_A/L^2) \cos \psi . \qquad (I.21)$$

The distance L can be computed from the simple sketch given in Figure 11, below, where, by inspection,

$$a = r \cos \Theta - R,$$
$$b = r \sin \Theta ,$$
$$L = \sqrt{a^2 + b^2} = r\sqrt{1 + \lambda^2 - 2\lambda \cos \Theta} , \qquad (I.22)$$

where $\lambda = R/r$.

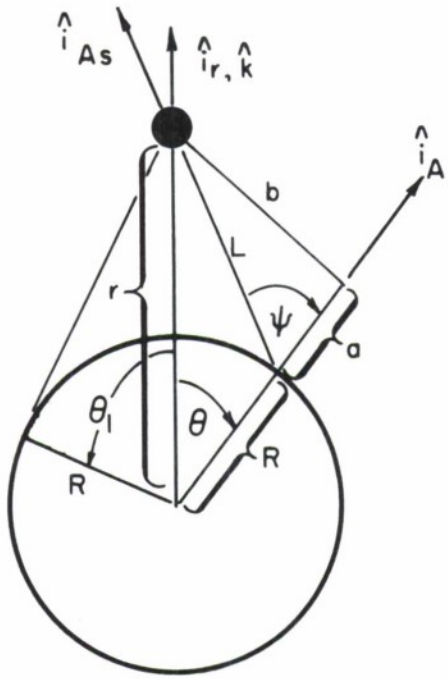

FIGURE 11. SKETCH FOR COMPUTING
SURFACE-TO-SATELLITE DISTANCE L.

Now we develop $\hat{i}_{As}$ by subtracting the geocentric vector to dA from the vector $\underline{r} = r\hat{k}$ and dividing by the distance L:

$$\hat{i}_{As} = \frac{-\lambda (\sin \phi \cos \phi)\, \hat{i} - \lambda (\sin \theta \sin \phi)\, \hat{j} + (1 - \lambda \cos \theta)\, \hat{k}}{\sqrt{1 + \lambda^2 - 2\lambda \cos \theta}} \quad . \tag{I.23}$$

Then, from (I.19),

$$\cos \psi = \hat{i}_A \cdot \hat{i}_{As} = \frac{\cos \theta - \lambda}{\sqrt{1 + \lambda^2 - 2\lambda \cos \theta}} \quad . \tag{I.24}$$

Because of the symmetry about the $(\hat{i}, \hat{k})$ plane, the solar pressure at the satellite's location due to dA has its component out of that plane

cancelled by another area element on the other side of the plane. The in-plane components are, of course, doubled in magnitude by that other area element. Hence, restricting ϕ to be between 0 and π, we find that the incremental pressure at the satellite due to the reflected light from dA is

$$d\underline{p}\,(\theta, \phi, \alpha) = 2\left[I(\psi)/c\right](\hat{i}_{As})_{i,k}, \qquad 0 \leq \phi \leq \pi \tag{I.25}$$

where $(\hat{i}_{As})_{i,k}$ = the projection of $\hat{i}_{As}$ on the $(\hat{i},\hat{k})$ plane.

For simplicity, now, let us normalize the solar pressure by removing the environmentally dependent quantity (qI_s/c). We define the residual expression as the differential illumination factor

$$d\underline{C}(\theta, \phi, \alpha) = d\underline{p}(\theta, \phi, \alpha)/(qI_s/c). \tag{I.26}$$

From (I.25), we find that

$$d\underline{C}(\theta,\phi,\alpha) = (2/\pi)\frac{\lambda^2(\cos\theta - \lambda)(\sin\theta)(\cos\alpha\cos\theta + \sin\alpha\sin\theta\cos\phi)}{(1 + \lambda^2 - 2\lambda\cos\theta)^2}$$

$$\cdot \left[-\lambda(\sin\theta\cos\phi)\,\hat{i} + (1 - \lambda\cos\theta)\,\hat{k}\right] d\theta\, d\phi,$$

which we can express more compactly as

$$d\underline{C}(\theta,\phi,\alpha) = (2\lambda^2/\pi)\left[\cos\alpha\,(I_1\hat{i}+I_2\hat{k}) + \sin\alpha\,(I_3\hat{i}+I_4\hat{k})\right] d\theta\, d\phi, \tag{I.27}$$

where

$$I_1 = \frac{\lambda\cos\theta\sin^2\theta\cos\phi\,(\cos\theta - \lambda)}{(\lambda^2 + 1 - 2\lambda\cos\theta)^2},$$

$$I_2 = \frac{\cos\theta\sin\theta\,(1 - \lambda\cos\theta)\,(\cos\theta - \lambda)}{(\lambda^2 + 1 - 2\lambda\cos\theta)^2},$$

$$I_3 = - \frac{\lambda \sin^3 \theta \cos^2 \phi \, (\cos \theta - \lambda)}{(\lambda^2 + 1 - 2\lambda \cos \theta)^2} \quad ,$$

$$I_4 = \frac{\sin^2 \theta \cos \phi \, (1 - \lambda \cos \theta) \, (\cos \theta - \lambda)}{(\lambda^2 + 1 - 2\lambda \cos \theta)^2} \quad .$$

The total earth-shine illumination factor is the integral of (I.27) taken over that part of the earth's sunlit surface that is visible to the satellite:

$$\underline{C}(\alpha) = \int_{\theta = \theta_o}^{\theta_1} \int_{\phi = 0}^{\phi_1} d\underline{C}(\theta, \phi, \alpha). \qquad \text{(I.28)}$$

The upper limit on θ is always

$$\theta_1 = \cos^{-1} (R/r) = \cos^{-1} \lambda, \qquad \text{(I.29)}$$

as is quickly discernible from Figure 11. The lower limit on θ and the upper limit on ϕ depend on the satellite-earth-sun geometry: i.e., on α and λ. The situation decomposes into four distinct cases.

Case A. The Satellite Sees an Earth which Is Entirely Sunlit

$(0 \leq \alpha \leq \pi/2 - \theta_1)$.

This is the only case that can be integrated analytically. Figure 10 indicates that $\theta_o = 0$, $\phi_1 = \pi$. Hence, from (I.28),

$$\underline{C}(\alpha) = \lambda \, (\hat{k} \, J_k \cos \alpha + \hat{i} \, J_i \sin \alpha) \quad , \qquad \text{(I.30)}$$

where

$$J_k = (2\lambda/\pi) \int_{\theta = 0}^{\theta_1} \int_{\phi = 0}^{\pi} I_2 d\phi \, d\theta = -(1/2)(B_1 + B_2 B_3 + k B_4),$$

$$J_i = (2\lambda/\pi) \int_{\theta=0}^{\theta_1} \int_{\phi=0}^{\pi} I_3 \, d\phi \, d\theta = (1/4) \left[B_1 - (\lambda+2k)(1-\lambda) + \right.$$
$$\left. + (3k^2+2k\lambda-1)B_3 - (k+\lambda)B_4 \right] ,$$

$$B_1 = (1-\lambda^2)/2$$

$$B_2 = 1-k^2$$

$$B_3 = \log\left[\frac{1+k}{\lambda+k}\right]$$

$$B_4 = B_2 \left[\frac{1}{1+k} - \frac{1}{\lambda+k}\right]$$

$$k = (\lambda^2+1)/(-2\lambda) \quad .$$

Case B. The Satellite Sees a Dark Region Which Covers Less Than Half the Visible Earth ($\pi/2 - \theta_1 \leq \alpha < \pi/2$).

We approximate the sun as a point source of light at infinity. Then the terminator (the line on the surface of the earth that separates night from day) is a great circle. The terminator intersects the horizon circle of the satellite at the two points A and B shown in Figure 12, below. If α is less than 90°, i.e., if less than half the visible cap is dark, as shown, then there will be a circle (circle 0 in the figure) which will be concentric with the horizon circle and tangent to the terminator at point C within which ϕ can range freely from 0 to π. The circle is at $\theta = \pi/2 - \alpha$.

For θ in the range $\theta_1 \geq \theta > \pi/2 - \alpha$, the range on ϕ will be a constrained function of α and θ, having upper limit

$$\phi_t = \cos^{-1}(-\cot \alpha \cot \theta). \qquad (I.31)$$

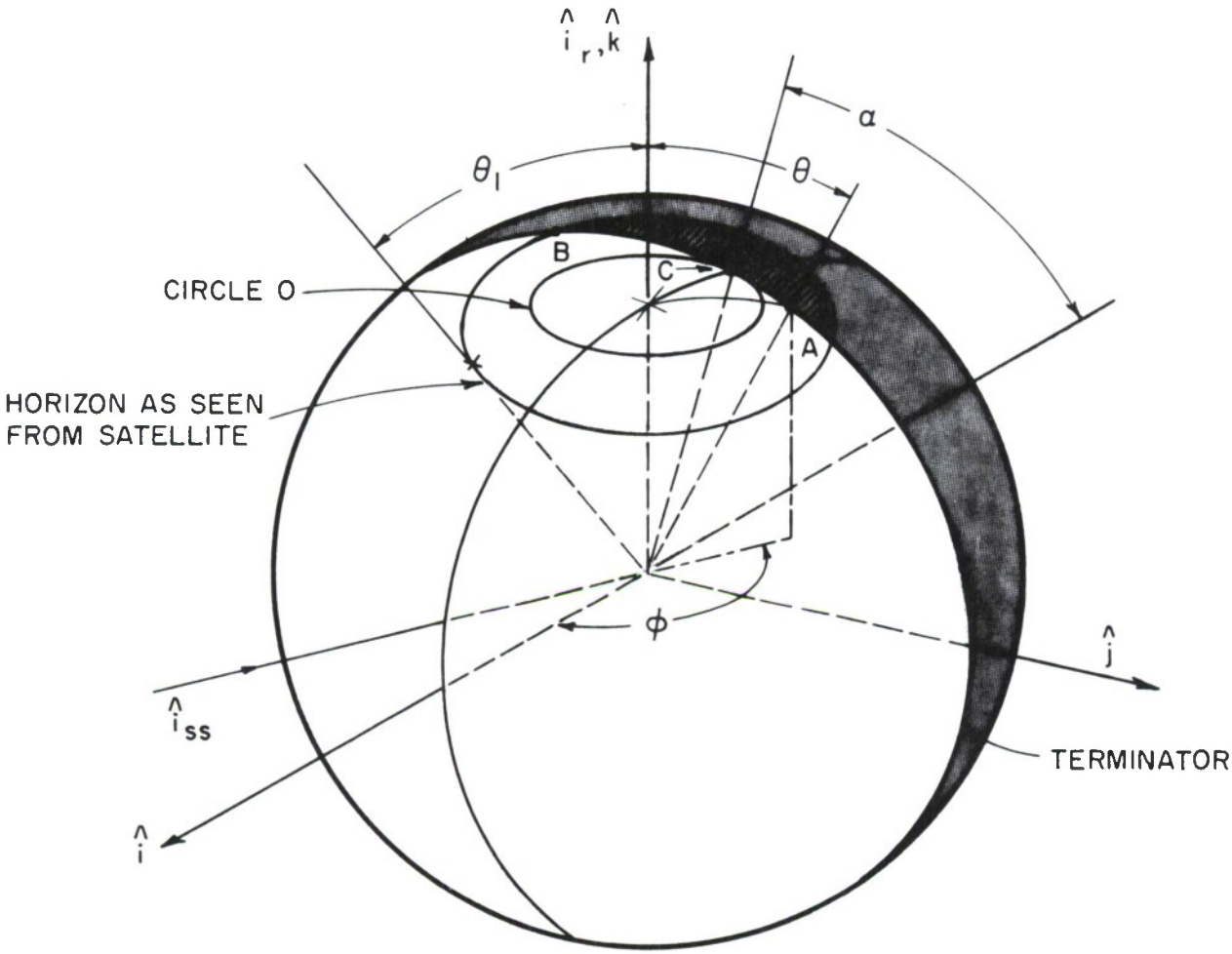
$\hat{i}_r, \hat{k}$
α
θ_1
θ
B
C
CIRCLE O
A
HORIZON AS SEEN
FROM SATELLITE
ϕ
$\hat{j}$
$\hat{i}_{ss}$
TERMINATOR
$\hat{i}$

FIGURE 12.

This derives from Figure 13, below, wherein the following relations apply:

$$c = R \sin \Theta \sin \phi,$$

$$d = R\sqrt{1 - c^2} = R\sqrt{1 - \sin^2 \Theta \sin^2 \phi},$$

$$e = d \cos \alpha = R\sqrt{1 - \sin^2 \Theta \sin^2 \phi}\cos \alpha.$$

The length e can also be obtained as

$$e = - R \sin \Theta \cos \phi.$$

Equating the two versions of e, we obtain (I.31).

Now (I.28) becomes

$$\underline{C}(\alpha) = (2\lambda^2/\pi)\left[\hat{k} \cos \alpha \int_{\Theta=0}^{\pi/2-\alpha} \int_{\phi=0}^{\pi} I_2 d\phi d\Theta + \hat{i} \sin \alpha \int_{\Theta=0}^{\pi/2-\alpha} \int_{\phi=0}^{\pi} I_3 d\phi d\Theta + \right.$$

$$+ \cos \alpha \int_{\pi/2-\alpha}^{\Theta_1} \int_{0}^{\phi_t} (\hat{i} I_1 + \hat{k} I_2)\, d\phi d\Theta +$$

$$\left. + \sin \alpha \int_{\pi/2-\alpha}^{\Theta_1} \int_{0}^{\phi_t} (\hat{i} I_3 + \hat{k} I_4)\, d\phi d\Theta \right] \qquad (I.32)$$

Case C. The Satellite Sees a Dark Region Which Covers More Than Half the Visible Earth $(\pi/2 \leq \alpha < \pi/2 + \Theta_1)$.

We refer again to Figure 12, except that now the terminator lies on the other side of the $\hat{k}$ axis (overhanging the positive $\hat{i}$ axis). No Circle O now exists within which ϕ has an unconstrained range between 0 and π. Hence

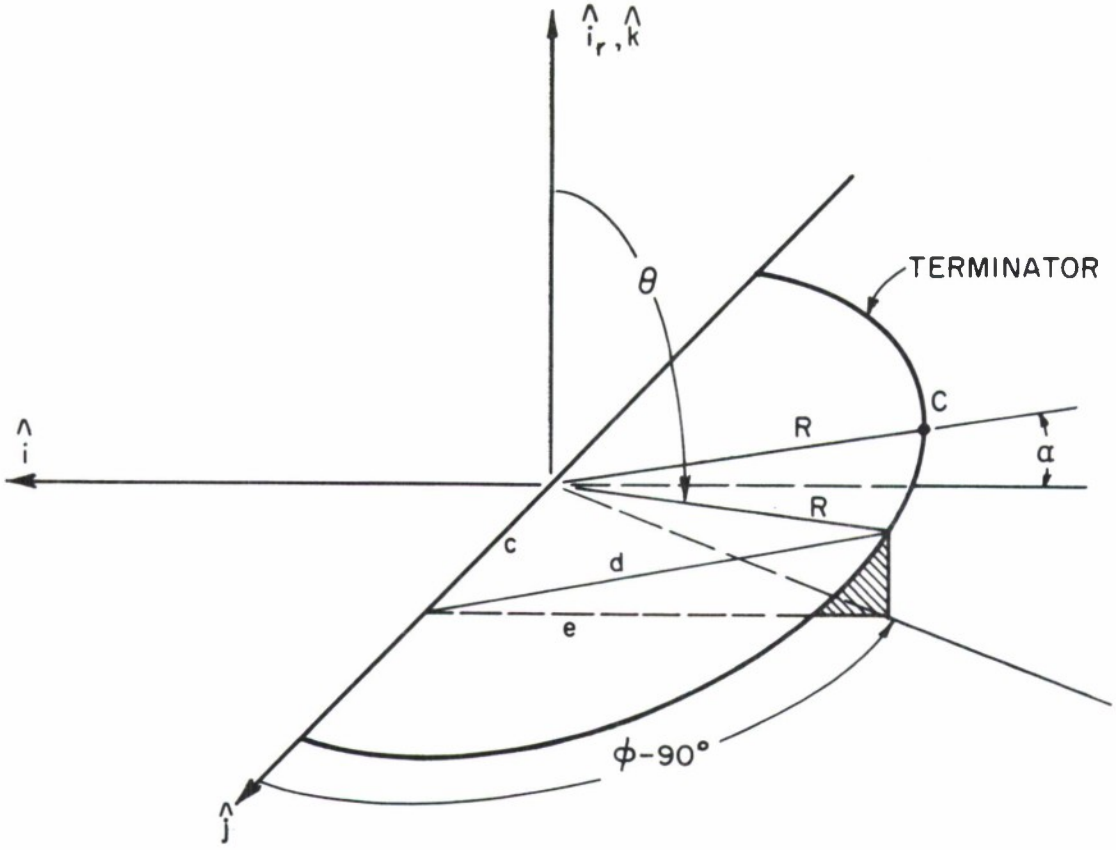

FIGURE 13.

$$\underline{C}(\alpha) = (2\lambda^2/\pi) \left[\cos\alpha \int_{\alpha-\pi/2}^{\Theta_1} \int_0^{\phi_t} (\hat{i}\, I_1 + \hat{k} I_2)\, d\phi d\Theta \right.$$

$$\left. + \sin\alpha \int_{\alpha-\pi/2}^{\Theta_1} \int_0^{\phi_t} (\hat{i} I_3 + \hat{k} I_4)\, d\phi d\Theta \right] \qquad (I.33)$$

Case D. The Satellite Sees a Completely Dark Earth ($\pi/2+\Theta_1 \leq \alpha \leq \pi$).

No earth shine, hence $\underline{C}(\alpha) \equiv 0$. Note, also, that this corresponds to the satellite's being in the umbral region specified by the first line of (I.17'). Hence there is no solar pressure whatsoever.

2. Earth Shine Calculations

The evaluation of (I.31) and the numerical integration of (I.32) and (I.33) yield the magnitude and angle curves of Figure 14, below. The vertical slash on the right end of each curve denotes the value $\alpha = \pi/2 + \theta_1$, where the satellite begins to see a wholly dark earth. Note that in the vicinity of α equals 80° or 90°, the magnitude curves cross. That is, the illumination for large-enough sun-satellite angles is not a monotone decreasing function of altitude. This contradicts Dennison's[29] interpretation of his previously published results, which were somewhat more complicated than those of Figure 14 and provided no angle information.

That our results are qualitatively correct is clear if we consider the following thought experiment. Put a satellite just off the surface of the earth at, say, $\alpha = 91^\circ$. It is in complete dark, and hence $\underline{C}(\alpha) = 0$. Somewhat higher, at a 100 km altitude, the satellite sees a good patch of sunlit earth, and so $\underline{C}(\alpha) \neq 0$. But most of what it can see is dim due to the glancing incidence of the sun's rays. As it goes yet higher, it sees more and more of the directly lit earth, and so $||\underline{C}(\alpha)||$ keeps increasing for a while. Eventually, however, the $(R/r)^2$ dependence of the received illumination begins to take effect, and $||\underline{C}(\alpha)||$ begins to drop with further increases in altitude. Hence the illumination for

FIGURE 14. MAGNITUDE AND ANGLE PLOTS FOR EARTH-SHINE ILLUMINATION FACTOR AT SATELLITE.

large-enough α cannot be monotonic with altitude.

For purposes of digital computation, it is convenient to represent the curves of Figure 14 in an approximate analytic form. Since the direct solar radiation impinges in the direction $\hat{i}_{ss}$, the approximation will be resolved into $\hat{i}_{ss}$ and $\hat{i}_r$ components, as follows.

$$\underline{C}(\alpha) \approx q_1 \hat{i}_r + q_2 \hat{i}_{ss}, \tag{I.34}$$

where

$$q_1 = \begin{cases} \lambda\,(a_1 + a_2)\cos\alpha, & |\alpha| \le \pi/2 - \theta_1; \\ \lambda\, a_r, & \pi/2-\theta_1 \le |\alpha| \le \pi/2 + \theta_1; \\ 0, & \text{elsewhere;} \end{cases}$$

$$q_2 = \begin{cases} \lambda\, a_2, & |\alpha| \le \pi/2 - \theta_1; \\ \lambda\, a_{ss}, & \pi/2-\theta_1 \le |\alpha| \le \pi/2 + \theta_1; \\ 0, & \text{elsewhere;} \end{cases}$$

$$a_1 = (1/3)(-.0417 + .5431\,\lambda),$$

$$a_2 = (1/3)(.0444 - 3.17(\lambda-.77)^3 + .0045(\lambda-.77)\sin\left[14.3(\lambda-.77)\pi\right]),$$

$$a_{ss} = (a_2/2)\left[1 + s - s\,e^{sy\tau} - e^{-\tau}\,y(2+sy)\right],$$

$$a_r = \left\{a_{ss} + (a_1/2)\left[s+1 - s(1+sy)^d\right]\right\}\cos\alpha +$$

$$+ (1/6)\left\{\frac{\lambda^2\left[(1/\lambda - \sin\alpha)^3 + (\lambda - \sin\alpha)^3\right]}{(1 + \lambda^2 - 2\lambda\sin\alpha)^{3/2}} - \frac{(1-\lambda^2)^{3/2}}{\lambda}\right\}\sin\alpha,$$

$$\tau = -4 + 9.3\,\lambda,$$

$$y = (\alpha - \pi/2)/\theta_1,$$

$$s = \begin{cases} -1, & y \ge 0; \\ 1, & y < 0; \end{cases}$$

$$d = 3.7 + 59\,(\lambda-.77)^2.$$

Figures 15 and 16, below, provide a comparison of the approximate and exact values as decomposed into the $\hat{k}$ and $-\hat{i}$ (radial and cross-radial) components

$$C_k(\alpha) = q_1 - q_2 \cos \alpha,$$
$$-C_i(\alpha) = q_2 \sin \alpha.$$

E. FINAL RESULTS

A combination of all the details for a spherical satellite yields finally

$$\ddot{\underline{r}}_{solar} = \ddot{\underline{r}}_{direct} + (qI_s/c)\underline{C}(\alpha),$$
$$= u_3 \underline{\gamma}(\underline{x}, t), \qquad (I.35)$$

where

$u_3 = (1 + 4 k_d/\alpha)(I_{nom}/c)(A/m)$ is a solar "ballistic" coefficient,

$$\underline{\gamma}(\underline{x},t) = \begin{bmatrix} \gamma_1 \\ \gamma_2 \\ \gamma_3 \end{bmatrix} = (R_{es}/r_{es})^2(p_1\hat{i}_r + p_2\hat{i}_{ss}),$$

$p_1 = qq_1$,

$p_2 = qq_2$,

all other terms having been defined in the body of this appendix. Equation (3.6), in the main text of the report, summarizes all these details in a concise way.

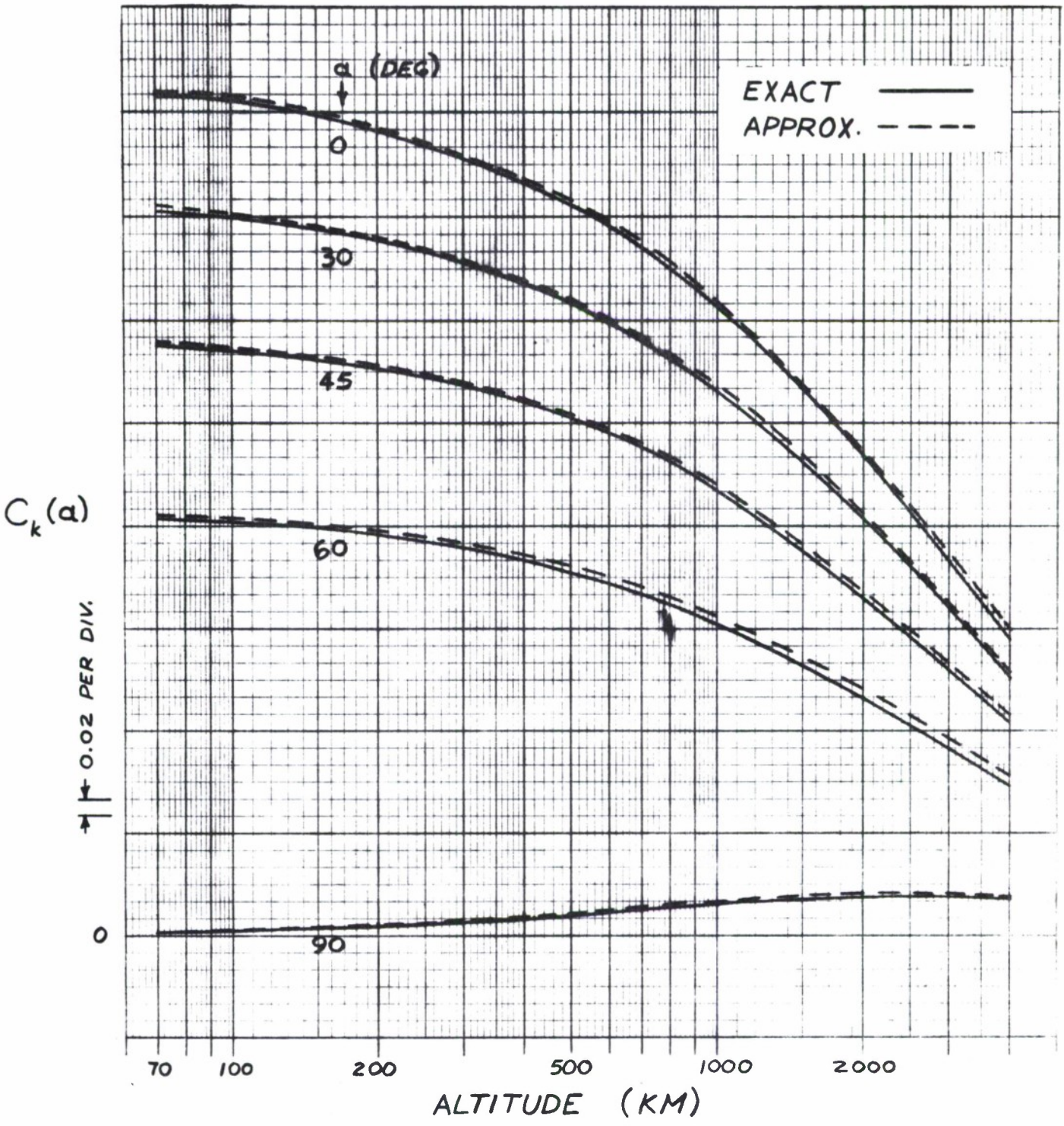

FIGURE 15. APPROXIMATE AND EXACT VALUES OF RADIAL EARTH-SHINE ILLUMINATION FACTOR

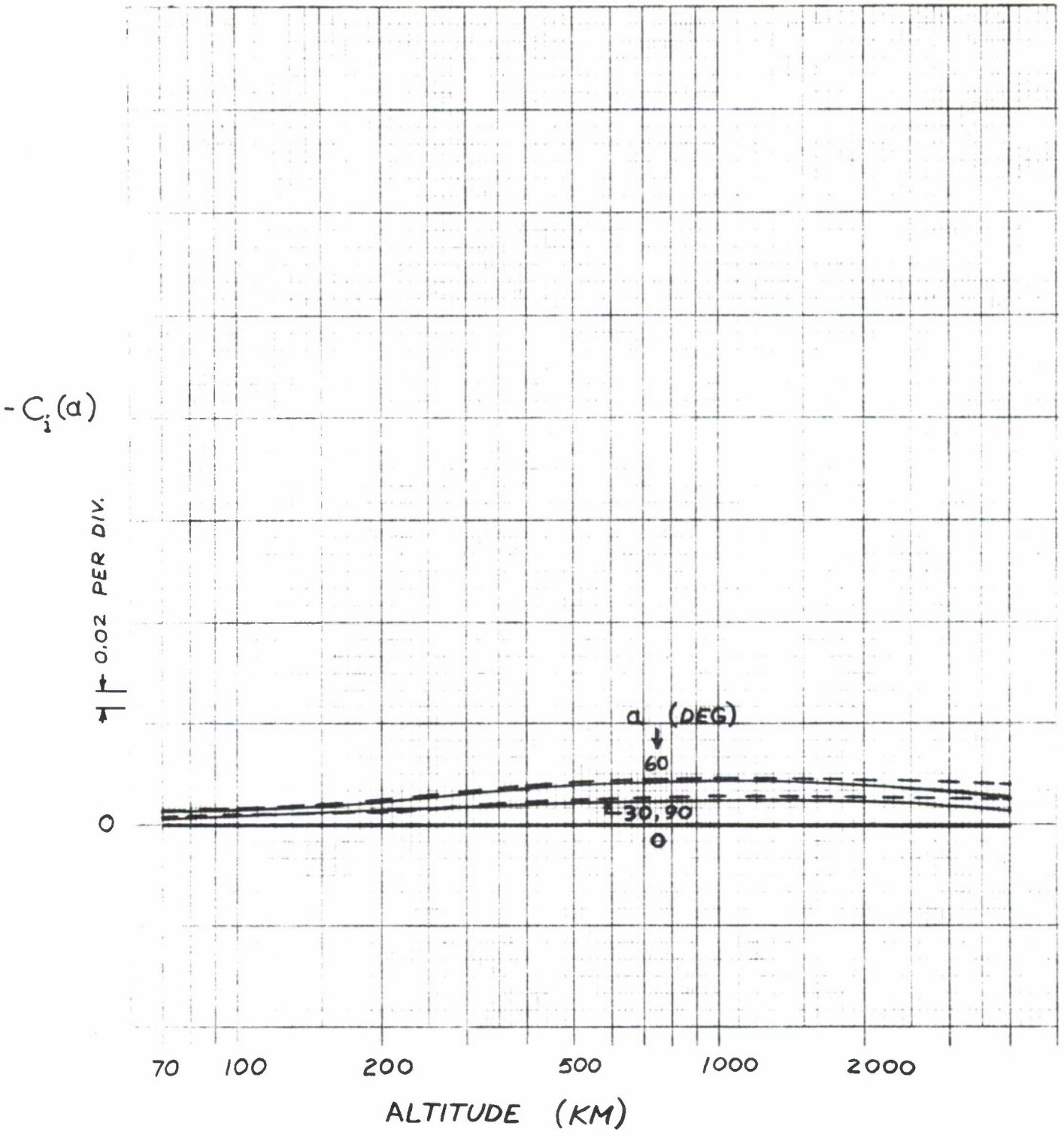

FIGURE 16. APPROXIMATE AND EXACT VALUES OF CROSS-RADIAL EARTH-SHINE ILLUMINATION FACTOR

F. CLOSING DISCUSSION

Mainly as a result of its effect on the orbit of Echo I, solar radiation is regarded as the most significant perturbative effect for orbits whose perigees exceed 1000 km. Large variations in the eccentricity and geocentric perigee distance for such orbits are almost wholly attributable to the effects of sunlight pressure.

Radiation pressure has no effect on the period if the orbit is circular. However, if the orbit is non-circular and is partly in shadow, the satellite can enter and leave the shadow region at different distances from the sun, resulting in a net gain or loss of energy from the radiation field. Even if the orbit does not pass through the earth's shadow, the radiation pressure has the effect of pushing the orbit "sideways," so that its effect on the perigee does not vanish even for circular orbits.

The force exerted on the satellite by direct solar radiation is known to within about 2% if K(A/m) is known perfectly. Therefore, the effect of the radiation is highly dependent upon the accuracy to which K, A, and m are known. The effect of thermal terrestial re-radiation has been neglected, since it is in the same direction as that of the principal gravitational term and its magnitude is negligible in comparison. A more exact analysis is available in Harvey[16] and Fitz, et. al[18]., although this accuracy is unnecessary.

APPENDIX II

ELECTROMAGNETIC AND ATMOSPHERIC DRAG ON SPHERICAL SATELLITES

DEFINITION OF SYMBOLS

q = satellite charge

e = electron charge -1.6065×10^{-19} coulombs

μ_o = permeability of free space $4\pi \times 10^{-7}$ (MKS units)

ϵ_o = permittivity of free space 8.85×10^{-12} (MKS units)

M = earth's magnetic dipole moment

R_s = satellite radius

r = satellite distance from earth's center

Q_s = satellite potential

v_s = satellite velocity

B = magnetic field strength

n = number of neutral particles per unit volume

n_i = number of ions per unit volume

m_i = ion mass

m_n = neutral particle mass

b_i = effective satellite radius

A. GENERAL

There are basically four types of forces, other than solar radiation and geopotential forces, which produce effects upon earth satellites. These four are all true drag forces. In order to determine their significance it is necessary to have a reasonable estimate of their magnitude.

B. ELECTROMOTIVE CHARGE DRAG

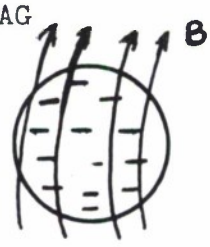

A satellite accumulates a charge q while moving through the ionosphere. Since the satellite moves through the earth's magnetic field, it experiences a force given by the basic equation governing the force on a charged particle moving in a magnetic field. According to Bechner[19], the magnitude of this force is

$$F_{mag} = \frac{q\mu_o M v_s}{2\pi r^3} \cos(\theta - 11.4^\circ) \qquad (II.1)$$

for a polar orbit with the ascending node at 70.1°. Here μ_o is the permeability of free space, M is the magnetic dipole moment of the earth, v_s is satellite velocity, r is satellite distance from the earth's center, and θ is the angle between the radial vector to the satellite and the earth's rotational axis.

In order to perform a sample computation cos (θ - 11.4°) will be assigned its maximum value of 1. The charge q is

$$q = 4\pi \epsilon_o R_s Q_s$$

where ϵ_o is permittivity of free space, R_s is satellite radius, and Q_s is the satellite potential. According to Brundin in Ref. 20, Q_s has a maximum negative potential in the neighborhood of 0.75V. For computational purposes Q_s will be assigned a value of -1.0V.

Assuming a spherical satellite of radius $R_s = 5.0$m at an altitude of 200 km,

$$q = 4\pi(8.85X10^{-12})(5)(1) \quad \text{coulombs}$$

$$v_s = 7.787X10^{3} \text{ m/sec}$$

$$\frac{\mu_o M}{4\pi} = 8.1X10^{15} \text{ weber-m}$$

$$r = 6.578X10^{6} \text{ m.}$$

The pressure is $F_{mag}/\pi R_s^2$ and equals $3.14X10^{-12} n/m^2$.

C. INDUCED DRAG

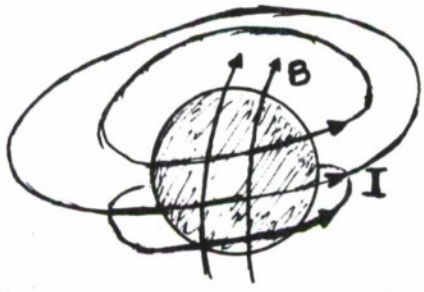

The motion of a conducting satellite in the earth's magnetic field will cause a current flow and, hence, a resultant force. This force has been treated by Brundin[20] and found to have a magnitude of

$$F_{ind} = -en_i v_s \pi R_s^3 B\left(1 - \frac{eBR_s}{m_i v_s}\right) \qquad \text{(II.2)}$$

below the hydrogen region, where the photoelectric emission has little

effect upon the effective current. At higher altitudes, the photoelectric emission current may produce forces one or two orders of magnitude higher than the force yielded by this equation. Because of the difficulties in predicting photoemission currents, only forces at lower altitudes ($\leq$ 800km) will be considered. For a more detailed discussion of photoemission current see Ref. 20.

Here,

e = electron charge

n_i*= number of ions per cubic meter = 3.857×10^{15} at 200km

R_s = 5 meters

B = magnetic field strength = $\dfrac{\mu_o M}{4\pi r^3}$

m_i = ion mass = 2.5×10^{-26} kg at 200km

The pressure at 200km is

$$F_{ind}/\pi R_s^2 = \left(\frac{(1.6065)(3.857)(5)(8.1)\times 10^{11}}{\pi(6.578)^3 \times 10^{18}}\right)\left(1-\frac{(1.6065)(8.1)(5)\times 10^{-4}}{(2.5)(7.787)(6.578)^3 \times 10^{-5}}\right)$$

$$= 2.44 \times 10^{-4} n/m^2$$

D. COULOMB DRAG

The term coulomb drag is given to that force caused by incident ions which hit the satellite because of the satellite's accumulated charge. This force is given by

$$F_{coul} = \pi m_i n_i v_s^2 (b_i^2 - R_s^2) \qquad \text{(II.3)}$$

where $b_i = R_s\left(1+\dfrac{2eQ_s}{m_i v_s^2}\right)^{\frac{1}{2}}$ is the effective radius according to Ref. 20.

* All data concerning atmospheric structure was obtained from Ref. 21, MODEL 10, HOUR 0.

This force will not be considered independently, as it is a component of atmospheric drag and will be treated as such.

E. ATMOSPHERIC DRAG

Atmospheric drag is produced by the collision of satellite and air particles. It therefore includes the aforementioned coulomb drag. It may be instructive to consider the atmospheric drag on nonconducting as well as conducting satellites, thereby obtaining some appreciation of the coulomb drag effect.

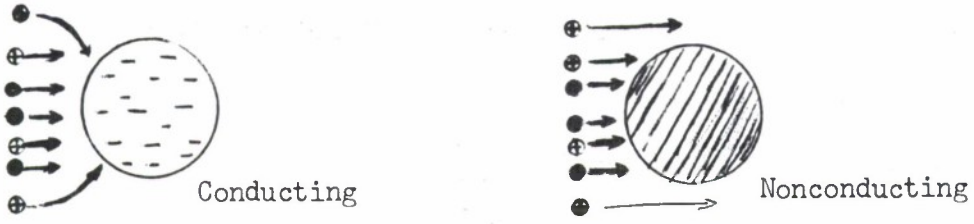

(a) Atmospheric drag on a conducting satellite

$$F_{atm} = F_n + F_i$$

where F_n is drag due to neutral particles and F_i is due to incident ions.

If n is the number of neutral particles encountered per unit volume,

$$F_n = \pi R_s^2 m_n n v_s^2 \qquad \text{(II.4)}$$

$$F_i = \pi b_i^2 m_i n_i v_s^2$$

$$= \pi R_s^2 \left(1 + \frac{2eQ_s}{m_i v_s^2}\right) m_i n_i v_s^2 \qquad \text{(II.5)}$$

Hence,

$$F_i = \frac{m_i n_i}{m_n n} \left(1 + \frac{2eQ_s}{m_i v_s^2}\right) F_n \qquad \text{(II.6)}$$

and

$$F_{atm} = \left\{1+ \frac{m_i n_i}{m_n n}\left(1+\frac{2eQ_s}{m_i v_s^2}\right)\right\} F_n \qquad \text{(II.7)}$$

This yields a reasonable upper bound of

$$F_{atm} = \left(1 + 0.625 \frac{n_i}{n}\right) F_n \qquad \text{(II.8)}$$

since $m_i/m_n \lesssim 0.5$ and $\dfrac{2eQ_s}{m_i v_s^2}$ has a least upper bound of 0.25 in the region being considered.

$$P_n = F_n/\pi R_s^2$$

$$= m_n n v_s^2$$

where $v_s^2 = GM_e/r$. G is the gravitational constant and M_e is the earth's mass. $(GM_e = 3.98866 \times 10^{14}\ m^3/sec^2)$

$$P_n = 1.624 \times 10^{-2}\ n/m^2 \text{ at } 200km$$

and

$$P = F/\pi R_s^2$$

$$= 2.26 \times 10^{-2}\ n/m^2$$

(b) Atmospheric drag on nonconducting satellite

The force equation for atmospheric drag on a nonconducting satellite is identical to that for a conducting satellite (II.7). In the case of the nonconductor, Q_s is zero and, therefore, the equation reduces to

$$F_{atm} = \left(1 + 0.5 \frac{n_i}{n}\right) F_n \qquad \text{(II.9}$$

Thus the ratio of nonconducting drag to conducting drag is

$$\frac{1 + 0.5 \frac{n_i}{n}}{1 + 0.625 \frac{n_i}{n}} \quad . \qquad \text{(II.10)}$$

F. RELATIVE MACNITUDES

The accompanying table and figure allow comparison of the four drag effects. In addition, the solar pressure due to the direct radiation of the sun is imposed on the figure for the cases of pure specular reflection and pure diffuse total reflection.

TABLE 1.

DRAG PRESSURES (n/m^2)

SPHERICAL SATELLITES

ALTITUDE (km)	AIR_1	AIR_2	INDUCED*	ELECTROMOTIVE CHARGE
200	$2.26X10^{-2}$	$2.14X10^{-2}$	$2.44X10^{-4}$	$3.14X10^{-12}$
300	$2.83X10^{-3}$	$2.54X10^{-3}$	$5.29X10^{-5}$	$2.98X10^{-12}$
500	$1.64X10^{-4}$	$1.36X10^{-4}$	$4.81X10^{-6}$	$2.68X10^{-12}$
800	$6.91X10^{-6}$	$5.54X10^{-6}$	$2.26X10^{-7}$	$2.31X10^{-12}$

Air_1 - Atmospheric drag on conducting satellite

Air_2 - Atmospheric drag on nonconducting satellite

* Helium considered to be charged particles

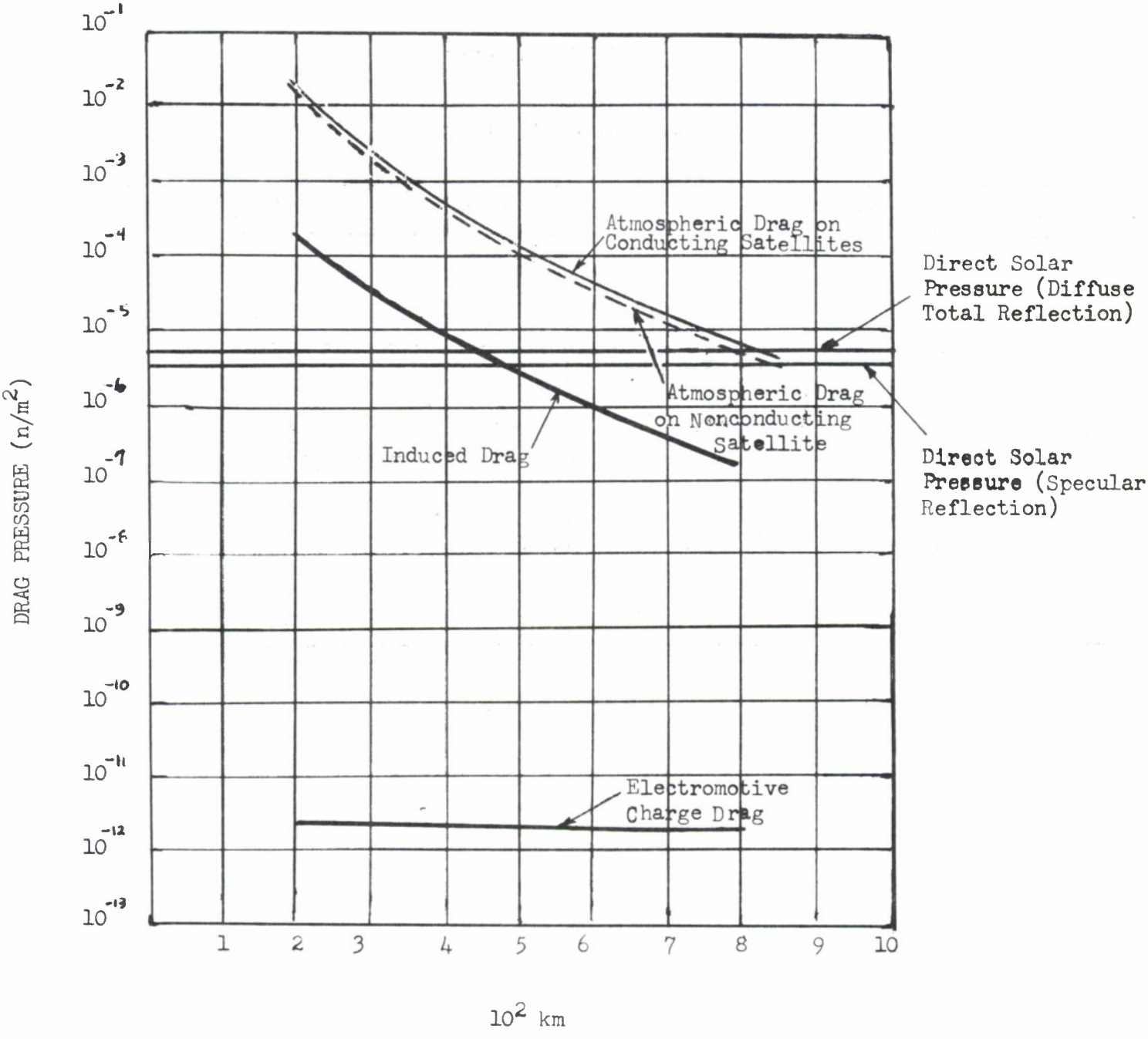

FIGURE 17. Drag Pressure Versus Altitude for Spherical Satellites

APPENDIX III

THE EARTH'S GEOPOTENTIAL FIELD

A. INTRODUCTION

The potential function $\phi(x)$ for the geopotential field of the earth can be written as an infinite series of associated Legendre polynomials. In truncated form, this may be expressed as

$$\phi(x) = \mu/r^2 + \phi_o(x), \tag{III.1}$$

where

$$\phi_o(x) = \sum_{n=2}^{N} \sum_{m=0}^{n} (C_{nm} U_n^m + S_{nm} V_n^m) \tag{III.2}$$

is the potential due to the oblateness (more generally, the asphericity) of the earth. The oblateness acceleration $\underline{F}_o(\underline{x},J)$ is the gradient of ϕ_o with respect to $\underline{r}$:

(III.3)

$$\underline{F}_o(\underline{x}) = T \sum_{n=2}^{N} \sum_{m=0}^{n} (C_{nm}\,\mathrm{grad}\, U_n^m + S_{nm}\,\mathrm{grad}\, V_n^m),$$

where T = the rotation transformation that takes the earth-fixed geocentric coordinate system (X^1, Y^1, Z^1), defined as the right-hand system with X^1 at Greenwich and Z^1 along the north-directed polar axis at time t, into the inertial geocentric coordinate system (X, Y, Z) defined in Figure 1,

C_{nm}, S_{nm} = the geopotential coefficients from (n, m) equal to (2, 2) upto (N, N) whose published values have constant but unknown biases on them,

$$\mathrm{grad} = \mathrm{column}\left(\frac{\partial}{\partial x^1}, \frac{\partial}{\partial y^1}, \frac{\partial}{\partial z^1}\right),$$

$$\begin{Bmatrix} U_n^m \\ V_n^m \end{Bmatrix} = (\mu/r)\,(R/r)^n\, P_n^m(\sin\beta) \begin{Bmatrix} \cos m\lambda \\ \sin m\lambda \end{Bmatrix},$$

where μ = earth's gravitational constant,

r = the geocentric distance to the satellite at time t,

R = earth's mean equatorial radius,

$P_n^m(\sin\beta)$ = associated Legendre polynomials, *

β, λ = satellite latitude and longitude, respectively, at time t.

The rotation matrix T consists of a precession and a nutation necessary to align the polar axis at time t with the polar axis at time 0^h January 1, and then a rotation around the polar axis to align the Greenwich meridians. (See Reference 4.)

The gradients in (III.3) are given by[27]

$$\text{grad } U_n^m = (1/R) \begin{bmatrix} \frac{1}{2} A_n^m U_{n+1}^{m-1} - \frac{1}{2} U_{n+1}^{m+1} \\ -\frac{1}{2} A_n^m V_{n+1}^{m-1} - \frac{1}{2} V_{n+1}^{m+1} \\ -(n-m+1)\, U_{n+1}^m \end{bmatrix},$$

*We use the definition

$$P_n^m(x) = \frac{1}{2^n n!}\,(1-x^2)^{m/2}\,\frac{d^{m+n}}{dx^{m+n}}\,(x^2-1)^n.$$

$$\text{grad } V_n^m = (1/R) \begin{bmatrix} \frac{1}{2} A_n^m V_{n+1}^{m-1} - \frac{1}{2} V_{n+1}^{m+1} \\ \frac{1}{2} A_n^m U_{n+1}^{m-1} + \frac{1}{2} U_{n+1}^{m+1} \\ -(n-m+1) V_{n+1}^m \end{bmatrix}, \qquad \text{(III.4)}$$

where $A_n^m = (n-m+1)(n-m+2)$.

Note that with the vector $\underline{J}$ defined to be the column array of geopotential coefficients

$$\underline{J} = \text{column } (C_{20}, C_{30}, \ldots C_{22}; C_{31}, \ldots, C_{33}; \ldots S_{22}; S_{31}, \ldots, S_{33}; \ldots), \qquad \text{(III.5)}$$

the sensitivity matrix $\frac{\partial \underline{F}_o}{\partial \underline{J}}$ can be written as

$$\frac{\partial \underline{F}_o}{\partial \underline{J}} = T \left[\text{gradU}_2^0, \text{gradU}_3^0, \ldots \text{gradU}_2^2; \text{grad } U_3^1 \ldots \right.$$
$$\left. \text{gradU}_3^3; \ldots \text{gradV}_2^2; \text{gradV}_3^1, \ldots, \text{gradV}_3^3; \ldots \right] \qquad \text{(III.6)}$$

The gradient - gradient of ϕ_o can also be found:[27]

$$\left[\frac{\partial^2 \phi_o}{\partial x_i \, \partial x_j} \right]_{i,j=1,2,3} = \frac{\partial \underline{F}_o}{\partial \underline{r}} = T \sum_{n=2}^{N} \sum_{m=0}^{N} (C_{nm} \text{ grad-grad } U_n^m + S_{nm} \text{ grad-grad } V_n^m) \, T^T, \qquad \text{(III.7)}$$

$$\text{grad-grad } U_n^m = \frac{1}{2R} \begin{bmatrix} A_n^m (\text{grad } U_{n+1}^{m-1})^T - (\text{grad } U_{n+1}^{m+1})^T \\ -A_n^m (\text{grad } V_{n+1}^{m-1})^T - (\text{grad } V_{n+1}^{m+1})^T \\ -2 (n-m+1) (\text{grad } U_{n+1}^m)^T \end{bmatrix}$$

$$\text{grad-grad } V_n^m = \frac{1}{2R}\begin{bmatrix} A_n^m \,(\text{grad } V_{n+1}^{m-1})^T - (\text{grad } V_{n+1}^{m+1})^T \\ A_n^m \,(\text{grad } U_{n+1}^{m-1})^T + (\text{grad } U_{n+1}^{m+1})^T \\ -2\,(n-m+1)\,(\text{grad } V_{n+1}^{m})^T \end{bmatrix} .$$

Note that both the gradient and gradient-gradient expressions require the negative-order expression for efficient computer calculation.

$$\begin{Bmatrix} U_n^{-m} \\ V_n^{-m} \end{Bmatrix} = (-1)^m \frac{(n-m)!}{(n+m)!} \begin{Bmatrix} U_n^m \\ -V_n^m \end{Bmatrix} \qquad \text{(III.8)}$$

Note, for purposes of numerical checks, that $\frac{\partial \underline{F}_o}{\partial \underline{r}}$ is clearly symmetric and, moreover, its diagonal elements are the Laplacian of ϕ_o and hence must vanish identically in free space:

$$\nabla^2 \phi_o = \frac{\partial^2 F_{ox}}{\partial x^2} + \frac{\partial^2 F_{oy}}{\partial y^2} + \frac{\partial^2 F_{oz}}{\partial z^2} \equiv 0. \qquad \text{(III.9)}$$

B. GEOPOTENTIAL MODEL COEFFICIENTS

The geopotential model to be used will be the essentially eighth-order model published at the 1966 COSPAR by Gaposchkin[23] and reproduced by Wackernagel.[24] It consists of Kozai's[22] thirteen zonal coefficients $C_{20} = -J_2$ to $C_{14,0} = -J_{14}$, plus the thirty-four pairs of tesseral coefficients (2,2), (3,1) to (3,3), ..., (8,1) to (8,8), plus the sixteen pairs of resonance terms (9,1), (9,2), (9,9), (10,1) to (10,4), (11,1), (12,1), (13,12), (13,13), (14,1), and (15,12) to (15,14). The unnormalized zonals are presented in Table 2 and the normalized tesserals are in Table 3.

The term "normalized" applies when the conventional spherical harmonics $P_n^m(x)$ are replaced with the fully normalized spherical harmonics

$$\bar{P}_n^m(x) = \sqrt{(n-m)!\ (2n+1)\ k/(n+m)!}\ \ P_n^m(x) = N(n,m)P_n^m(x) \tag{III.10}$$

where

$$k = \begin{cases} 1, & m = 0; \\ 2, & m \neq 0. \end{cases}$$

The coefficients C_{nm}, S_{nm} are then replaced with their normalized versions:

$$\bar{C}_{nm} = C_{nm}/N(n,m),$$

$$\bar{S}_{nm} = S_{nm}/N(n,m), \tag{III.11}$$

wherever the $\bar{P}_n^m(x)$ appear.

The geopotential-coefficient covariance matrix P_{JJ} is 113 x 113, although the majority of its elements are zero. Tables 4 and 6 present the standard deviations on the coefficients, and Tables 5 and 7 their correlation matrix. We were unable to fine the standard deviations for the (9,9) terms and therefore used the rule-of-thumb value 0.2×10^{-7} commonly applied to these normalized coefficients. This pair was determined from the special resonance properties of MIDAS, and hence are uncorrelated to any other coefficients.[23]

The coefficients form essentially three uncorrelated groups: the even zonals, the odd zonals, and the tesserals. The correlation matrix, therefore, is presented in three parts, one for each of these groups.

Because of its size, the tesseral correlation matrix is presented in thirty-one pages. The placement of these pages is keyed to the correlation-matrix map in Figure 18.

$J_2 = 1082.645 \times 10^{-6}$, $J_3 = -2.546 \times 10^{-6}$,

$J_4 = -1.649 \times 10^{-6}$, $J_5 = -0.210 \times 10^{-6}$,

$J_6 = 0.646 \times 10^{-6}$, $J_7 = -0.333 \times 10^{-6}$,

$J_8 = -0.270 \times 10^{-6}$, $J_9 = -0.053 \times 10^{-6}$,

$J_{10} = -0.054 \times 10^{-6}$, $J_{11} = 0.302 \times 10^{-6}$,

$J_{12} = -0.357 \times 10^{-6}$, $J_{13} = -0.114 \times 10^{-6}$,

$J_{14} = 0.179 \times 10^{-6}$.

Table 2. Unnormalized Zonal Coefficients

n	m	$\bar{C} \times 10^6$	$\bar{S} \times 10^6$	n	m	$\bar{C} \times 10^6$	$\bar{S} \times 10^6$
2	2	2.379	-1.351	7	7	0.055	0.096
3	1	1.936	0.266	8	1	-0.075	0.065
3	2	0.734	-0.538	8	2	0.026	0.039
3	3	0.561	1.620	8	3	-0.037	0.004
4	1	-0.572	-0.469	8	4	-0.212	-0.012
4	2	0.330	0.661	8	5	-0.053	0.118
4	3	0.851	-0.190	8	6	-0.017	0.318
4	4	-0.053	0.230	8	7	-0.0087	0.031
5	1	-0.079	-0.103	8	8	-0.248	0.102
5	2	0.631	-0.232	9	1	0.117	0.012
5	3	-0.520	0.007	9	2	-0.0040	0.035
5	4	-0.265	0.064	9	9	-0.065	0.0909
5	5	0.156	-0.592	10	1	0.105	-0.126
6	1	-0.047	-0.027	10	2	-0.105	-0.042
6	2	0.069	-0.366	10	3	-0.065	0.030
6	3	-0.054	0.031	10	4	-0.074	-0.111
6	4	-0.044	0.518	11	1	-0.053	0.015
6	5	-0.313	0.458	12	1	-0.163	-0.071
6	6	-0.040	-0.155	12	2	-0.103	-0.0051
7	1	0.197	0.156	13	12	-0.058	0.048
7	2	0.364	0.163	13	13	-0.075	0.010
7	3	0.250	0.018	14	1	-0.015	0.0053
7	4	-0.152	-0.102	15	12	-0.062	0.058
7	5	0.076	0.054	15	13	-0.063	-0.066
7	6	-0.209	0.063	15	14	0.0083	-0.0201

Table 3. Normalized Tesseral Coefficients

J2	6.0-09	J3	2.0-08
J4	1.6-08	J5	2.5-08
J6	3.0-08	J7	3.9-08
J8	5.0-08	J9	6.0-08
J10	5.0-08	J11	3.5-08
J12	4.7-08	J13	8.4-08
J14	6.3-08		

Table 4. Geopotential Coefficient Standard Deviations (Unormalized) - Zonal Coefficients

	J2	J4	J6	J8	J10	J12	J14
J2	1.00	-.60	.80	-.89	.79	-.71	.83
J4		1.00	-.86	.80	-.85	.91	-.47
J6			1.00	-.79	.96	-.88	.60
J8				1.00	-.80	.84	-.84
J10					1.00	-.80	.70
J12						1.00	-.50
J14							1.00

	J3	J5	J7	J9	J11	J13
J3	1.00	-.93	.98	-.94	.48	-.86
J5		1.00	-.96	.86	-.69	.75
J7			1.00	-.92	.57	-.82
J9				1.00	-.27	.97
J11					1.00	-.12
J13						1.00

Table 5. Geopotential Coefficient Correlation Matrix - Zonal Coefficients

C2,2	1.3760-08	C7,7	2.1940-08	S6,4	2.2400-08	C11,1	1.9730-08
C3,1	1.3450-08	C8,1	1.3480-08	S6,5	9.3780-09	C12,1	1.9920-08
C3,2	1.2510-08	C8,2	2.1790-08	S6,6	2.3950-08	C12,2	2.6770-08
C3,3	1.7730-08	C8,3	1.5460-08	S7,1	2.2610-08	C13,12	1.8590-08
C4,1	8.0960-09	C8,4	1.9410-08	S7,2	1.1270-08	C13,13	6.1730-09
C4,2	1.2420-08	C8,5	1.7550-08	S7,3	1.5940-08	C14,1	1.5730-08
C4,3	7.7960-09	C8,6	2.4750-08	S7,4	1.4790-08	C15,12	8.6970-09
C4,4	2.7300-08	C8,7	1.3290-08	S7,5	2.0930-08	C15,13	1.6880-09
C5,1	1.0810-08	C8,8	1.9890-08	S7,6	1.7450-08	C15,14	2.1210-10
C5,2	1.1790-08	S2,2	1.3810-08	S7,7	2.1230-08	S9,1	2.2440-08
C5,3	1.3880-08	S3,1	1.3840-08	S8,1	1.2120-08	S9,2	1.1590-08
C5,4	1.5160-08	S3,2	1.2310-08	S8,2	2.1450-08	S9,9	2.0000-08
C5,5	2.2200-08	S3,3	1.8590-08	S8,3	1.4100-08	S10,1	1.3210-08
C6,1	6.9180-09	S4,1	7.2110-09	S8,4	2.0920-08	S10,2	2.1850-08
C6,2	1.1530-08	S4,2	1.2320-08	S8,5	1.7180-08	S10,3	2.2270-08
C6,3	1.2820-08	S4,3	7.4480-09	S8,6	2.4240-08	S10,4	1.8740-08
C6,4	2.0470-08	S4,4	3.0320-08	S8,7	1.4780-08	S11,1	2.0230-08
C6,5	9.8010-09	S5,1	1.1390-08	S8,8	1.9400-08	S12,1	1.7500-08
C6,6	2.4480-08	S5,2	1.1200-08	C9,1	2.2540-08	S12,2	2.6340-08
C7,1	2.1140-08	S5,3	1.3810-08	C9,2	1.1510-08	S13,12	1.8630-08
C7,2	1.1730-08	S5,4	1.3860-08	C9,9	2.0000-08	S13,13	6.1980-09
C7,3	1.5940-08	S5,5	2.2320-08	C10,1	1.4360-08	S14,1	1.4420-08
C7,4	1.5670-08	S6,1	6.4980-09	C10,2	2.1650-08	S15,12	8.7160-09
C7,5	2.0590-08	S6,2	1.2130-08	C10,3	2.4330-08	S15,13	1.7020-09
C7,6	1.8640-08	S6,3	1.1450-08	C10,4	1.8230-08	S15,14	2.1700-10

Table 6. Geopotential Ceofficient Standard Deviations (Normalized)--Tesseral Coefficients

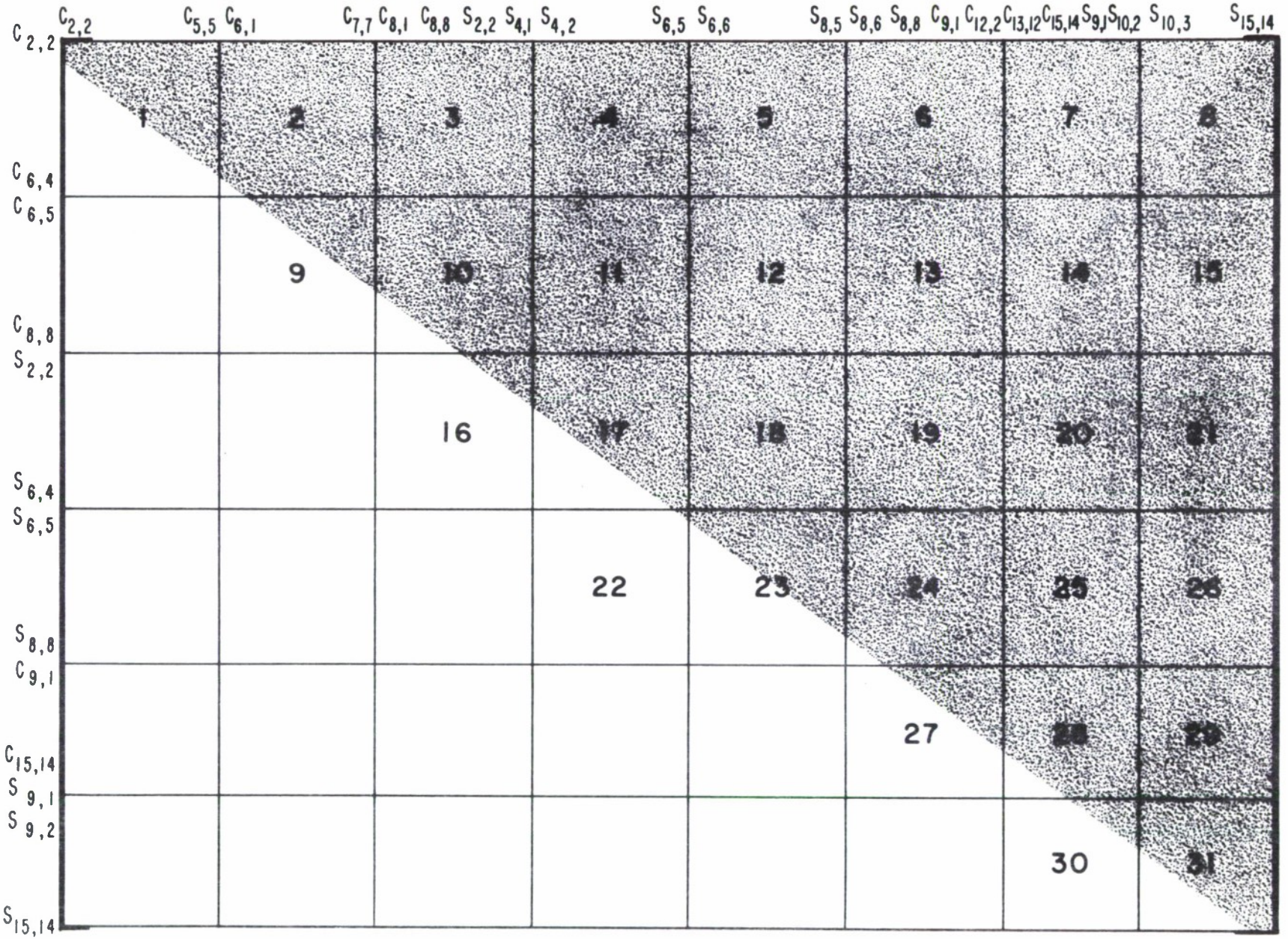

FIGURE 18. Geopotential Coefficient Correlation Matrix - Tesseral Coefficient Reference Chart for Table C.6

	C2,2	C3,1	C3,2	C3,3	C4,1	C4,2	C4,3	C4,4	C5,1	C5,2	C5,3	C5,4	C5,5	
C2,2	1.00	-.02	-.01	.02	-.06	.85	.03	.09	.01	-.03	.01	.02	.01	C2,2
C3,1		1.00	.02	-.06	.03	.01	.04	-.14	.37	.02	.07	-.05	-.03	C3,1
C3,2			1.00	.13	-.05	.08	-.04	.04	.03	.16	.04	.07	.09	C3,2
C3,3				1.00	-.02	.04	.07	.01	.02	.12	.27	.13	-.09	C3,3
C4,1					1.00	-.07	.12	.03	-.08	-.01	-.00	-.01	.02	C4,1
C4,2						1.00	.01	.09	.03	.04	.07	.03	.01	C4,2
C4,3							1.00	.11	.04	.01	-.05	.04	.00	C4,3
C4,4								1.00	-.08	.03	-.05	-.03	.00	C4,4
C5,1									1.00	.06	.01	-.04	-.04	C5,1
C5,2										1.00	.01	-.01	.09	C5,2
C5,3											1.00	.11	-.09	C5,3
C5,4												1.00	.04	C5,4
C5,5													1.00	C5,5

TABLE 7. GEOPOTENTIAL COEFFICIENT CORRELATION MATRIX - TESSERAL COEFFICIENTS (PART 1 of 31)

	C6,1	C6,2	C6,3	C6,4	C6,5	C6,6	C7,1	C7,2	C7,3	C7,4	C7,5	C7,6	C7,7	
C2,2	.02	.49	.04	.07	-.01	-.04	-.03	-.00	.02	-.01	.01	.02	.06	C2,2
C3,1	-.04	-.08	-.03	-.13	-.05	.00	.85	.01	.00	-.01	.06	.03	.08	C3,1
C3,2	.06	.00	-.03	.03	-.04	-.08	.03	.39	-.01	-.04	.08	.18	.05	C3,2
C3,3	.08	.12	-.00	.04	-.20	-.08	-.03	.06	.23	.09	-.05	.02	.11	C3,3
C4,1	-.47	-.04	.09	.01	.05	.08	-.01	-.01	-.01	.04	.04	.04	.05	C4,1
C4,2	.02	.24	.05	.08	-.03	-.05	-.01	.03	-.01	-.05	.02	-.04	.02	C4,2
C4,3	-.04	.01	.55	.09	.09	.06	.03	.01	-.04	-.00	-.06	.06	.05	C4,3
C4,4	-.01	.08	.23	.88	-.01	-.06	-.15	.02	-.04	-.06	.01	-.03	.03	C4,4
C5,1	.17	-.04	-.03	-.11	-.06	-.04	.45	.05	.02	-.04	-.02	-.00	.08	C5,1
C5,2	.05	.09	-.00	.05	-.06	-.11	.02	.12	-.03	-.00	.02	.12	.08	C5,2
C5,3	.01	.03	.06	.00	-.14	-.10	.06	-.03	.32	.11	.02	.00	.09	C5,3
C5,4	.01	-.02	-.04	.03	-.04	.02	-.04	-.01	.04	.05	-.00	.10	.03	C5,4
C5,5	.02	.02	-.02	-.02	.22	-.11	-.06	.07	-.05	-.02	.33	.01	.01	C5,5
C6,1	1.00	.06	.01	.01	-.08	-.02	.05	.01	-.00	-.07	-.06	-.05	-.08	C6,1
C6,2		1.00	-.00	.08	-.05	-.04	-.09	-.01	.04	.00	.01	-.09	-.04	C6,2
C6,3			1.00	.21	.06	.00	-.05	.01	-.01	.02	.04	.04	.07	C6,3
C6,4				1.00	-.05	-.04	-.17	.03	-.01	-.02	.01	-.01	.02	C6,4

TABLE 7. GEOPOTENTIAL COEFFICIENT CORRELATION MATRIX - TESSERAL COEFFICIENTS (PART 2 of 31)

	C8,1	C8,2	C8,3	C8,4	C8,5	C8,6	C8,7	C8,8	S2,2	S3,1	S3,2	S3,3	S4,1	
C2,2	-.04	.47	.05	.09	.01	-.03	-.00	-.01	.15	-.03	-.01	-.01	-.06	C2,2
C3,1	.01	.01	-.03	-.12	.07	.03	-.05	-.01	-.11	.05	.07	-.06	.02	C3,1
C3,2	-.04	.08	.02	.06	.02	.02	-.02	-.08	.01	.13	-.10	-.17	.04	C3,2
C3,3	-.02	.03	.07	.08	-.08	.03	.18	-.16	.04	-.02	-.14	.03	-.02	C3,3
C4,1	.84	-.04	.06	-.00	.04	.04	.03	.04	-.07	.01	.04	.04	.03	C4,1
C4,2	-.03	.70	.04	.07	.04	-.03	.02	-.02	.14	.05	-.10	-.01	-.02	C4,2
C4,3	.13	.00	.53	.07	.02	.08	.11	.08	-.05	.03	.07	-.04	-.09	C4,3
C4,4	.05	.05	.25	.78	.04	-.05	-.03	-.00	-.03	.06	.01	-.02	-.05	C4,4
C5,1	-.16	.01	-.00	-.08	-.01	-.01	-.07	-.00	-.07	-.00	.04	-.10	-.00	C5,1
C5,2	-.02	-.04	-.01	.03	-.02	-.03	-.02	-.08	-.00	.05	-.12	-.08	.07	C5,2
C5,3	-.01	.05	-.03	-.02	-.08	-.01	.12	-.11	.02	-.04	-.11	.05	-.04	C5,3
C5,4	-.05	.02	-.01	-.03	-.05	-.01	.05	-.11	.03	.18	-.01	-.12	-.04	C5,4
C5,5	.03	-.01	-.03	-.05	.10	-.01	-.10	-.13	-.09	-.09	-.02	-.15	.03	C5,5
C6,1	-.58	.00	.05	.03	-.02	.04	-.03	-.03	.05	-.11	-.00	-.07	.00	C6,1
C6,2	-.04	-.32	.03	.10	.03	-.03	.03	-.03	.13	-.08	-.07	-.03	.00	C6,2
C6,3	.14	.04	.63	.17	.10	.00	.07	.04	-.06	-.02	-.04	-.01	-.10	C6,3
C6,4	.04	.04	.24	.75	.02	-.00	-.02	-.04	-.00	.02	-.05	-.08	-.05	C6,4

TABLE 7. GEOPOTENTIAL COEFFICIENT CORRELATION MATRIX - TESSERAL COEFFICIENTS (PART 3 of 31)

	S4,2	S4,3	S4,4	S5,1	S5,2	S5,3	S5,4	S5,5	S6,1	S6,2	S6,3	S6,4	S6,5	
C2,2	.13	.01	.06	-.02	.02	.01	-.02	.08	-.01	.09	.03	.05	.02	C2,2
C3,1	-.12	-.12	.00	.03	.13	.01	.00	.12	-.05	-.12	.05	.05	.05	C3,1
C3,2	-.02	-.12	-.01	.13	-.06	.02	.03	-.14	-.19	-.02	.02	.02	.14	C3,2
C3,3	-.02	.05	-.06	-.08	-.06	.08	.02	-.00	-.09	-.05	.01	-.00	-.04	C3,3
C4,1	-.06	.00	-.17	-.03	.08	.04	.08	.02	.02	.00	.00	-.11	-.01	C4,1
C4,2	.11	.01	.06	-.02	.01	-.04	-.06	-.02	-.06	.10	.04	.04	-.00	C4,2
C4,3	.01	.04	-.10	-.03	.05	-.03	.07	.03	-.01	-.00	.03	-.04	.02	C4,3
C4,4	-.00	.07	-.01	-.06	.02	.02	.02	-.01	-.06	-.06	-.00	-.03	-.03	C4,4
C5,1	-.14	-.11	.10	-.05	-.01	-.03	-.02	.10	-.03	-.16	.03	.06	.02	C5,1
C5,2	-.03	-.12	-.04	-.00	-.04	.02	-.06	-.22	-.18	.03	-.06	-.01	-.03	C5,2
C5,3	-.00	-.01	.03	.07	.02	.08	-.03	.03	.17	-.01	.05	.02	-.06	C5,3
C5,4	.05	.09	.02	.19	.01	-.02	.07	.04	.12	.03	.01	.07	-.09	C5,4
C5,5	.01	-.13	-.07	-.11	.08	-.08	.02	-.04	.01	.08	-.06	-.08	.14	C5,5
C6,1	-.03	.01	.07	-.12	-.20	-.10	-.16	-.05	-.05	-.04	-.02	-.09	.02	C6,1
C6,2	.13	.00	.08	-.08	-.10	-.03	-.02	-.09	-.08	.11	-.06	.06	-.03	C6,2
C6,3	-.04	.02	-.09	-.04	.06	-.01	.09	.02	.02	-.04	.05	-.08	.01	C6,3
C6,4	.02	.05	-.00	-.03	-.00	-.03	.02	.00	-.04	-.03	.02	-.01	-.10	C6,4

TABLE 7. GEOPOTENTIAL COEFFICIENT CORRELATION MATRIX - TESSERAL COEFFICIENTS (PART 4 of 31)

	S6,6	S7,1	S7,2	S7,3	S7,4	S7,5	S7,6	S7,7	S8,1	S8,2	S8,3	S8,4	S8,5	
C2,2	.03	-.03	.03	-.02	-.02	.06	.00	-.02	-.05	.04	.04	.05	-.01	C2,2
C3,1	.00	.02	.03	.07	.14	-.06	-.06	.04	.04	-.05	.00	.07	-.02	C3,1
C3,2	.08	.11	-.04	.01	.04	.09	-.08	-.06	.02	.00	.02	-.03	.13	C3,2
C3,3	.07	-.02	-.02	.07	-.07	.08	.17	-.21	-.01	-.01	.02	-.01	-.01	C3,3
C4,1	-.09	.02	.10	.00	.07	-.02	.05	.00	.01	-.01	-.02	-.09	-.03	C4,1
C4,2	.05	-.01	-.01	-.01	.05	.04	.04	-.01	-.03	.03	.01	.06	.04	C4,2
C4,3	-.02	.05	.06	.02	.01	.09	.21	-.02	-.11	.04	.01	-.03	.07	C4,3
C4,4	.14	-.01	-.01	.03	-.01	.00	-.04	.05	-.09	.04	-.03	-.03	.03	C4,4
C5,1	.05	-.01	.05	.06	.06	.07	-.04	.03	.05	-.05	.05	.16	.04	C5,1
C5,2	.07	.04	-.05	.11	.04	-.03	-.01	-.13	.02	-.02	.04	.05	.06	C5,2
C5,3	-.06	.03	.05	.07	.06	.01	.06	-.09	-.11	-.04	.00	.07	.06	C5,3
C5,4	.00	.24	-.03	.04	.05	.08	.10	-.12	.00	-.01	.05	.08	.03	C5,4
C5,5	-.10	-.16	.09	-.04	.06	-.01	-.05	.13	.05	.04	-.04	-.10	.08	C5,5
C6,1	.06	-.08	-.10	.04	-.10	.10	-.03	-.01	.04	-.01	.02	-.00	.06	C6,1
C6,2	.06	-.10	-.02	-.08	-.06	.03	.10	-.02	-.01	.05	-.05	.05	-.00	C6,2
C6,3	-.05	-.00	.02	.04	-.03	-.02	.04	-.02	-.18	.05	.03	-.03	.02	C6,3
C6,4	.15	.01	-.04	.02	.00	-.02	-.01	-.10	-.09	.04	-.03	-.02	.04	C6,4

TABLE 7. GEOPOTENTIAL COEFFICIENT CORRELATION MATRIX - TESSERAL COEFFICIENTS (PART 5 of 31)

	S8,6	S8,7	S8,8	C9,1	C9,2	C9,9	C10,1	C10,2	C10,3	C10,4	C11,1	C12,1	C12,2	
C2,2	.03	.02	.02	.02	-.06	.00	.04	.41	.04	.08	-.03	-.06	.56	C2,2
C3,1	-.03	-.00	-.05	.20	.02	.00	-.04	-.01	-.01	-.09	.80	.00	.04	C3,1
C3,2	.01	-.08	.01	.00	-.13	.00	.04	-.04	.02	.05	.02	-.01	.07	C3,2
C3,3	.05	-.25	.03	.03	-.03	.00	.07	.03	.05	.07	-.03	-.00	.01	C3,3
C4,1	-.03	.03	-.02	-.06	.02	.00	-.39	-.05	.07	-.01	-.02	.68	-.04	C4,1
C4,2	.02	-.03	.03	.01	-.06	.00	.01	.15	.05	.08	-.03	-.04	.71	C4,2
C4,3	.04	-.08	-.14	.00	.01	.00	-.06	.00	.58	.02	.01	.06	.01	C4,3
C4,4	.09	-.01	.02	-.07	-.02	.00	-.01	.04	.26	.65	-.15	.02	.03	C4,4
C5,1	-.01	-.01	-.05	.84	.03	.00	.18	.00	-.02	-.05	.19	-.16	.05	C5,1
C5,2	.05	-.04	.03	.04	.32	.00	.03	.09	.01	.05	-.01	-.03	-.02	C5,2
C5,3	-.06	-.15	.01	.02	-.04	.00	.03	.03	-.01	-.04	.05	-.03	.06	C5,3
C5,4	.08	-.00	.09	-.02	-.05	.00	-.01	-.01	-.02	.04	-.02	-.02	.04	C5,4
C5,5	.01	.17	-.02	-.05	.02	.00	-.01	-.00	-.03	-.02	-.07	.01	-.01	C5,5
C6,1	-.04	-.06	.03	.09	-.04	.00	.67	.03	.02	.02	.05	-.43	.00	C6,1
C6,2	.03	-.08	.06	-.05	.01	.00	.09	.70	.02	.08	-.09	-.08	-.18	C6,2
C6,3	-.05	-.05	-.12	-.03	.03	.00	-.03	-.01	.76	.09	-.05	.04	.04	C6,3
C6,4	.08	-.09	.09	-.11	-.01	.00	.01	.03	.26	.61	-.16	.01	.03	C6,4

TABLE 7. GEOPOTENTIAL COEFFICIENT CORRELATION MATRIX - TESSERAL COEFFICIENTS (PART 6 of 31)

	C13,12	C13,13	C14,1	C15,12	C15,13	C15,14	S9,1	S9,2	S9,9	S10,1	S10,2	
C2,2	.01	-.01	.00	.01	-.00	-.01	.01	.02	.00	.01	.10	C2,2
C3,1	.04	.00	-.01	.04	-.01	-.00	.03	.02	.00	.01	-.05	C3,1
C3,2	.01	-.01	.03	.01	-.01	.04	.11	.01	.00	-.14	.02	C3,2
C3,3	.02	-.04	.05	.02	-.02	.02	-.05	.06	.00	-.06	-.01	C3,3
C4,1	-.01	-.01	-.01	-.01	-.00	-.01	-.06	-.01	.00	-.03	-.02	C4,1
C4,2	-.00	.01	-.02	-.00	.02	.01	.00	.04	.00	-.01	.11	C4,2
C4,3	.03	-.01	-.09	.03	-.01	-.01	.00	.02	.00	.03	.06	C4,3
C4,4	.01	.02	-.03	.01	.02	.00	-.07	.00	.00	-.03	.03	C4,4
C5,1	.02	.01	.15	.02	.01	.01	-.03	.09	.00	-.02	-.00	C5,1
C5,2	-.00	-.02	.04	-.00	-.01	.07	-.02	.07	.00	-.15	.06	C5,2
C5,3	.03	-.04	.04	.02	-.03	.01	.07	.11	.00	.17	.02	C5,3
C5,4	.03	-.04	.02	.03	-.03	-.00	.17	.01	.00	.10	.04	C5,4
C5,5	-.15	.03	-.02	-.15	.03	.01	-.14	.10	.00	-.02	.01	C5,5
C6,1	-.01	.02	.37	-.01	.01	.01	-.07	.03	.00	-.02	.04	C6,1
C6,2	-.01	.03	.07	-.01	.03	.00	-.08	.02	.00	-.08	.07	C6,2
C6,3	.01	-.01	-.09	.01	-.01	-.00	-.03	.08	.00	.06	.07	C6,3
C6,4	.03	.01	-.02	.03	.01	.01	-.01	.01	.00	-.02	.06	C6,4

TABLE 7. GEOPOTENTIAL COEFFICIENT CORRELATION MATRIX - TESSERAL COEFFICIENTS (PART 7 of 31)

	S10,3	S10,4	S11,1	S12,1	S12,2	S13,12	S13,13	S14,1	S15,12	S15,13	S15,14	
C2,2	.05	.04	-.03	-.05	.06	.01	-.01	.03	.01	-.01	.00	C2,2
C3,1	.03	.01	.01	.00	-.01	.02	.00	-.02	.02	.01	.01	C3,1
C3,2	.07	.01	.09	.02	-.01	-.01	-.04	-.09	-.01	-.05	.02	C3,2
C3,3	-.02	-.01	-.00	.01	.03	-.03	-.07	-.01	-.03	-.07	-.01	C3,3
C4,1	-.02	-.11	.04	.06	.02	.01	-.01	-.04	.01	-.02	.01	C4,1
C4,2	.02	.04	.00	-.04	.05	-.00	-.01	.02	-.00	-.00	-.01	C4,2
C4,3	-.02	-.03	.08	-.05	.09	.01	-.04	.07	.01	-.04	-.03	C4,3
C4,4	-.02	-.03	.02	-.03	.09	-.02	-.00	.01	-.02	-.00	.01	C4,4
C5,1	.02	.14	-.02	.01	-.03	.02	.00	-.01	.02	.01	.01	C5,1
C5,2	.02	-.03	.04	.01	-.01	.02	-.05	-.09	.02	-.04	.01	C5,2
C5,3	-.01	.05	.01	-.07	-.03	-.03	-.03	.19	-.03	-.02	-.02	C5,3
C5,4	.01	.09	.20	-.01	.00	.02	-.03	.06	.02	-.01	.03	C5,4
C5,5	.04	-.05	-.16	.03	-.02	-.01	-.03	-.03	-.01	-.03	.08	C5,5
C6,1	-.01	.06	-.08	-.00	-.03	-.01	.03	.01	-.01	.05	-.01	C6,1
C6,2	-.09	.05	-.07	.02	.01	.00	-.01	-.04	.00	-.01	-.01	C6,2
C6,3	.00	-.01	.04	-.07	.10	.03	-.01	.12	.03	-.01	-.02	C6,3
C6,4	-.04	-.02	.03	-.04	.10	-.03	-.02	.03	-.03	-.02	-.02	C6,4

TABLE 7. GEOPOTENTIAL COEFFICIENT CORRELATION MATRIX - TESSERAL COEFFICIENTS (PART 8 of 31)

	C6,1	C6,2	C6,3	C6,4	C6,5	C6,6	C7,1	C7,2	C7,3	C7,4	C7,5	C7,6	C7,7	
C6,5					1.00	-.04	-.12	-.04	-.08	-.08	.06	.03	-.04	C6,5
C6,6						1.00	.03	-.10	-.08	.05	-.03	-.07	-.07	C6,6
C7,1							1.00	.01	.01	.02	.02	.04	.09	C7,1
C7,2								1.00	-.06	-.06	.05	.12	.09	C7,2
C7,3									1.00	.04	.00	-.01	.03	C7,3
C7,4										1.00	-.03	.02	.08	C7,4
C7,5											1.00	.06	.00	C7,5
C7,6												1.00	.01	C7,6
C7,7													1.00	C7,7

TABLE 7. GEOPOTENTIAL COEFFICIENT CORRELATION MATRIX - TESSERAL COEFFICIENTS (PART 9 of 31)

	C8,1	C8,2	C8,3	C8,4	C8,5	C8,6	C8,7	C8,8	S2,2	S3,1	S3,2	S3,3	S4,1	
C6,5	.05	-.01	.01	-.10	.12	-.03	-.03	.07	-.03	-.05	-.00	-.11	.07	C6,5
C6,6	.09	-.04	.00	-.06	-.04	.73	.03	.16	.00	.03	-.04	.04	.04	C6,6
C7,1	-.02	-.02	-.05	-.16	.01	.03	-.07	-.01	-.09	.03	.05	-.07	.01	C7,1
C7,2	-.01	.18	.02	.02	-.00	-.00	-.04	-.07	.02	.05	-.08	-.03	.04	C7,2
C7,3	-.01	-.01	.03	-.03	-.04	-.04	.05	-.05	.04	-.01	.02	.02	-.08	C7,3
C7,4	.04	-.07	-.03	.06	-.05	.03	.03	-.14	.03	-.01	-.05	-.02	-.06	C7,4
C7,5	.07	.02	.02	-.05	.19	.02	-.04	-.05	.00	.07	-.11	-.07	.02	C7,5
C7,6	.01	-.02	.04	-.04	-.03	.08	-.04	.02	-.02	.16	.21	-.15	.00	C7,6
C7,7	.02	-.03	.08	.00	-.02	-.02	.19	-.13	-.01	.04	.10	.18	-.07	C7,7
C8,1	1.00	-.00	.10	.02	.07	.06	.03	.04	-.05	.03	-.05	.01	.04	C8,1
C8,2		1.00	.01	.03	.00	-.01	.01	-.01	.06	.04	-.09	-.02	-.00	C8,2
C8,3			1.00	.20	.11	.01	.05	.01	-.04	.04	.01	-.00	-.08	C8,3
C8,4				1.00	-.02	-.02	.00	-.06	.01	-.01	.02	-.10	-.04	C8,4
C8,5					1.00	-.04	.00	.05	.00	.08	-.10	-.01	.02	C8,5
C8,6						1.00	.01	.03	-.01	.01	.03	-.06	.01	C8,6
C8,7							1.00	-.00	.02	-.01	-.02	.17	-.04	C8,7
C8,8								1.00	-.01	.00	.03	.05	.03	C8,8

TABLE 7. GEOPOTENTIAL COEFFICIENT CORRELATION MATRIX - TESSERAL COEFFICIENTS (PART 10 of 31)

	S4,2	S4,3	S4,4	S5,1	S5,2	S5,3	S5,4	S5,5	S6,1	S6,2	S6,3	S6,4	S6,5	
C6,5	.04	-.09	-.00	-.03	.12	-.07	.12	-.02	-.05	.12	-.08	.02	.08	C6,5
C6,6	.01	.12	-.04	.08	-.09	.10	.01	.10	.05	-.00	.16	-.02	.07	C6,6
C7,1	-.17	-.14	.07	.01	.06	.01	-.03	.12	-.00	-.18	.05	.07	.07	C7,1
C7,2	.03	-.12	.02	.01	-.01	.03	-.02	-.22	-.10	.02	-.01	.06	-.09	C7,2
C7,3	.01	-.02	.03	.05	-.03	.04	-.00	.05	.08	.06	.01	.00	-.00	C7,3
C7,4	-.02	-.01	-.01	.07	-.06	-.02	.05	.05	.17	.06	.06	.04	-.11	C7,4
C7,5	-.01	-.14	-.03	-.00	.10	-.06	-.05	-.00	-.04	.02	.00	-.02	.06	C7,5
C7,6	-.04	-.26	-.01	.18	.17	-.00	-.01	-.03	-.03	-.06	-.01	.02	.05	C7,6
C7,7	-.02	-.05	-.08	.04	.16	.14	.08	-.03	.04	-.03	.03	.05	-.12	C7,7
C8,1	-.02	-.00	-.23	.02	.11	.05	.06	-.01	.03	-.03	.00	-.19	-.01	C8,1
C8,2	.04	.06	.01	.00	.03	-.02	-.01	-.07	-.03	.05	.07	.01	-.01	C8,2
C8,3	-.03	.01	-.08	-.05	-.01	.04	.03	.04	-.08	-.09	.05	-.08	-.01	C8,3
C8,4	.01	.09	.00	-.09	-.08	-.38	.03	.03	-.07	-.03	-.01	-.01	-.08	C8,4
C8,5	.00	-.06	-.01	-.01	.01	-.13	-.04	.00	-.02	.03	-.05	-.03	.04	C8,5
C8,6	.00	-.04	-.02	.05	-.01	.03	-.06	-.03	.05	.00	.12	-.01	-.00	C8,6
C8,7	.03	.14	-.02	.02	-.01	.08	-.01	-.09	.03	.06	.07	.06	-.13	C8,7
C8,8	.01	.12	-.00	.01	-.01	.00	-.07	.05	-.03	.01	.10	-.04	.14	C8,8

TABLE 7. GEOPOTENTIAL COEFFICIENT CORRELATION MATRIX - TESSERAL COEFFICIENTS (PART 11 of 31)

	S6,6	S7,1	S7,2	S7,3	S7,4	S7,5	S7,6	S7,7	S8,1	S8,2	S8,3	S8,4	S8,5	
C6,5	-.14	-.10	.12	-.04	.14	-.01	.11	.17	.05	.05	-.05	.00	.03	C6,5
C6,6	-.03	.06	-.10	.11	.05	.10	.13	-.02	.07	-.02	.10	-.00	.04	C6,6
C7,1	.01	.00	.00	.08	.04	-.00	-.09	.04	.02	-.08	.05	.10	.02	C7,1
C7,2	.03	.01	-.02	.04	-.03	-.05	-.03	-.13	-.02	.03	-.04	.07	-.04	C7,2
C7,3	-.10	.06	.07	.06	-.01	-.02	.00	-.01	-.02	-.02	.06	-.00	.00	C7,3
C7,4	-.06	.06	-.04	.03	.04	-.00	.05	-.14	-.07	-.04	-.05	.09	-.10	C7,4
C7,5	-.11	.01	.03	-.05	.06	-.02	-.04	.06	.03	.04	-.07	-.06	.01	C7,5
C7,6	-.09	.21	.16	.05	.01	.07	-.03	-.06	.01	.00	.11	-.01	.04	C7,6
C7,7	-.01	.08	.17	.08	.16	.00	-.07	-.07	-.06	-.01	.07	.18	-.06	C7,7
C8,1	-.11	.00	.06	-.03	.06	-.05	.06	.01	.00	.03	-.04	-.18	-.04	C8,1
C8,2	.03	.00	-.03	.00	.04	-.06	.02	.01	-.02	.01	.04	.01	-.01	C8,2
C8,3	-.01	.03	.07	.01	.04	.08	-.04	-.04	-.12	.05	.04	-.06	.05	C8,3
C8,4	.16	-.00	-.06	-.01	-.04	.04	.03	-.20	-.06	.03	-.02	-.01	-.02	C8,4
C8,5	-.10	.01	.07	-.08	.13	.00	-.01	.11	.03	.06	-.06	.02	.01	C8,5
C8,6	-.00	.02	-.01	.10	.04	.11	.09	-.01	.04	-.01	.12	-.03	.08	C8,6
C8,7	-.01	.04	-.01	.02	.07	-.03	.14	-.13	-.03	.04	.02	.13	-.07	C8,7
C8,8	-.10	.03	-.00	-.02	-.08	.06	.10	.13	.03	.04	.07	-.06	.06	C8,8

TABLE 7. GEOPOTENTIAL COEFFICIENT CORRELATION MATRIX - TESSERAL COEFFICIENTS (PART 12 of 31)

	S8,6	S8,7	S8,8	C9,1	C9,2	C9,9	C10,1	C10,2	C10,3	C10,4	C11,1	C12,1	C12,2	
C6,5	-.01	.14	-.11	-.09	-.01	.00	-.11	-.03	-.00	-.07	-.12	.01	-.02	C6,5
C6,6	-.01	.03	.10	-.02	-.04	.00	-.05	-.02	.00	-.09	.06	.04	-.04	C6,6
C7,1	-.03	.02	-.07	.26	-.00	.00	.00	-.02	-.02	-.13	.90	.01	.03	C7,1
C7,2	.01	.01	.02	.02	-.06	.00	-.01	-.17	.00	.02	-.02	-.01	.11	C7,2
C7,3	-.12	-.06	.01	-.00	-.05	.00	-.01	.06	-.06	-.05	.02	.01	.03	C7,3
C7,4	-.03	-.04	.10	-.00	.01	.00	-.08	-.02	.00	-.06	.03	.04	-.06	C7,4
C7,5	-.09	-.04	-.07	-.05	-.03	.00	-.07	-.01	-.02	-.10	.02	.04	.01	C7,5
C7,6	-.02	.05	-.10	.01	.04	.00	-.06	.00	-.01	-.05	.05	.01	.02	C7,6
C7,7	-.01	-.11	-.15	.08	.07	.00	-.10	-.01	.06	-.01	.06	.01	-.00	C7,7
C8,1	-.07	.01	-.00	-.11	.01	.00	-.58	-.03	.12	.01	-.03	.75	-.00	C8,1
C8,2	.00	-.05	.00	.01	-.14	.00	-.02	-.41	.03	.05	-.04	-.00	.83	C8,2
C8,3	-.04	-.04	-.08	-.01	-.02	.00	.02	-.00	.68	.13	-.05	.00	.02	C8,3
C8,4	.08	-.14	.14	-.09	-.02	.00	.05	.04	.24	.56	-.16	.01	.01	C8,4
C8,5	-.10	.05	-.05	-.06	-.02	.00	-.07	-.00	.03	-.01	.00	.03	-.00	C8,5
C8,6	-.01	-.07	.03	-.01	.01	.00	.02	-.01	.02	-.08	.04	.02	-.02	C8,6
C8,7	.04	-.04	-.03	-.07	-.03	.00	-.05	.01	.01	.01	-.05	.01	.01	C8,7
C8,8	-.04	.08	-.02	-.01	-.04	.00	-.04	-.00	-.02	-.05	-.00	.01	.01	C8,8

TABLE 7. GEOPOTENTIAL COEFFICIENT CORRELATION MATRIX - TESSERAL COEFFICIENTS (PART 13 of 31)

	C13,12	C13,13	C14,1	C15,12	C15,13	C15,14	S9,1	S9,2	S9,9	S10,1	S10,2	
C6,5	-.04	.03	-.09	-.04	.02	-.10	-.06	.10	.00	-.09	.04	C6,5
C6,6	.07	-.00	-.07	.07	-.00	-.06	.08	-.10	.00	.01	-.05	C6,6
C7,1	.03	-.00	.04	.03	-.01	.02	.02	-.01	.00	.06	-.07	C7,1
C7,2	.00	-.03	-.01	.00	-.03	.07	-.01	.03	.00	-.15	.04	C7,2
C7,3	.01	-.03	-.03	-.02	.01	-.02	.07	.06	.00	.02	.02	C7,3
C7,4	.03	-.03	-.06	.03	-.03	-.00	.08	-.06	.00	.21	-.00	C7,4
C7,5	-.08	.01	-.10	-.08	-.01	-.01	-.04	.14	.00	-.04	.07	C7,5
C7,6	.03	-.18	-.03	.03	-.18	-.03	.17	.05	.00	-.02	-.00	C7,6
C7,7	.02	-.01	-.06	.02	-.01	.20	.06	.10	.00	.06	.01	C7,7
C8,1	-.03	.01	-.36	-.03	.01	-.01	-.01	-.03	.00	-.01	-.01	C8,1
C8,2	-.01	.01	-.04	-.01	.01	-.00	.00	.02	.00	-.01	.08	C8,2
C8,3	.00	-.01	-.06	.00	-.01	.01	-.02	.02	.00	-.04	.06	C8,3
C8,4	.04	.02	.03	.04	.02	.01	-.05	-.10	.00	-.05	.03	C8,4
C8,5	-.04	.02	-.10	-.04	.01	-.06	-.05	.14	.00	-.05	.06	C8,5
C8,6	.02	-.03	-.01	.02	-.03	-.02	.06	-.04	.00	.03	-.05	C8,6
C8,7	.14	.01	-.05	.14	.02	.06	.05	-.01	.00	.04	.03	C8,7
C8,8	.05	-.11	-.05	.05	-.09	-.09	.02	-.03	.00	-.05	.02	C8,8

TABLE 7. GEOPOTENTIAL COEFFICIENT CORRELATION MATRIX - TESSERAL COEFFICIENTS (PART 14 of 31)

	S10,3	S10,4	S11,1	S12,1	S12,2	S13,12	S13,13	S14,1	S15,12	S15,13	S15,14	
C6,5	-.02	-.00	-.11	.04	-.00	-.01	.04	-.07	-.01	.02	.01	C6,5
C6,6	.01	-.00	.04	.01	-.03	-.00	-.02	-.03	-.00	-.03	-.05	C6,6
C7,1	.04	.07	.01	-.00	-.02	.02	.01	.01	.02	.01	.02	C7,1
C7,2	.06	.13	.00	-.00	.03	.04	-.03	-.10	.04	-.03	.01	C7,2
C7,3	-.01	.07	.03	.00	-.01	-.02	-.00	.01	-.02	.00	-.00	C7,3
C7,4	-.01	.02	.06	-.06	-.00	.02	-.05	.16	.02	-.04	.03	C7,4
C7,5	.00	.03	.01	.02	-.01	-.01	.00	-.05	-.01	.02	.03	C7,5
C7,6	.16	-.01	.18	.00	.01	.06	-.01	-.01	.06	-.01	.03	C7,6
C7,7	.07	.14	.09	-.05	.03	.18	-.11	.05	.18	-.08	.06	C7,7
C8,1	-.03	-.15	.03	.05	.09	-.00	.00	-.04	-.00	-.01	.00	C8,1
C8,2	.06	.01	-.00	-.03	.04	-.01	-.00	.02	-.01	.00	-.01	C8,2
C8,3	.02	.01	.05	-.03	.11	.04	-.01	.05	.04	-.00	-.01	C8,3
C8,4	-.04	-.02	.06	-.02	.09	-.04	-.03	-.01	-.04	-.03	-.04	C8,4
C8,5	-.03	.01	.02	-.00	.03	-.06	.03	-.07	-.06	.05	.01	C8,5
C8,6	.05	-.03	.01	-.01	-.02	.00	-.07	-.01	.00	-.07	-.01	C8,6
C8,7	-.05	.09	.04	-.02	.01	-.02	-.00	.05	-.02	.00	.00	C8,7
C8,8	.01	-.04	.03	.02	.02	-.09	.10	-.05	-.09	.08	-.04	C8,8

TABLE 7. GEOPOTENTIAL COEFFICIENT CORRELATION MATRIX - TESSERAL COEFFICIENTS (PART 15 of 31)

	C8,1	C8,2	C8,3	C8,4	C8,5	C8,6	C8,7	C8,8	S2,2	S3,1	S3,2	S3,3	S4,1	
S2,2									1.00	.03	-.05	.03	-.03	S2,2
S3,1										1.00	.01	-.10	.02	S3,1
S3,2											1.00	.03	-.04	S3,2
S3,3												1.00	-.03	S3,3
S4,1													1.00	S4,1

TABLE 7. GEOPOTENTIAL COEFFICIENT CORRELATION MATRIX - TESSERAL COEFFICIENTS (PART 16 of 31)

	S4,2	S4,3	S4,4	S5,1	S5,2	S5,3	S5,4	S5,5	S6,1	S6,2	S6,3	S6,4	S6,5	
S2,2	.86	.02	.16	.02	-.06	.01	-.03	.01	.01	.53	-.00	.13	-.03	S2,2
S3,1	.01	-.06	.04	.47	.09	.00	.05	-.06	-.10	-.03	-.03	.04	-.08	S3,1
S3,2	-.04	-.02	-.01	.01	-.03	.06	.09	-.01	-.03	-.11	-.02	-.01	-.00	S3,2
S3,3	.03	.14	-.01	-.12	.01	.33	-.10	.16	-.01	-.01	.02	.03	-.05	S3,3
S4,1	-.01	.01	.00	-.12	-.03	-.02	-.01	-.05	-.47	-.01	-.02	.00	.04	S4,1
S4,2	1.00	.04	.12	.02	-.04	.00	.03	-.01	.02	.30	-.02	.12	-.02	S4,2
S4,3		1.00	-.15	-.10	-.13	.02	.04	.02	-.01	.01	.44	-.13	.00	S4,3
S4,4			1.00	.07	-.06	-.03	-.05	-.01	.01	.13	-.21	.89	-.02	S4,4
S5,1				1.00	.10	.00	.04	-.06	.14	-.00	-.01	.08	-.06	S5,1
S5,2					1.00	.03	.04	-.01	.04	.03	-.01	-.02	-.07	S5,2
S5,3						1.00	-.01	.09	.09	-.04	.08	.01	.01	S5,3
S5,4							1.00	.01	.05	-.01	-.01	.04	-.04	S5,4
S5,5								1.00	.11	-.02	.02	-.01	.12	S5,5
S6,1									1.00	.03	.07	-.02	-.06	S6,1
S6,2										1.00	-.04	.14	.01	S6,2
S6,3											1.00	-.19	-.00	S6,3
S6,4												1.00	-.04	S6,4

TABLE 7. GEOPOTENTIAL COEFFICIENT CORRELATION MATRIX - TESSERAL COEFFICIENTS (PART 17 of 31)

	S6,6	S7,1	S7,2	S7,3	S7,4	S7,5	S7,6	S7,7	S8,1	S8,2	S8,3	S8,4	S8,5	
S2,2	.01	.03	.04	.01	-.04	.03	.02	-.00	-.01	.46	.01	.13	-.03	S2⁄2
S3,1	-.00	.87	.06	.04	.08	.03	.07	-.03	.04	.01	.01	.07	.06	S3⁄1
S3,2	-.05	.04	.33	.04	-.02	.05	-.03	.05	.03	.00	.06	-.02	.01	S3⁄2
S3,3	-.05	-.13	.01	.22	-.05	-.01	-.08	.11	-.03	.02	.02	.08	-.03	S3⁄3
S4,1	-.06	.01	-.05	-.09	-.01	.03	.02	-.00	.83	.01	-.04	-.08	.00	S4⁄1
S4,2	-.00	.01	.06	-.02	-.05	-.02	.01	-.01	.00	.69	-.02	.09	-.00	S4⁄2
S4,3	.07	-.04	-.13	-.03	-.06	-.05	.07	-.03	.03	.01	.40	-.09	-.05	S4⁄3
S4,4	.15	.06	-.06	-.02	-.04	-.00	-.01	.06	-.01	.00	-.18	.79	-.02	S4⁄4
S5,1	-.06	.51	.07	.08	.09	-.03	.11	-.05	-.15	.01	.04	.09	-.04	S5⁄1
S5,2	-.14	.05	-.00	.01	.15	.00	-.07	.05	-.04	-.07	.00	-.01	-.04	S5⁄2
S5,3	-.10	-.00	.03	.31	.03	.09	-.10	.06	-.06	-.01	-.00	.04	-.08	S5⁄3
S5,4	-.05	.07	.06	.03	-.08	-.02	.07	-.01	-.01	.02	.01	-.05	-.08	S5,4
S5,5	-.06	-.03	.03	.03	-.04	.32	-.01	.07	-.01	-.02	.02	-.02	.04	S5,5
S6,1	-.05	-.03	.07	.11	.02	-.10	-.02	.02	-.57	-.00	.05	.03	-.04	S6⁄1
S6,2	-.01	-.02	.00	.01	.06	-.02	.02	-.02	-.02	-.28	-.04	.15	-.03	S6⁄2
S6,3	-.03	.02	-.05	.03	.03	-.00	.02	-.00	-.00	.01	.55	-.13	.03	S6⁄3
S6,4	.15	.07	-.04	.00	-.00	-.01	.01	.00	-.01	.01	-.19	.77	-.05	S6⁄4

TABLE 7. GEOPOTENTIAL COEFFICIENT CORRELATION MATRIX - TESSERAL COEFFICIENTS (PART 18 of 31)

	S8,6	S8,7	S8,8	C9,1	C9,2	C9,9	C10,1	C10,2	C10,3	C10,4	C11,1	C12,1	C12,2	
S2,2	-.01	-.03	.04	-.04	.01	.00	.04	.05	-.06	-.02	-.09	-.05	.03	S2,2
S3,1	.01	-.03	.01	-.03	-.01	.00	-.11	-.04	.03	.05	.05	.02	.06	S3,1
S3,2	.05	.07	-.05	.04	-.02	.00	.06	-.00	-.02	-.02	.06	-.05	-.04	S3,2
S3,3	.02	.26	-.02	-.08	.04	.00	-.09	-.02	.02	-.10	-.03	.02	-.03	S3,3
S4,1	-.06	-.00	.04	-.01	.01	.00	.01	-.02	-.09	-.00	.01	.01	-.01	S4,1
S4,2	.00	.00	.03	-.12	.02	.00	-.04	.05	-.04	.00	-.13	-.01	.01	S4,2
S4,3	.06	.01	.08	-.09	-.09	.00	.02	.01	.03	.09	-.10	.01	.07	S4,3
S4,4	.09	-.02	.02	.09	.01	.00	.11	.01	-.08	.01	.04	-.14	-.02	S4,4
S5,1	-.03	-.04	.02	-.05	.03	.00	-.13	.02	-.03	-.09	.03	.01	.02	S5,1
S5,2	-.05	-.01	-.08	-.04	.03	.00	-.25	-.02	.02	.01	.06	.11	.03	S5,2
S5,3	-.04	.18	-.07	-.02	.05	.00	-.12	-.03	-.01	-.08	.03	.04	-.02	S5,3
S5,4	-.04	-.06	-.08	-.04	-.05	.00	-.11	-.04	.08	-.01	-.01	.05	-.03	S5,4
S5,5	-.03	.05	-.04	.07	-.13	.00	-.03	-.05	.01	.00	.10	-.00	-.03	S5,5
S6,1	-.01	.03	-.03	.02	-.00	.00	-.07	-.01	-.05	-.09	-.02	.03	-.01	S6,1
S6,2	.00	.00	.03	-.15	.03	.00	.00	.01	-.10	-.04	-.17	-.05	-.00	S6,2
S6,3	-.05	-.01	.01	.03	-.10	.00	-.01	.04	.02	.01	.03	-.00	.12	S6,3
S6,4	.14	-.01	.00	.06	.03	.00	.01	.01	-.07	-.00	.06	-.09	-.03	S6,4

TABLE 7. GEOPOTENTIAL COEFFICIENT CORRELATION MATRIX - TESSERAL COEFFICIENTS (PART 19 of 31)

	C13,12	C13,13	C14,1	C15,12	C15,13	C15,14	S9,1	S9,2	S9,9	S10,1	S10,2	
S2,2	.01	-.00	.01	.01	-.00	-.01	.02	-.05	.00	.01	.40	S2,2
S3,1	.01	-.02	-.12	.01	.00	.01	.28	.06	.00	-.08	.03	S3,1
S3,2	.03	-.01	.08	.03	-.02	-.00	.02	-.20	.00	-.03	-.10	S3,2
S3,3	.07	.00	-.07	.07	.01	.00	-.14	-.02	.00	-.01	-.03	S3,3
S4,1	.00	.01	.02	.00	.01	-.02	-.08	.01	.00	-.35	-.01	S4,1
S4,2	.01	-.00	-.08	.01	-.00	-.01	.02	-.03	.00	-.01	.15	S4,2
S4,3	.05	.02	.02	.05	.02	-.03	-.06	-.13	.00	-.01	.00	S4,3
S4,4	-.01	.01	.17	-.01	.02	-.01	.06	-.03	.00	.02	.02	S4,4
S5,1	.01	-.03	-.13	.01	-.03	.01	.84	.01	.00	.15	-.01	S5,1
S5,2	-.01	-.03	-.21	-.01	-.03	.00	.06	.34	.00	.10	.09	S5,2
S5,3	.06	-.02	-.09	.06	-.02	.00	-.02	-.01	.00	.06	-.04	S5,3
S5,4	-.02	.05	-.09	-.02	.03	.02	.03	-.03	.00	.03	-.03	S5,4
S5,5	.04	-.04	-.01	.04	-.04	-.05	-.03	.04	.00	.09	-.01	S5,5
S6,1	.01	-.01	-.05	.01	-.02	.01	.07	-.03	.00	.66	-.01	S6,1
S6,2	.01	-.00	.03	.01	.00	-.01	.00	.06	.00	.03	.69	S6,2
S6,3	.02	-.01	-.01	.02	-.01	-.01	.02	-.04	.00	.06	.01	S6,3
S6,4	.01	-.00	.10	.01	-.00	.01	.07	-.03	.00	.00	.01	S6,4

TABLE 7. GEOPOTENTIAL COEFFICIENT CORRELATION MATRIX - TESSERAL COEFFICIENTS (PART 20 of 31)

	S10,3	S10,4	S11,1	S12,1	S12,2	S13,12	S13,13	S14,1	S15,12	S15,13	S15,14	
S2,2	-.01	.12	.04	-.02	.50	.01	-.00	-.02	.01	.01	-.01	S2,2
S3,1	.05	.06	.82	.03	.03	.03	-.04	-.09	.03	-.05	-.00	S3,1
S3,2	.08	-.01	.02	.02	-.01	.06	.02	-.06	.06	.01	.02	S3,2
S3,3	-.03	.07	-.11	-.01	.02	-.01	.02	-.02	-.01	.03	.01	S3,3
S4,1	-.00	-.03	-.03	.63	-.01	.01	.02	.08	.01	.01	-.01	S4,1
S4,2	-.01	.09	.01	-.01	.65	.01	.00	-.02	.01	.00	-.01	S4,2
S4,3	.47	-.05	.01	.03	.03	-.03	.00	-.02	-.03	-.00	-.05	S4,3
S4,4	-.20	.65	.04	-.02	-.06	.01	.02	.03	.01	.02	.01	S4,4
S5,1	.02	.06	.31	-.15	.03	.04	-.04	.02	.04	-.02	-.01	S5,1
S5,2	.07	-.02	.02	-.08	-.04	.03	.00	.06	.03	.01	.03	S5,2
S5,3	.01	.03	-.02	-.05	-.01	.01	-.00	.11	.01	.00	.02	S5,3
S5,4	.01	.03	.08	.01	.05	.02	-.03	.01	.02	-.03	.02	S5,4
S5,5	.01	-.00	-.00	-.01	.00	-.11	-.04	.06	-.11	-.03	.02	S5,5
S6,1	.01	.06	.01	-.39	.01	.01	.00	.32	.01	.01	.02	S6,1
S6,2	-.05	.11	-.02	-.03	-.19	-.00	.01	.01	.00	.01	-.02	S6,2
S6,3	.70	-.08	.02	-.02	.02	-.02	-.02	.03	-.02	-.01	-.01	S6,3
S6,4	-.21	.61	.05	-.01	-.06	.04	.00	.01	.04	.00	.01	S6,4

TABLE 7. GEOPOTENTIAL COEFFICIENT CORRELATION MATRIX - TESSERAL COEFFICIENTS (PART 21 of 31)

	S4,2	S4,3	S4,4	S5,1	S5,2	S5,3	S5,4	S5,5	S6,1	S6,2	S6,3	S6,4	S6,5	
S6,5													1,00	S6,5

TABLE 7. GEOPOTENTIAL COEFFICIENT CORRELATION MATRIX - TESSERAL COEFFICIENTS (PART 22 of 31)

	S6,6	S7,1	S7,2	S7,3	S7,4	S7,5	S7,6	S7,7	S8,1	S8,2	S8,3	S8,4	S8,5	
S6,5	-.05	-.10	-.05	-.01	-.10	.06	-.09	.04	.05	.03	-.02	-.08	.11	S6,5
S6,6	1.00	.01	-.16	-.07	-.02	.02	-.01	-.05	-.08	-.04	-.04	.07	.01	S6,6
S7,1		1.00	.02	.08	.07	.02	.13	-.11	.03	.00	.04	.09	.01	S7,1
S7,2			1.00	.03	.10	.03	-.09	.05	-.03	.19	.06	-.01	-.01	S7,2
S7,3				1.00	.06	.06	-.06	.01	-.08	-.05	.07	.03	-.01	S7,3
S7,4					1.00	-.03	-.01	.02	-.00	-.03	-.02	.15	-.03	S7,4
S7,5						1.00	-.01	-.01	.06	-.01	.03	-.03	.19	S7,5
S7,6							1.00	-.07	.01	.01	-.01	-.01	-.03	S7,6
S7,7								1.00	.01	-.03	.02	-.05	-.01	S7,7
S8,1									1.00	.01	.00	-.02	.01	S8,1
S8,2										1.00	-.00	.02	.02	S8,2
S8,3											1.00	-.15	.05	S8,3
S8,4												1.00	-.06	S8,4
S8,5													1.00	S8,5

TABLE 7. GEOPOTENTIAL COEFFICIENT CORRELATION MATRIX - TESSERAL COEFFICIENTS (PART 23 of 31)

	S8,6	S8,7	S8,8	C9,1	C9,2	C9,9	C10,1	C10,2	C10,3	C10,4	C11,1	C12,1	C12,2	
S6,5	-.01	.17	-.03	.04	-.15	.00	.02	-.01	-.05	-.06	.08	-.00	.01	S6,5
S6,6	.76	-.06	.07	.05	-.03	.00	.12	.03	.05	.13	-.02	-.03	.02	S6,6
S7,1	-.01	-.06	.02	-.02	-.03	.00	-.05	-.03	.02	.02	.03	-.00	.04	S7,1
S7,2	-.04	-.03	-.09	-.00	.05	.00	-.01	.03	-.02	-.14	-.03	-.02	.02	S7,2
S7,3	-.05	.07	-.06	.05	.02	.00	.05	-.03	.02	-.08	.07	-.07	-.01	S7,3
S7,4	-.00	-.09	-.11	.00	.02	.00	-.16	.01	-.01	.01	-.01	.03	.02	S7,4
S7,5	.06	-.09	-.05	.09	-.13	.00	.08	-.07	.03	-.02	-.03	-.06	-.05	S7,5
S7,6	.05	-.01	.08	-.05	-.01	.00	-.01	.02	-.05	.04	-.08	.05	-.00	S7,6
S7,7	-.02	-.17	-.14	.03	-.08	.00	-.01	.01	-.04	-.16	.03	.01	.01	S7,7
S8,1	-.09	.01	.04	.03	-.01	.00	.06	-.01	-.16	-.03	.03	-.03	-.00	S8,1
S8,2	-.02	.00	-.01	-.07	.03	.00	-.09	.03	.01	.00	-.07	.04	-.00	S8,2
S8,3	-.05	-.00	-.02	.03	-.01	.00	.02	.04	.02	-.07	.05	-.03	.12	S8,3
S8,4	.08	.02	.00	.12	.12	.00	.00	.02	-.06	-.01	.03	-.12	-.01	S8,4
S8,5	.01	.04	.00	.04	-.13	.00	.07	-.04	.04	-.02	.01	-.04	.02	S8,5
S8,6	1.00	-.01	.03	.01	-.01	.00	.01	.03	.00	.06	-.02	-.00	.01	S8,6
S8,7		1.00	-.03	.01	.05	.00	-.08	-.05	-.02	-.11	.04	.01	-.03	S8,7
S8,8			1.00	-.06	.01	.00	.03	.01	-.02	.12	-.07	.00	-.02	S8,8

TABLE 7. GEOPOTENTIAL COEFFICIENT CORRELATION MATRIX - TESSERAL COEFFICIENTS (PART 24 of 31)

	C13,12	C13,13	C14,1	C15,12	C15,13	C15,14	S9,1	S9,2	S9,9	S10,1	S10,2	
S6,5	.04	-.07	.02	.04	-.06	-.05	-.07	-.05	.00	-.05	.00	S6,5
S6,6	-.01	.06	.14	-.01	.06	.04	-.02	-.11	.00	-.00	-.03	S6,6
S7,1	.04	-.03	-.06	.04	-.01	.02	.30	.01	.00	-.05	.02	S7,1
S7,2	-.02	-.04	-.04	-.02	-.03	-.01	.01	-.08	.00	.10	-.10	S7,2
S7,3	.04	-.02	.03	.04	-.02	.00	.05	.02	.00	.06	.01	S7,3
S7,4	-.02	.04	-.11	-.02	.04	.03	.08	.16	.00	.03	.05	S7,4
S7,5	.04	-.03	.10	.04	-.03	-.02	-.02	-.01	.00	-.06	-.01	S7,5
S7,6	-.04	.00	-.01	-.04	.01	-.01	.11	-.05	.00	-.03	.01	S7,6
S7,7	-.17	.11	-.02	-.17	.09	-.07	-.11	.03	.00	.01	-.03	S7,7
S8,1	.01	.02	.05	.01	.02	-.03	-.09	.02	.00	-.57	-.01	S8,1
S8,2	.01	-.01	-.12	.01	-.01	-.00	-.01	-.11	.00	-.04	-.41	S8,2
S8,3	.00	-.03	.02	.00	-.02	.00	.05	-.04	.00	.03	.01	S8,3
S8,4	.04	-.02	.09	.04	-.01	.03	.08	.03	.00	.04	.05	S8,4
S8,5	.07	-.04	.07	.07	-.05	-.02	-.05	-.03	.00	-.03	.01	S8,5
S8,6	-.00	.06	.06	-.00	.07	.00	-.02	-.05	.00	.02	-.03	S8,6
S8,7	.03	-.03	-.06	.03	-.03	-.06	-.06	-.07	.00	.00	-.03	S8,7
S8,8	.09	-.06	.02	.09	-.04	-.00	.03	-.05	.00	-.05	-.01	S8,8

TABLE 7. GEOPOTENTIAL COEFFICIENT CORRELATION MATRIX - TESSERAL COEFFICIENTS (PART 25 of 31)

	S10,3	S10,4	S11,1	S12,1	S12,2	S13,12	S13,13	S14,1	S15,12	S15,13	S15,14	
S6,5	-.00	-.05	-.11	.04	-.02	-.03	.04	-.04	-.03	.03	-.06	S6,5
S6,6	-.05	-.01	.04	-.04	-.04	.03	.02	.03	.03	-.00	-.03	S6,6
S7,1	.04	.08	.92	.05	.02	.03	-.05	-.04	.04	-.05	-.01	S7,1
S7,2	.06	.00	.00	.01	.17	.02	-.00	-.01	.02	-.01	.03	S7,2
S7,3	-.00	.00	.05	-.06	-.03	.01	-.02	.05	.01	-.03	.02	S7,3
S7,4	-.01	-.02	.04	-.01	-.05	.03	-.02	.02	.03	-.02	.02	S7,4
S7,5	.00	.02	.05	.07	-.02	-.05	.00	-.07	-.05	.00	.00	S7,5
S7,6	-.06	-.02	.10	.00	-.00	-.02	-.15	-.02	-.02	-.13	-.03	S7,6
S7,7	.03	-.04	-.13	.01	-.04	-.02	-.01	-.01	-.02	-.01	.17	S7,7
S8,1	.03	-.03	-.02	.73	-.01	.02	.03	-.27	.02	.02	.00	S8,1
S8,2	-.01	.05	.01	.03	.81	-.01	.01	-.05	-.01	.01	-.02	S8,2
S8,3	.60	-.08	.04	-.03	.03	-.01	-.03	-.01	-.01	-.02	.01	S8,3
S8,4	-.18	.58	.07	-.04	-.05	.05	.01	.05	.05	.01	.01	S8,4
S8,5	-.00	-.03	.04	.02	.03	-.03	.01	-.03	-.03	-.02	-.04	S8,5
S8,6	-.03	-.02	.01	-.07	-.03	.01	-.01	.04	.01	-.03	-.01	S8,6
S8,7	.01	.04	-.06	-.01	-.01	.09	.06	-.02	.09	.06	.09	S8,7
S8,8	-.04	-.00	.01	.01	-.02	.01	-.11	-.06	.01	-.10	-.05	S8,8

TABLE 7. GEOPOTENTIAL COEFFICIENT CORRELATION MATRIX - TESSERAL COEFFICIENTS (PART 26 of 31)

	S8,6	S8,7	S8,8	C9,1	C9,2	C9,9	C10,1	C10,2	C10,3	C10,4	C11,1	C12,1	C12,2	
C9,1				1.00	.02	.00	.21	-.00	-.03	-.07	-.03	-.19	.04	C9,1
C9,2					1.00	.00	-.06	.16	-.02	-.04	-.03	-.01	-.18	C9,2
C9,9						1.00	.00	.00	.00	.00	.00	.00	.00	C9,9
C10,1							1.00	.06	.00	.03	-.03	-.79	.00	C10,1
C10,2								1.00	-.01	.04	-.03	-.07	-.08	C10,2
C10,3									1.00	.15	-.02	.05	.02	C10,3
C10,4										1.00	-.13	.02	.03	C10,4
C11,1											1.00	.05	.02	C11,1
C12,1												1.00	-.00	C12,1
C12,2													1.00	C12,2

TABLE 7. GEOPOTENTIAL COEFFICIENT CORRELATION MATRIX - TESSERAL COEFFICIENTS (PART 27 of 31)

	C13,12	C13,13	C14,1	C15,12	C15,13	C15,14	S9,1	S9,2	S9,9	S10,1	S10,2	
C9,1	.00	-.00	.21	.00	.00	.03	-.02	.06	.00	.03	-.01	C9,1
C9,2	-.00	-.03	-.05	-.00	-.03	.05	.01	.02	.00	-.01	.01	C9,2
C9,9	.00	.00	.00	.00	.00	.00	.00	.00	.00	.00	.00	C9,9
C10,1	-.01	.02	.75	-.01	.02	.01	-.08	-.04	.00	-.04	.07	C10,1
C10,2	-.01	.01	.03	-.01	.01	-.00	.04	.02	.00	-.00	.05	C10,2
C10,3	-.01	.00	-.07	-.01	-.00	.02	-.03	.03	.00	.00	.03	C10,3
C10,4	.03	.03	.02	.03	.03	.02	-.04	-.01	.00	-.04	.01	C10,4
C11,1	.03	-.01	-.03	.03	-.02	.02	.04	-.08	.00	.05	-.09	C11,1
C12,1	-.00	.02	-.51	-.00	.01	-.00	-.01	-.06	.00	.01	-.10	C12,1
C12,2	-.05	-.00	.00	-.04	-.05	-.00	.03	.02	.00	.01	.10	C12,2
C13,12	1.00	-.05	-.00	1.00	-.04	-.05	.03	-.04	.00	.01	-.01	C13,12
C13,13		1.00	.01	-.05	.92	.07	-.03	-.02	.00	-.00	-.01	C13,13
C14,1			1.00	-.00	.01	.01	-.10	-.07	.00	-.05	.03	C14,1
C15,12				1.00	-.04	-.05	.03	-.04	.00	.01	-.01	C15,12
C15,13					1.00	.06	-.04	-.01	.00	-.02	-.01	C15,13
C15,14						1.00	.03	-.00	.00	.02	.00	C15,14
S9,1							1.00	-.02	.00	.18	.00	S9,1

TABLE 7. GEOPOTENTIAL COEFFICIENT CORRELATION MATRIX - TESSERAL COEFFICIENTS (PART 28 of 31)

	S10,3	S10,4	S11,1	S12,1	S12,2	S13,12	S13,13	S14,1	S15,12	S15,13	S15,14	
C9,1	.06	.09	-.03	-.01	-.02	.02	.00	.04	.02	.00	.02	C9,1
C9,2	-.04	.04	-.05	-.07	.03	.05	-.01	.01	.05	-.00	.01	C9,2
C9,9	.00	.00	.00	.00	.00	.00	.00	.00	.00	.00	.00	C9,9
C10,1	-.00	.03	-.05	.02	-.07	-.01	.03	.02	-.01	.03	-.01	C10,1
C10,2	.02	-.00	-.05	-.02	.04	-.01	.00	-.00	-.01	-.00	-.01	C10,2
C10,3	.02	-.06	.05	-.07	.11	.04	-.01	.08	.04	-.01	-.00	C10,3
C10,4	-.01	-.01	.07	-.02	.03	-.02	-.02	-.02	-.02	-.01	-.03	C10,4
C11,1	.04	.01	.04	.01	-.02	.02	.01	.00	.02	.01	.03	C11,1
C12,1	-.02	-.13	.03	-.02	-.00	.01	.05	-.00	.02	-.02	-.00	C12,1
C12,2	.12	.00	.04	.07	.01	-.00	.00	.01	.00	-.07	-.00	C12,2
C13,12	-.03	.03	.04	-.03	-.00	.01	-.00	.00	.01	.00	-.07	C13,12
C13,13	-.02	-.01	-.02	.01	-.01	-.01	.04	-.01	-.01	.03	.07	C13,13
C14,1	.01	.06	-.04	.01	-.13	.00	.02	.00	.00	.02	-.01	C14,1
C15,12	-.03	.03	.04	-.03	-.00	.01	-.00	.00	.01	.00	-.07	C15,12
C15,13	-.02	-.01	-.00	.01	-.01	-.01	.04	-.02	-.01	.03	.06	C15,13
C15,14	.02	.03	.03	-.01	.01	.10	-.02	.03	.10	-.01	.00	C15,14
S9,1	.02	.04	.05	-.19	.02	.03	-.04	.12	.03	-.02	-.01	S9,1

TABLE 7. GEOPOTENTIAL COEFFICIENT CORRELATION MATRIX - TESSERAL COEFFICIENTS (PART 29 of 31)

	C13,12	C13,13	C14,1	C15,12	C15,13	C15,14	S9,1	S9,2	S9,9	S10,1	S10,2	
S9,2								1.00	.00	-.02	.20	S9,2
S9,9									1.00	.00	.00	S9,9
S10,1										1.00	.01	S10,1
S10,2											1.00	S10,2

TABLE 7. GEOPOTENTIAL COEFFICIENT CORRELATION MATRIX - TESSERAL COEFFICIENTS (PART 30 of 31)

	S10,3	S10,4	S11,1	S12,1	S12,2	S13,12	S13,13	S14,1	S15,12	S15,13	S15,14	
S9,2	.02	.02	-.01	.01	-.14	-.02	-.01	.01	-.01	-.01	.02	S9,2
S9,9	.00	.00	.00	.00	.00	.00	.00	.00	.00	.00	.00	S9,9
S10,1	.02	.03	-.05	-.79	-.01	.01	-.00	.73	.01	.01	.02	S10,1
S10,2	-.00	.06	.02	-.03	-.09	-.02	.01	.01	-.02	.02	-.01	S10,2
S10,3	1.00	-.12	.04	.00	.03	-.01	-.03	-.02	-.01	-.03	.03	S10,3
S10,4		1.00	.07	-.04	-.00	.04	.02	.02	.04	.02	.01	S10,4
S11,1			1.00	.08	.03	.03	-.04	-.10	.03	-.05	-.01	S11,1
S12,1				1.00	-.01	.00	-.04	-.01	.00	-.00	-.00	S12,1
S12,2					1.00	-.02	.00	-.02	-.02	.00	-.01	S12,2
S13,12						1.00	-.03	-.01	1.00	-.02	-.03	S13,12
S13,13							1.00	-.01	-.03	.92	.03	S13,13
S14,1								1.00	-.01	.00	.01	S14,1
S15,12									1.00	-.02	-.03	S15,12
S15,13										1.00	.02	S15,13
S15,14											1.00	S15,14

TABLE 7. GEOPOTENTIAL COEFFICIENT CORRELATION MATRIX - TESSERAL COEFFICIENTS (PART 31 of 31)

APPENDIX IV

TRANSITION MATRIX $\Phi(t,t_o)$ IN RECTANGULAR COORDINATES

Repeating equations (2.2),

$$\underline{r} = \underline{r}_0 \, f(\Delta E) + \dot{\underline{r}}_0 \, g(\Delta E),$$

$$\dot{\underline{r}} = d\underline{r}/dt = \underline{r}_0 \, f_t(\Delta E) + \dot{\underline{r}}_0 \, g_t(\Delta E), \qquad \text{(IV.1)}$$

where the f and g functions are defined with equations (2.2). From (2.6), the Keplerian transition matrix is

$$\Phi(t,t_0) = \left[\begin{array}{c|c} \partial \underline{r}/\partial \underline{r}_0 & \partial \underline{r}/\partial \dot{\underline{r}}_0 \\ \hline \partial \dot{\underline{r}}/\partial \underline{r}_0 & \partial \dot{\underline{r}}/\partial \dot{\underline{r}}_0 \end{array}\right] \qquad \text{(IV.2)}$$

evaluated on the two-body orbit (IV.1), where the state vector is, of course,

$$\underline{x} = \left[\begin{array}{c} \underline{r} \\ \hline \dot{\underline{r}} \end{array}\right] .$$

From (IV.1), the four 3 x 3 submatrices are

$$\partial \underline{r}/\partial \underline{r}_0 = fI + \underline{r}_0(\partial f/\partial \underline{r}_0) + \dot{\underline{r}}_0 (\partial g/\partial \underline{r}_0) ,$$

$$\partial \underline{r}/\partial \dot{\underline{r}}_0 = \underline{r}_0(\partial f/\partial \dot{\underline{r}}_0) + gI + \dot{\underline{r}}_0 (\partial g/\partial \dot{\underline{r}}_0) ,$$

$$\partial \dot{\underline{r}} / \partial \underline{r}_0 = f_t I + \underline{r}_0 (\partial f_t / \partial \underline{r}_0) + \dot{\underline{r}}_0 (\partial g_t / \partial \underline{r}_0) ,$$

$$\partial \dot{\underline{r}} / \partial \dot{\underline{r}}_0 = \underline{r}_0 (\partial f_t / \partial \dot{\underline{r}}_0) + g_t I + \dot{\underline{r}}_0 (\partial g_t / \partial \dot{\underline{r}}_0) , \qquad \text{(IV.3)}$$

where, for example, the row vector

$$(\partial f / \partial \underline{r}_0) = (\partial f / \partial x_{01}, \partial f / \partial x_{02}, \partial f / \partial x_{03}).$$

Noting that

$$x_{i+3} = \dot{x}_i , \qquad 1 \leq i \leq 3,$$

we can employ for the sake of clarity the convention that the x subscripts will never exceed 3 and derivatives will be denoted by ($\cdot$) rather than by the subscripts 4 to 6. Then

$$\underline{r} = \begin{bmatrix} x_1 \\ x_2 \\ x_3 \end{bmatrix} , \qquad \dot{\underline{r}} = \begin{bmatrix} \dot{x}_1 \\ \dot{x}_2 \\ \dot{x}_3 \end{bmatrix} ,$$

$$r = (x_1^2 + x_2^2 + x_3^2)^{\frac{1}{2}}, \qquad \dot{r} = (\dot{x}_1^2 + \dot{x}_2^2 + \dot{x}_3^2)^{\frac{1}{2}},$$

$$\underline{r}_0 = \begin{bmatrix} x_{01} \\ x_{02} \\ x_{03} \end{bmatrix} , \qquad \dot{\underline{r}}_0 = \begin{bmatrix} \dot{x}_{01} \\ \dot{x}_{02} \\ \dot{x}_{03} \end{bmatrix}$$

$$r_0 = (x_{01}^2 + x_{02}^2 + x_{03}^2)^{\frac{1}{2}}, \qquad \dot{r}_0 = (\dot{x}_{01}^2 + \dot{x}_{02}^2 + \dot{x}_{03}^2)^{\frac{1}{2}}.$$

In these terms, we can write the semi-major axis as

$$a = \mu r_0 / \ (2\mu - r_0 \dot{r}_0^2);$$

the inner product

$$d_0 = \underline{r}_0 \cdot \dot{\underline{r}}_0 = x_{01}\dot{x}_{01} + x_{02}\dot{x}_{02} + x_{03}\dot{x}_{03}$$

will also be useful.

From the definitions of the f and g functions,

$$\partial f/\partial x_{0i} = \left[\frac{a x_{0i} - r_0^2 (\partial a/\partial x_{oi})}{r_0^3}\right] (1-\cos \Delta E) - (a/r_0)\sin \Delta E \frac{\partial(\Delta E)}{\partial x_{0i}},$$

$$\partial f/\partial \dot{x}_{0i} = - \frac{(\partial a/\partial \dot{x}_{0i})}{r_0} (1 - \cos \Delta E) - (a/r_0) \sin \Delta E \frac{\partial(\Delta E)}{\partial \dot{x}_{0i}},$$

$$\partial g/\partial x_{0i} = \frac{(\mu a)^{\frac{1}{2}} x_{oi} \sin \Delta E + a r_0 \dot{x}_{0i}(1-\cos \Delta E)}{\mu r_0} + A_1(\partial a/\partial x_{0i}) + A_5 \frac{\partial(\Delta E)}{\partial x_{0i}},$$

$$\partial g/\partial \dot{x}_{0i} = (a/\mu) x_{0i} (1-\cos \Delta E) + A_1 (\partial a/\partial \dot{x}_{0i}) + A_5 \frac{\partial(\Delta E)}{\partial \dot{x}_{0i}},$$

$$\partial f_t/\partial x_{0i} = A_2 \left[2r x_{0i} + 2a r_0^2 \frac{\partial(r/a)}{\partial x_{0i}} + (r/a) r_0^2 \frac{\partial a}{\partial x_{0i}}\right] - \frac{(ua)^{\frac{1}{2}}}{r r_0} \cos \Delta E \frac{\partial(\Delta E)}{\partial x_{0i}}$$

$$\partial f_t/\partial \dot{x}_{0i} = A_2 r_0^2 \left[2a \frac{\partial(r/a)}{\partial \dot{x}_{0i}} + (r/a) \frac{\partial a}{\partial \dot{x}_{0i}}\right] - \frac{(ua)^{\frac{1}{2}}}{r r_0} \cos \Delta E \frac{\partial(\Delta E)}{\partial \dot{x}_{0i}}$$

$$\partial g_t/\partial x_{0i} = A_3 \frac{\partial(r/a)}{\partial x_{0i}} - (a/r) \sin \Delta E \frac{\partial(\Delta E)}{\partial x_{0i}},$$

$$\partial g_t/\partial \dot{x}_{0i} = A_3 \frac{\partial(r/a)}{\partial \dot{x}_{0i}} - (a/r) \sin \Delta E \frac{\partial(\Delta E)}{\partial \dot{x}_{0i}}. \qquad \text{(IV.4)}$$

The partials that appear in (IV.4) are simply

$$\partial a/\partial x_{0i} = \frac{x_{0i}\,(\mu + a\dot{r}_0^{\,2})}{r_0(2\mu - r_0\dot{r}_0^{\,2})} \quad ,$$

$$\partial a/\partial \dot{x}_{0i} = \frac{2\mu r_0^{\,2}\dot{x}_{0i}}{(2\mu - r_0\dot{r}_0^{\,2})^2} \quad ,$$

$$\frac{\partial(r/a)}{\partial x_{0i}} = \frac{\mu^{-1}x_{0i}\cos\Delta E + a^{-2}r_0\dot{x}_{0i}\sin\Delta E}{\mu^{-\frac{1}{2}}a r_0} - A_4(\partial a/\partial x_{0i})$$

$$+ A_6\,(\partial\Delta E/\partial x_{0i}),$$

$$\frac{\partial(r/a)}{\partial \dot{x}_{0i}} = \frac{x_{0i}\sin\Delta E}{(\mu a)^{\frac{1}{2}}} - A_4(\partial a/\partial \dot{x}_{0i})$$

$$+ A_6(\partial\Delta E/\partial \dot{x}_{0i}) \quad ,$$

where

$$\frac{\partial\Delta E}{\partial x_{0i}} = A_8\left[A_7(\partial a/\partial x_{0i}) - \frac{\sin\Delta E}{a r_0}\,x_{0i} - \frac{(1-\cos\Delta E)}{(\mu a)^{\frac{1}{2}}}\,\dot{x}_{0i}\right]$$

$$\frac{\partial\Delta E}{\partial \dot{x}_{0i}} = A_8\left[A_7(\partial a/\partial \dot{x}_{0i}) - \frac{(1-\cos\Delta E)}{(\mu a)^{\frac{1}{2}}}\,x_{0i}\right]$$

and the parameters A_1 through A_8 are

$$A_1 = \frac{\mu^{\frac{1}{2}}r_0\sin\Delta E + 2a^{\frac{1}{2}}d_0(1-\cos\Delta E)}{2\mu a^{\frac{1}{2}}} \quad ,$$

$$A_2 = \frac{(\mu a)^{\frac{1}{2}}\sin\Delta E}{2r^2 r_0^{\,3}} \quad ,$$

$$A_3 = (a/r)^2(1-\cos \Delta E),$$

$$A_4 = \frac{2\mu^{\frac{1}{2}} r_0 \cos \Delta E + a^{\frac{1}{2}} d_0 \sin \Delta E}{2\mu^{\frac{1}{2}} a^2}$$

$$A_5 = \frac{(au)^{\frac{1}{2}} r_0 \cos \Delta E + a d_0 \sin \Delta E}{u},$$

$$A_6 = (1 - r_0/a) \sin \Delta E + d_0(\cos \Delta E)/(ua)^{\frac{1}{2}},$$

$$A_7 = (r_0/a^2) \sin \Delta E + \frac{d_0(1 - \cos \Delta E)}{2\,(ua^3)^{\frac{1}{2}}} - (3/2)(u/a^5)^{\frac{1}{2}} \Delta t,$$

$$A_8 = \frac{1}{1 + d_0 (\sin \Delta E)/(ua)^{\frac{1}{2}} - (1-r_0/a) \cos \Delta E}.$$

Clearly, when $r_0 \dot{r}_0^2$ approaches 2μ, the elements of the transition matrix tend to be ill-conditioned because of $\underline{a}$ and its partials. This corresponds to a near-parabolic orbit. Although this case does not apply to the present study, it was considered in the development of MINIVAR, and hence the so-called NASA orbital-element states are used there. Only one of the states reflects $\underline{a}$, and the ill-conditionedness of the corresponding transition matrix is virtually avoided in the near-parabolic case.

To go from the transition matrix of this appendix to the form used in MINIVAR requires only a point transformation, as outlined in Reference 4. A comparison of this sort was programmed, and in all cases the two transition matrices agreed to within round-off tolerances. Thus, both the algebraic details developed here and the MINIVAR development are sustantiated.

APPENDIX V

COMPARISON OF MAXIMUM LIKELIHOOD AND MINIMUM-VARIANCE ESTIMATION OF SPACE-VEHICLE MASS

Suppose that the sequence $\{\underline{x}(k);\ k = 0,1,\ldots\}$ of real random n-vectors $\underline{x}(k)$ is governed by the recursive equation

$$\underline{x}(k+1) = \Phi(k+1,\ k)\ \underline{x}(k) + \underline{f}(k) + \alpha\underline{g}(k), \tag{V.1}$$

where $\Phi(k+1,\ k)$ is a given n x n transition matrix, α is an unknown system parameter (such as the area-to-mass ratio of the main report) which will be regarded as a real random variable having a *priori* mean $\bar{\alpha}$ and variance σ^2; $\underline{f}(k)$ and $\underline{g}(k)$ are random n-vectors with means $\bar{\underline{f}}(k)$ and $\bar{\underline{g}}(k)$ respectively, and $\underline{x}(0)$ is a random n-vector with mean $\bar{\underline{x}}(0)$ and covariance matrix P_0. In addition, suppose that for each k = 1, 2, ..., N, we have available an m x 1 observation vector $\underline{z}(k)$ given by

$$\underline{z}(k) = H(k)\underline{x}(k) + \underline{v}(k), \tag{V.2}$$

where H(k) is a given m x n matrix and $\underline{v}(k)$ is a random m-vector of observation errors having mean zero and covariance matrix R(k). Finally, we will assume that all of the vectors $\underline{x}(0)$, $\underline{f}(0)$, $\underline{f}(1),\ldots,$ $\underline{g}(0)$, $\underline{g}(1),\ldots,$ $\underline{v}(1), \underline{v}(2),\ldots,$ are pairwise uncorrelated, and that the random parameter α is strictly independent of all of these vectors. Using the available observations, we wish to determine an optimal

(in some well-defined sense) a posteriori estimate of the parameter α.

For any random vector $\underline{y}$, if $\bar{\underline{y}}$ is the a priori (unconditional) mean of $\underline{y}$, we will write $\tilde{\underline{y}} = \underline{y} - \bar{\underline{y}}$; i.e., $\underline{y} = \bar{\underline{y}} + \tilde{\underline{y}}$ is a well-defined decomposition of $\underline{y}$ into a deterministic part and a zero mean random part. In equation (V.1), we then define $\underline{e}(k) = \tilde{\underline{f}}(k) + \alpha\tilde{\underline{g}}(k)$, and note that $\underline{e}(k)$ is orthogonal to $\tilde{\underline{x}}(0)$, $\underline{v}(1)$, $\underline{v}(2),\ldots,$ $\tilde{\alpha}$, and to each $\underline{e}(j)$ for $j \neq k$. With this notation we have

$$\underline{x}(k+1) = \Phi(k+1,k)\underline{x}(k) + \bar{\underline{f}}(k) + \alpha\bar{\underline{g}}(k) + \underline{e}(k). \qquad \text{(V.1a)}$$

The covariance matrix of the zero mean random vector $\underline{e}(k)$ will be denoted by $Q(k)$.

If h_1 and h_2 are zero mean real random variables with finite variances, we define the scalar product $(h_1, h_2) = Eh_1h_2$ (where $E(.)$ is the expectation operator), and the norm $\|h\| = (h,h)^{\frac{1}{2}}$. Let $\mathcal{H}$ denote the Hilbert space which is the closure in this norm of the linear manifold generated by all the components of $\tilde{\underline{x}}(0)$, $\underline{e}(1)$, $\underline{e}(2),\ldots,$ $\underline{v}(1)$, $\underline{v}(2),\ldots,$ and by $\tilde{\alpha}$. Clearly, for each $k = 1, 2,\ldots,$ the components of $\tilde{\underline{x}}(k)$ and $\tilde{\underline{z}}(k)$ are elements of $\mathcal{H}$, since each of these components is expressible as a finite linear sum of elements of the generating set. For each positive integer N, let $\mathcal{M}(N)$ be the finite subspace of $\mathcal{H}$ which is spanned by the components of $\tilde{\underline{z}}(1),\ldots,$ $\tilde{\underline{z}}(N)$, and let K_N be the orthogonal projection on $\mathcal{M}(N)$.

If h_N is an arbitrary element of $\mathcal{M}(N)$, then

$$\|\tilde{\alpha} - h_N\| = \|\tilde{\alpha} - K_N\tilde{\alpha}\| + \|K_N\tilde{\alpha} - h_N\|, \qquad \text{(V.3)}$$

since $K_N\tilde{\alpha} - h_N \in \mathcal{M}(N)$ and $\tilde{\alpha} - K_N\tilde{\alpha} \perp \mathcal{M}(N)$ by the orthogonal projection theorem. From (E.3) it follows that $K_N\tilde{\alpha}$ is the unique element of $\mathcal{M}(N)$ which minimizes the distance from $\tilde{\alpha}$ to $\mathcal{M}(N)$; i.e., $K_N\tilde{\alpha}$ is the unique (up to equivalence) minimum-variance, linear estimate of $\tilde{\alpha}$ with respect to the observations $\underline{\tilde{z}}(1),\ldots, \underline{\tilde{z}}(N)$.

If the components of $\underline{\tilde{z}}(1),\ldots\underline{\tilde{z}}(N)$ are all linearly independent, then the projection $K_N\tilde{\alpha}$ can be represented as follows. Let $\underline{\tilde{Z}}_N$ denote the vector whose transpose is defined as $\underline{\tilde{Z}}_N^T = \left[\underline{\tilde{z}}^T(1),\ldots, \underline{\tilde{z}}^T(N)\right]$. The linear independence of the components of $\underline{\tilde{Z}}_N$ means that the matrix $\text{cov}\,(\underline{\tilde{Z}}_N) = E\underline{\tilde{Z}}_N\underline{\tilde{Z}}_N^T$, which we will henceforth call U_N, is positive definite. Setting $\underline{\tilde{Y}}_N = U_N^{-\frac{1}{2}}\underline{\tilde{Z}}_N$, we see that $\text{cov}\,(\underline{\tilde{Y}}_N) = I$. Therefore, the components of $\underline{\tilde{Y}}_N$ comprise an orthonormal basis for $\mathcal{M}(N)$, and we can write

$$K_N\tilde{\alpha} = (E\tilde{\alpha}\underline{\tilde{Y}}_N)^T\underline{\tilde{Y}}_N = (E\tilde{\alpha}\underline{\tilde{Z}}_N)^T U_N^{-1}\underline{\tilde{Z}}_N, \qquad (V.4)$$

where the components of $E\tilde{\alpha}\underline{\tilde{Y}}_N$ are the Fourier coefficients of $\tilde{\alpha}$ with respect to the orthonormalized observations. Since $\tilde{\alpha} = \alpha - \bar{\alpha}$, the minimum-variance, linear estimate of α based on N observation points is given by

$$\hat{\alpha}(N) = \bar{\alpha} + (E\tilde{\alpha}\underline{\tilde{Z}}_N)^T U_N^{-1}(\underline{Z}_N - \underline{\bar{Z}}_N). \qquad (V.5)$$

The variance of the estimation error may be computed as follows:

$$E(\alpha - \hat{\alpha}(N))^2 = \| \tilde{\alpha} - K_N \tilde{\alpha} \|^2$$

$$= \sigma^2 - (E\tilde{\alpha}\underline{\tilde{Z}}_N)^T U_N^{-1} (E\tilde{\alpha}\underline{\tilde{Z}}_N). \qquad (V.6)$$

REMARK: We note that even if the components of $\underline{\tilde{Z}}_N$ are not all linearly independent, equations (V.4), (V.5) and (V.6) remain valid if we replace U_N^{-1} by $U_N^{\dagger}$, the generalized inverse of the positive semi-definite matrix U_N in the sense of Penrose[10]. The question of linear independence, which we will not consider in this appendix, is probably most easily discussed using the notation of the sequential estimation procedure of Kalman, described below. A sufficient, but by no means necessary, condition for the linear independence of the components of the $\underline{\tilde{z}}(i)$'s is that rank $(R(k)) = m$ for each k.

Let us suppose for a moment that the random variable $\tilde{\alpha}$ and each of the random vectors $\underline{\tilde{x}}(0)$, $\underline{e}(0)$, $\underline{e}(1),\ldots$, $\underline{v}(1)$, $\underline{v}(2),\ldots$, has a Gaussian distribution. In this case, the orthogonality of these random quantities implies that they are actually strictly independent of one another. For our purposes, the important fact is that $\tilde{\alpha}$ and the components of $\underline{\tilde{Z}}_N$ will then have a joint Gaussian distribution. Hence, it is quite easy to obtain the maximum likelihood estimate of α given $\underline{\tilde{Z}}_N$. For this and later computations, we will need the

following result.

LEMMA: Let the symmetric, positive definite matrix M be partitioned as

$$M = \begin{bmatrix} A & B \\ B^T & C \end{bmatrix}$$

where A is p x p, B is p x q, and C is q x q. Then the matrices A, C, $A - BC^{-1}B^T$ and $C-B^TA^{-1}B$ are each positive definite. Furthermore, if $\underline{x}$ and $\underline{u}$ are p-vectors and $\underline{y}$ and $\underline{v}$ are q-vectors, then the bilinear form

$$Q(\underline{x}, \underline{y}, \underline{u}, \underline{v}) = [\underline{x}^T, \underline{y}^T] \begin{bmatrix} A & B \\ B^T & C \end{bmatrix}^{-1} \begin{bmatrix} \underline{u} \\ \underline{v} \end{bmatrix}$$

admits the expansions

(i) $Q(\underline{x}, \underline{y}, \underline{u}, \underline{v}) = \underline{x}^TA^{-1}\underline{u} + (\underline{y} - B^TA^{-1}\underline{x})^T(C-B^TA^{-1}B)^{-1}(\underline{v}-B^TA^{-1}\underline{u})$,

and

(ii) $Q(\underline{x}, \underline{y}, \underline{u}, \underline{v}) = \underline{y}^TC^{-1}\underline{v} + (\underline{x} - BC^{-1}\underline{y})^T(A-BC^{-1}B^T)^{-1}(\underline{u} - BC^{-1}\underline{v})$.

PROOF: The positive definiteness of A and C is obvious.

Writing

$$\begin{bmatrix} A & B \\ B^T & C \end{bmatrix} = \begin{bmatrix} A & 0 \\ B^T & I \end{bmatrix} \begin{bmatrix} I & A^{-1}B \\ 0 & C-B^TA^{-1}B \end{bmatrix} ,$$

and taking determinants of both sides, we see that $|C-B^TA^{-1}B| > 0$, which shows that $(C-B^TA^{-1}B)^{-1}$ exists. Inverting both sides of the above decomposition then gives

$$\begin{bmatrix} A & B \\ B^T & C \end{bmatrix}^{-1} = \begin{bmatrix} I & -A^{-1}B(C-B^TA^{-1}B)^{-1} \\ 0 & (C-B^TA^{-1}B)^{-1} \end{bmatrix} \begin{bmatrix} A^{-1} & 0 \\ -B^TA^{-1} & I \end{bmatrix} .$$

If $Q(\underline{x}, \underline{y}, \underline{u}, \underline{v},)$ is computed using the representation of M^{-1} given by the above equation, (i) is obtained. Setting $\underline{x} = \underline{u} = 0$, $\underline{y} = \underline{v}$, the positive definiteness of $C-B^TA^{-1}B$ is apparent. The proof of the remaining statements is similar.

The maximum likelihood estimate of α given $\underset{\sim}{Z}_N$ is simply the value of α which minimizes the quadratic form

$$[\alpha, \underset{\sim}{Z}_N^T] \begin{bmatrix} \sigma^2 & E\alpha\underset{\sim}{Z}_N^T \\ E\alpha\underset{\sim}{Z}_N & U_N \end{bmatrix}^{-1} \begin{bmatrix} \alpha \\ \underset{\sim}{Z}_N \end{bmatrix} ,$$

which occurs in the exponential factor of the joint Gaussian density of α and $\underline{Z}_N$. Using expansion (ii) of the above lemma, this quadratic form may be written as

$$\frac{(\tilde{\alpha}-(E\tilde{\alpha}\tilde{\underline{Z}}_N)^T U_N^{-1}\tilde{\underline{Z}}_N)^2}{(\sigma^2-(E\tilde{\alpha}\tilde{\underline{Z}}_N)^T U_N^{-1}(E\tilde{\alpha}\tilde{\underline{Z}}_N))} + \tilde{\underline{Z}}_N^T U_N^{-1}\tilde{\underline{Z}}_N. \qquad (V.7)$$

From this last expression, we see that the maximum likelihood estimate of α given $\tilde{\underline{Z}}_N$ under the Gaussian assumptions is just the same as the general linear, minimum variance estimate (V.5), and the estimation error also has the same variance (V.6).

Returning now to the wide-sense, minimum-variance point of view, we note that not only for $\tilde{\alpha}$, but in fact for any element $\tilde{h} \in \mathcal{H}$, the projection

$$K_N\tilde{h} = (E\tilde{h}\tilde{\underline{Z}}_N^T)\, U_N^{-1}\tilde{\underline{Z}}_N \qquad (V.8)$$

is the optimum linear estimate of $\tilde{h}$ given $\tilde{\underline{Z}}_N$ in the sense of the norm of $\mathcal{H}$, i.e., in the minimum-variance sense. If $\underline{y}$ is a random vector such that the components of the associated vector $\tilde{\underline{y}}$ are elements of $\mathcal{H}$, we will denote by $K_N\tilde{\underline{y}}$ that vector whose components are the projections on $\mathcal{M}(N)$ of the components of $\tilde{\underline{y}}$. Hence, we can write

$$K_N\tilde{\underline{y}} = (E\tilde{\underline{y}}\tilde{\underline{Z}}_N^T)\, U_N^{-1}\tilde{\underline{Z}}_N. \qquad (V.9)$$

The covariance matrix of the estimation error will then be given by

$$\left[(\tilde{y}^i - K_N \tilde{y}^i,\ \tilde{y}^j - K_N \tilde{y}^j)\right]$$

$$= \text{cov}\,(\tilde{\underline{y}}) - (E\tilde{\underline{y}}\tilde{\underline{Z}}_N^T)\, U_N^{-1}\, (E\tilde{\underline{Z}}_N\tilde{\underline{y}}^T), \qquad \text{(V.10)}$$

where $\tilde{y}^i$ and $\tilde{y}^j$ denote the $i^{\underline{th}}$ and $j^{\underline{th}}$ components of the vector $\tilde{\underline{y}}$. The minimum-variance, linear estimate of the original vector $\underline{y}$ is then $\bar{\underline{y}} + K_N\tilde{\underline{y}}$, and the covariance matrix of the error involved in this estimate is also given by (V.10).

We will now re-write the system (V.1a) in the augmented form

$$\underline{y}(k+1) = \Phi_y(k+1,\ k)\ \underline{y}(k) + \underline{u}(k) + \underline{w}(k), \qquad \text{(V.11)}$$

where

$$\underline{y}(k) = \begin{bmatrix} \underline{x}(k) \\ \alpha \end{bmatrix} \quad ; \quad \underline{u}(k) = \begin{bmatrix} \bar{\underline{f}}(k) \\ 0 \end{bmatrix} \quad ; \quad \underline{w}(k) = \begin{bmatrix} \underline{e}(k) \\ 0 \end{bmatrix} \quad ;$$

and

$$\Phi_y(k+1,k) = \begin{bmatrix} \Phi(k+1,k) & \bar{\underline{g}}(k) \\ 0 & 1 \end{bmatrix} \quad .$$

If M(k) is defined as the m x (n+1) matrix $[\,H(k),\ 0\,]$, we then have

$$\underline{z}(k) = M(k)\,\underline{y}(k) + \underline{v}(k) \tag{V.12}$$

instead of equation (V.2). Together with (V.11) and (V.12), we have the associated equations

$$\bar{\underline{y}}(k+1) = \Phi_y(k+1,k)\bar{\underline{y}}(k) + \underline{u}(k), \tag{V.11a}$$

$$\tilde{\underline{y}}(k+1) = \Phi_y(k+1,k)\tilde{\underline{y}}(k) + \underline{w}(k) \tag{V.11b}$$

$$\bar{\underline{z}}(k) = M(k)\bar{\underline{y}}(k), \text{ and} \tag{V.12a}$$

$$\tilde{\underline{z}}(k) = M(k)\tilde{\underline{y}}(k) + \underline{v}(k). \tag{V.12b}$$

The optimal estimate of $\underline{y}(k)$ given $\tilde{\underline{Z}}_N = \underline{Z}_N - \bar{\underline{Z}}_N$ will be denoted by $\hat{\underline{y}}(k/N)$; hence,

$$\hat{\underline{y}}(k/N) = \bar{\underline{y}}(k) + K_N\tilde{\underline{y}}(k), \tag{V.13}$$

since the components of $\tilde{\underline{y}}(k)$ are obviously elements of $\mathcal{H}$. The estimation error associated with this estimate will be designated

as $\tilde{\underline{y}}(k/N)$, so that

$$\tilde{\underline{y}}(k/N) = \underline{y}(k) - \hat{\underline{y}}(k/N)$$

$$= \tilde{\underline{y}}(k) - K_N \tilde{\underline{y}}(k). \qquad (V.14)$$

setting $P_{yy}(k/N) = \text{cov}\,(\tilde{\underline{y}}(k/N))$, it follows from equation (V.10) that

$$P_{yy}(k/N) = \text{cov}\,(\tilde{\underline{y}}(k)) - (E\tilde{\underline{y}}(k)\tilde{\underline{Z}}_N^T)\, U_N^{-1}\, (E\tilde{\underline{Z}}_N\tilde{\underline{y}}^T(k)). \qquad (V.15)$$

Since $\underline{w}(k)$ and $\tilde{\underline{Z}}_k$ are orthogonal for each k, we compute

$$\hat{\underline{y}}(k/k-1) = \Phi_y(k,k-1)\bar{\underline{y}}(k-1) + \underline{u}(k-1) + K_{k-1}(\Phi_y(k,k-1)\tilde{\underline{y}}(k-1) + \underline{w}(k-1))$$

$$= \Phi_y(k,k-1)\hat{\underline{y}}(k-1/k-1) + \underline{u}(k-1). \qquad (V.16)$$

Subtracting (V.16) from (V.11) (after replacing k by k-1 in (V.11)), and evaluating the covariance matrix of the resulting expression, produces

$$P_{yy}(k/k-1) = \Phi_y(k,k-1)P_{yy}(k-1/k-1)\ \Phi_y^T(k,k-1) + \begin{bmatrix} Q(k-1) & 0 \\ 0 & 0 \end{bmatrix}. \qquad (V.17)$$

Applying expansion (i) of the above lemma, we now compute

$$K_k\tilde{\underline{y}}(k) = (E\tilde{\underline{y}}(k)\tilde{\underline{Z}}_k^T)\, U_k^{-1}\tilde{\underline{Z}}_k$$

$$= \left[E\tilde{\underline{y}}(k)\tilde{\underline{Z}}_{k-1}^T,\ E\tilde{\underline{y}}(k)\tilde{\underline{z}}^T(k)\right] \begin{bmatrix} U_{k-1} & E\tilde{\underline{Z}}_{k-1}\tilde{\underline{z}}^T(k) \\ E\tilde{\underline{z}}(k)\tilde{\underline{Z}}_{k-1}^T & E\tilde{\underline{z}}(k)\tilde{\underline{z}}^T(k) \end{bmatrix}^{-1} \begin{bmatrix} \tilde{\underline{Z}}_{k-1} \\ \tilde{\underline{z}}(k) \end{bmatrix}$$

$$= K_{k-1}\tilde{\underline{y}}(k) + B_y(k)\,(\tilde{\underline{z}}(k) - K_{k-1}\tilde{\underline{z}}(k)), \qquad (V.18)$$

where

$$B_y(k) = \left[E\tilde{\underline{y}}(k)\tilde{\underline{z}}^T(k) - (E\tilde{\underline{y}}(k)\tilde{\underline{Z}}_{k-1}^T)\, U_{k-1}^{-1}(E\tilde{\underline{Z}}_{k-1}\tilde{\underline{z}}^T(k))\right]$$

$$\cdot\left[E\tilde{\underline{z}}(k)\tilde{\underline{z}}^T(k) - (E\tilde{\underline{z}}(k)\tilde{\underline{Z}}_{k-1}^T)\, U_{k-1}^{-1}\,(E\tilde{\underline{Z}}_{k-1}\tilde{\underline{z}}^T(k))\right]^{-1}.$$

Since $\underline{v}(k)$ is orthogonal to both $\tilde{\underline{y}}(k)$ and $\tilde{\underline{Z}}_{k-1}$, we can substitute the right side of (V.12b) for $\tilde{\underline{z}}(k)$ in the latter expression, and obtain

$$B_y(k) = P_{yy}(k/k-1)M^T(k)\left[M(k)P_{yy}(k/k-1)M^T(k) + R(k)\right]^{-1} \qquad (V.19)$$

The orthogonality of $\underline{v}(k)$ and $\tilde{\underline{Z}}_{k-1}$ also implies that $K_{k-1}\tilde{\underline{z}}(k)$ $=$ $M(k)K_{k-1}\tilde{\underline{y}}(k)$; hence, the combination of (V.13) and (V.18) produces

$$\hat{\underline{y}}(k/k) = \bar{\underline{y}}(k) + K_{k-1}\tilde{\underline{y}}(k) + B_y(k)\left[\underline{z}(k) - M(k)\left[\bar{\underline{y}}(k) + K_{k-1}\tilde{\underline{y}}(k)\right]\right]$$

$$= \hat{\underline{y}}(k/k-1) + B_y(k)\left[\underline{z}(k) - M(k)\hat{\underline{y}}(k/k-1)\right]. \qquad (V.20)$$

From (V.11b), (V.12b), (V.14) and (V.18), we find

$$\tilde{\underline{y}}(k/k) = \tilde{\underline{y}}(k) - K_{k-1}\tilde{\underline{y}}(k) - B_y(k)M(k)\left[\tilde{\underline{y}}(k) - K_{k-1}\tilde{\underline{y}}(k)\right] - B_y(k)\underline{v}(k)$$

$$= (I-B_y(k)M(k))\tilde{\underline{y}}(k/k-1) - B_y(k)\underline{v}(k). \qquad (V.21)$$

Computing the covariance of the latter expression gives

$$P_{yy}(k/k) = (I-B_y(k)M(k))\ P_{yy}(k/k-1). \qquad (V.22)$$

Equations (V.16), (V.17), (V.19), (V.20), (V.21) and (V.22) are equivalent to those originally derived by Kalman[6] for the sequential estimation of the state vector of the system (V.11) based on observations of the form (V.12) (c.f. equations (3.5), (3.6), (3.14), (3.15), (3.16) and (3.17) of reference 11). In order to start the computation, it is clear that we should set

$$P_{yy}(0/0) = \begin{bmatrix} P_0 & 0 \\ 0 & \sigma^2 \end{bmatrix}, \quad \text{and } \hat{\underline{y}}(0/0) = \begin{bmatrix} \bar{\underline{x}}(0) \\ \bar{a} \end{bmatrix}. \qquad (V.23)$$

As the computation proceeds, the optimal estimate of the parameter α based on N observation points, which is given by equation (.5), is obviously the same as the last component of the vector $\hat{\underline{y}}(N/N)$.

APPENDIX VI

THE PSEUDO-INVERSE AND DATA EDITING

A. INTRODUCTION

The optimal noise-free solution for the Kalman filter derives from finding the gain $B_y(n)$ that satisfies the equation (4.39):

$$B_y \left[H_y \, P_{yy}(n/n-1) \, H_y^T \right] - P_{yy}(n/n-1) \, H_y^T = 0, \qquad \text{(VI.1)}$$

where the argument (n) is implicit in the B_y and H_y terms. In order for the processing of perfect observations to be meaningful, we can use a maximum of only three position measurements and three velocity measurements at any time t_n, for otherwise we would have some wholly redundant equations in the unknowns $x, y, z, \dot{x}, \dot{y}, \dot{z}$ without enhancing our knowledge of the mass parameters u_1, u_2, u_3. As long as we are dealing with a single sensor at time t_n, as long as t_n is not identical to t_{n-1} for all n (no matter how close they may get), and as long as the trajectory is randomly perturbed (with geopotential and drag uncertainties), then $H_y \, P_{yy} \, (n/n-1) H_y^T$ is <u>theoretically</u> nonsingular and the solution (4.40)

$$B_y(n) = P_{yy}(n/n-1) H_y^T \left[H_y P_{yy}(n/n-1) H_y^T \right]^{-1} \qquad \text{(VI.2)}$$

is theoretically possible.

In a practical sense, however, the inversion called out in (VI.2) often meets with severe numerical difficulties. The first of these arises because we may not be able to keep t_n distinct from t_{n-1} for all n.

1. Multiple-Sensors, Simultaneous Observations

Two or more sensors, each perfect, may be able to see the satellite at the same instant of time t_n. For any of the sensors of concern to us in the present work, $H_y P_{yy}(n/n-1) H_y^T$ would then be singular.

EXAMPLE 1.

Suppose two Baker-Nunn cameras sight a satellite at the same time t_n. Each of the cameras has an observation matrix

$$H_y = \begin{bmatrix} \partial\alpha/\partial\underline{y} \\ \partial\delta/\partial\underline{y} \end{bmatrix} = \begin{bmatrix} h_{11} & h_{12} & 0 & 0 & 0 & 0 & 0 & 0 & 0 \\ h_{21} & h_{22} & h_{23} & 0 & 0 & 0 & 0 & 0 & 0 \end{bmatrix},$$

where α = right ascension,

δ = declination,

$$h_{11} = \frac{y-y_s}{(\sec^2\alpha)(x-x_s)^2},$$

$$h_{12} = \frac{1}{(\sec^2\alpha)(x-x_s)^2},$$

$$h_{21} = \frac{-(z-z_s)(x-x_s)}{R^3 \cos\delta},$$

$$h_{22} = \frac{-(z-z_s)(y-y_s)}{R^3 \cos\delta},$$

$$h_{23} = \frac{R^2 - (z-z_s)^2}{R^3 \cos\delta},$$

where (x_s, y_s, z_s) are the coordinates of the camera in question, R is

the range from the camera to the satellite, and the h_{ij} are evaluated around nominal satellite values at t_n.

We can let t_n be itself for camera 1, and let it be t_{n+1} for camera 2. To make the computations easier, we will take both cameras at the same latitude such that $z = z_s$, and normalize where we can to obtain

$$\text{Camera 1:} \qquad H_{y1}(n) = \begin{bmatrix} 1 & 1 & 0 & 0 & 0 & 0 & 0 & 0 & 0 \\ 0 & 0 & 1 & 0 & 0 & 0 & 0 & 0 & 0 \end{bmatrix},$$

$$\text{Camera 2:} \quad H_{y2}(n+1) = H_{y2}(n) = \begin{bmatrix} a & b & 0 & 0 & 0 & 0 & 0 & 0 & 0 \\ 0 & 0 & c & 0 & 0 & 0 & 0 & 0 & 0 \end{bmatrix},$$

We will assume, without any real restriction, that

$$P_{yy}(n/n-1) = \sigma^2 I. \tag{VI.3}$$

Then we can show that

$$P_{yy}(n/n) = (\sigma^2/2) \begin{bmatrix} 1 & -1 & & & & & & & \\ -1 & 1 & & & & & & & \\ & & 1 & & & & & & \\ & & & 2 & & & & & \\ & & & & 2 & & & & \\ & & & & & 2 & & & \\ & & & & & & 2 & & \\ & & & & & & & 2 & \\ & & & & & & & & 2 \end{bmatrix} \tag{VI.4}$$

(This is also $P_{yy}(n+1/n)$ since the data from camera 2 occurs at $t_{n+1} = t_n$.) Note that the two angles from camera 1 removed two degrees of freedom (reduced the rank by 2) between (VI.3) and (VI.4). This occurred where it should, in the 3 x 3 submatrix in the upper left-hand corner, which

corresponds to position uncertainties. To remove the final uncertainty in that 3 x 3 submatrix, we should use only one more angle measured at that time: the right ascension reading from camera 2. Without a special procedure, however, we try to use both new angles:

$$H_{y2}(n+1)P_{yy}(n+1/n)H_{y2}^{T}(n+1) = H_{y2}(n+1)P_{yy}(n/n)H_{y2}^{T}(n+1)$$

$$= (\sigma^2/2)\begin{bmatrix} (a-b)^2 & 0 \\ 0 & 0 \end{bmatrix} \qquad \text{(VI.5)}$$

and we obtain an expression which cannot be inverted for (VI.2).

2. Round-Off

Even when the matrix is theoretically well-behaved, the finite precision of the computation equipment may present us with severe numerical problems. In the case of multiple sensors, two observations may not be truly simultaneous, but they may be so close in time that the trajectory perturbations have had essentially no effect on the orbit: i.e., the observations are treated numerically in much the same way as led to (VI.5). Note that the perturbations enter the covariance computations through $Q_{yy}(n-1)$ and $\frac{\partial \underline{y}}{\partial \underline{v}_2}(n, n-1)$, both of which are integrals of finite functions over the range (t_n, t_{n-1}),* and hence vanish as $t_n \rightarrow t_{n-1}$.

Problems can still arise with closely spaced observations after care has been taken to throw away redundant readings, such as the declination

*See equations (4.27) and (4.30).

measurement in the above example. The transition equations for the stochastic and deterministic estimates of drag are given respectively as

$$\hat{u}_1(n/n\text{-}1) = \hat{u}_1(n\text{-}1/n\text{-}1)\ e^{-(t_n - t_{n-1})/\tau_d}\ ,$$

$$u_2(n/n\text{-}1) = u_2(n\text{-}1/n\text{-}1). \qquad \text{(VI.6)}$$

If t_n is too close to t_{n-1}, the two equations are numerically difficult to distinguish, and since u_1 and u_2 appear in the equations of motion only as the sum $(u_1 + u_2)$, we find ourselves faced with a system which is essentially Kalman-unobservable.[6,30]

EXAMPLE 2.

Consider the hypothetically simplified example

$$\underline{x}(n+1) = \Phi\ (n+1,n)\ \underline{x}(n),$$

$$\underline{z}(n) = H(n)\ \underline{x}(n)\ , \qquad \text{(VI.7)}$$

where

$$\Phi\ (n+1,n) = \Phi = \begin{bmatrix} 1 & 1 & 0 & 0 \\ 0 & 1 & 1 & 1 \\ 0 & 0 & 1 & 0 \\ 0 & 0 & 0 & 1 \end{bmatrix}\ ,$$

$$H(n) = H = \begin{bmatrix} 1 & 2 & 0 & 0 \\ 3 & 4 & 0 & 0 \end{bmatrix}$$

Components x_3 and x_4, here, correspond to the u_1 and u_2 of our real system under the condition that t_n and t_{n+1} are so close together that the exponential in (VI.6) is numerically unity.

After one measurement, say at t_n,

$$\text{Cov} \begin{bmatrix} x_1 \\ x_2 \end{bmatrix} = 0.$$

We will assume that the overall covariance

$$P(n/n) = \begin{bmatrix} 0 & & & \\ & 0 & & \\ & & \sigma_3^2 & \\ & & & \sigma_4^2 \end{bmatrix}$$

Then

$$P(n+1/n) = \Phi\, P(n/n)\, \Phi^T = \begin{bmatrix} 0 & 0 & 0 & 0 \\ 0 & \sigma_3^2+\sigma_4^2 & \sigma_3^2 & \sigma_4^2 \\ 0 & \sigma_3^2 & \sigma_3^2 & 0 \\ 0 & \sigma_4^2 & 0 & \sigma_4^2 \end{bmatrix}$$

and

$$H\, P(n+1/n) H^T = 4(\sigma_3^2 + \sigma_4^2) \begin{bmatrix} 1 & 2 \\ 2 & 4 \end{bmatrix} \qquad \text{(VI.8)}$$

Again, we cannot perform the inversion required for (VI.2). What we should have done was to accept only one of the two observations at this time and estimate, in effect, only the sum of x_3 and x_4, rather than try to estimate them independently. Then, when we obtain some better-spaced future data that causes their behavior to separate, estimate them individually.

B. THE PSEUDO-INVERSE

Rather than attempt to throw away data in the conscious way just described, we can achieve the same effect by replacing the inverse in (VI.2) with a

pseudo-inverse. The general method of pseudo-inversion, with overtones for least-squares fitting, is described in Penrose,[10] and Kalman[30] alludes to it throughout his work without, however, going through the mechanics of what it achieves.

For our purposes, since we require it only for the observation-covariance matrix $H_y P_{yy}(n/n-1)H_y^T$, it suffices to specialize the pseudo-inversion to a symmetric k x k matrix, say A. Denoting the eigenvalues of A as $\lambda_1,\ldots,\lambda_k$, we can always transform A to the diagonal form

$$D = \begin{bmatrix} \lambda_1 & & & & \\ & \lambda_2 & & & \\ & & \cdot & & \\ & & & \cdot & \\ & & & & \lambda_k \end{bmatrix} = S^T A S, \qquad \text{(VI.9)}$$

by taking S to be a matrix whose k columns are the k distinct eigenvectors of A, normalized such that

$$S^T S = I = S S^T.$$

If some of the λ's are zero, say λ_{i+1}, λ_{i+2},..., λ_k, then the pseudo-inverse of A is defined as

$$A^{\#} = (SDS^T)^{\#} = S \begin{bmatrix} (1/\lambda_1) & & & & & \\ & (1/\lambda_2) & & & & \\ & & \ddots & & & \\ & & & (1/\lambda_i) & & \\ & & & & 0 & \\ & & & & & \ddots \\ & & & & & & 0 \end{bmatrix} S^T.$$

That is, the part of A that has a normal inverse is inverted normally; the part that has zero eigenvalues is pseudo-inverted to have zero eigenvalues.

APPLICATION TO EXAMPLE 1.

Consider the solution with the declination measurement thrown away by conscious editing. We use $(\ )'$ to denote the matrices so obtained for camera 2:

$$z' = \alpha,$$

$$H'_{yz} = \begin{bmatrix} a & b & 0 & 0 & 0 & 0 & 0 & 0 & 0 \end{bmatrix}$$

Then, from (VI.2), (VI.4), and (VI.5)

$$B'_y(n+1) = P_{yy}(n/n)H'^{T}_{y2}(n+1)\left[H'_{yz}(n+1)P_{yy}(n/n)H'^{T}_{yz}(n+1)\right]^{-1},$$

$$= (\sigma^2/2)\begin{bmatrix} a-b \\ a+b \\ 0 \\ \cdot \\ \cdot \\ \cdot \\ 0 \end{bmatrix} \left[(\sigma^2/2)(a-b)^2\right]^{-1} = \begin{bmatrix} \frac{1}{a+b} \\ \frac{1}{a-b} \\ 0 \\ \cdot \\ \cdot \\ \cdot \\ 0 \end{bmatrix} \qquad \text{(VI.10)}$$

Now we apply the pseudo-inverse, instead, to (VI.5) in the automatic way described:

$$B_y(n+1) = P_{yy}(n/n)H_{y2}(n+1)\left[H_{y2}(n+1)P_{yy}(n/n)H_{y2}(n+1)\right]^{\#}$$

$$= (\sigma^2/2) \begin{bmatrix} a-b & 0 \\ a+b & 0 \\ 0 & 0 \\ \cdot & \cdot \\ \cdot & \cdot \\ \cdot & \cdot \\ 0 & 0 \end{bmatrix} \begin{bmatrix} (\sigma^2/2)(a-b)^2 & 0 \\ 0 & 0 \end{bmatrix} = \begin{bmatrix} \frac{1}{a+b} & 0 \\ \frac{1}{a-b} & 0 \\ 0 & 0 \\ \cdot & \cdot \\ \cdot & \cdot \\ \cdot & \cdot \\ 0 & 0 \end{bmatrix}$$

(VI.11)

Relation (VI.10) directs that the first two position extrapolations be corrected by multiplying the right-ascension residuals by 1/(a+b) and 1/(a-b), respectively, and all others be left uncorrected; (VI.11) directs the same thing. Hence the results are the same.

APPLICATION TO EXAMPLE 2.

We accept only the z_1 measurement in the simplified example specified by (VI.7). Then

$$z' = z_1$$

$$H' = \begin{bmatrix} 1 & 2 & 0 & 0 \end{bmatrix}$$

and

$$B'(n+1) = 2 \begin{bmatrix} 0 \\ \sigma_3^2 + \sigma_4^2 \\ \sigma_3^2 \\ \sigma_4^2 \end{bmatrix} (4\sigma_3^2 + 4\sigma_4^2)^{-1} = \frac{1}{2(\sigma_3^2+\sigma_4^2)} \begin{bmatrix} 0 \\ \sigma_3^2 + \sigma_4^2 \\ \sigma_3^2 \\ \sigma_4^2 \end{bmatrix}$$

(VI.12)

The in-step covariance is

$$P'(n+1/n+1) = [I-B'(n+1)H']P(n+1/n),$$

$$= \frac{\sigma_3^2 \sigma_4^2}{\sigma_3^2+\sigma_4^2} \begin{bmatrix} 0 & 0 & 0 & 0 \\ 0 & 0 & 0 & 0 \\ 0 & 0 & 1 & -1 \\ 0 & 0 & -1 & 1 \end{bmatrix} \qquad \text{(VI.13)}$$

The pseudo-inverse approach employs the original unprimed matrices from Example 2. First we must find the eigenvalues of (VI.8): $\lambda_1 = 5$, $\lambda_2 = 0$. We then determine the matrix of eigenvectors to be

$$S = S^T = (1/\sqrt{5}) \begin{bmatrix} -2 & 1 \\ 1 & 2 \end{bmatrix}$$

Equation (VI.8) becomes

$$H\,P(n+1/n)H^T = 20\,(\sigma_3^2 + \sigma_4^2)\,S \begin{bmatrix} 0 & 0 \\ 0 & 1 \end{bmatrix} S,$$

so that

$$[H\,P(n+1/n)H^T]^{\#} = \frac{1}{20(\sigma_3^2+\sigma_4^2)}\, S \begin{bmatrix} 0 & 0 \\ 0 & 1 \end{bmatrix} S$$

$$= \frac{1}{100(\sigma_3^2+\sigma_4^2)} \begin{bmatrix} 1 & 2 \\ 2 & 4 \end{bmatrix} \qquad \text{(VI.14)}$$

Hence

$$B(n+1) = \frac{1}{10(\sigma_3^2+\sigma_4^2)} \begin{bmatrix} 0 & 0 \\ \sigma_3^2+\sigma_4^2 & 2(\sigma_3^2+\sigma_4^2) \\ \sigma_3^2 & 2\sigma_3^2 \\ \sigma_4^2 & 2\sigma_4^2 \end{bmatrix} \qquad \text{(VI.15)}$$

Comparison of (VI.15) with (VI.12) is not particularly enlightening. Hence we compute the in-step covariance with the unprimed values,

$$P(n+1/n) = \frac{\sigma_3^2\sigma_4^2}{\sigma_3^2+\sigma_4^2} \begin{bmatrix} 0 & 0 & 0 & 0 \\ 0 & 0 & 0 & 0 \\ 0 & 0 & 1 & -1 \\ 0 & 0 & -1 & 1 \end{bmatrix}$$

and find that it agrees with (VI.13), thus verifying that the pseudo-inverse automatically performs the desired editing.

C. NUMERICAL IMPLEMENTATION

Computer round-off usually prevents a calculation from yielding a true zero value when there should be one if the calculation involves more than a very few steps. Hence the examination of D for computed singularities will not always be sufficient.

There are two cases to consider. The first and most common arises when some diagonal entry σ_i^2 in P_{yy} should be zero, but is not. The entries in the row and column that contain σ_i^2 should also be zero if P_{yy} is to have the non-negative definite property that a covariance matrix must have. If these row and column entries are wholly due to round-off, it is very unlikely that P_{yy} will be non-negative definite (have only non-negative eigenvalues). Hence, one approach is to positive-semi-definitize the P_{yy} matrices.

TEST 1.

Check the diagonal entries in P_{yy}. If there are any negative entries,

say σ_i^2, set them and the ith column and row to zero. Set also the appropriate rows in P_{yJ} and P_{yv2} to zero. Perform the check for both the arguments (n/n) and (n/n-1).

TEST 2.

Compute the diagonal matrix of eigenvalues

$$D = S^T P_{yy} S$$

for arguments (n/n) and (n/n-1). If any eigenvalue is negative, set it to zero and reconstruct

$$P_{yy}' = SD'S^T,$$

where the primes denote the matrices after the negative eigenvalues are made zero. It is assumed that any negative eigenvalue is small enough in magnitude that setting it to zero has negligible effect on S.

TEST 3.

For some input parameter C, set the ith row and column in $P_{yy}(n/n)$ to zero if $\sigma_i^2 \leq C$.

TEST 4.

Having obtained a data value $z_i(n)$, and therefrom a residual

$$e_i = z_i(n) - h_i\left[\hat{\underline{x}}(n/n-1)\right] ,$$

set the ith element σ_{ei}^2 in $H_y(n)P_{yy}(n/n-1)H_y^T(n)$ to zero if

$$e_i^2 > K_1 \sigma_{ei}^2$$

for some input parameter K_1. However, set the residual e_i to zero if

$$K_1 \sigma_{ei}^2 \geq e_i^2 > K_2 \sigma_{ei}^2$$

for some input parameter K_2 ($< K_1$) and proceed with the covariance computations as if the data was used.

The second case arises when the P_{yy} matrices are numerically positive semi-definite, but some small σ_i^2 should be zero. There are two possible approaches. One is to diagonalize to the D matrix and set any λ_i to zero that is "very much" smaller than any other λ_i. There is a difficulty in assigning a number to the "very much", especially since some of the variances have the units of distance, some have the units of velocity, and some have units involving area-to-mass ratio. In general, however, it is better to discard good data (by setting a λ_i to zero that should not be) rather than to include bad, or meaningless data in the smoothing. The computed covariances will simply be a little larger than they should be.

A second approach, which also covers some of the problems encountered earlier, is to include a round-off "noise" matrix R_{rr} in the residual covariance

$$\left[H_y(n)P_{yy}(n/n-1)H_y^T(n) + R_{rr}(n)\right]$$

to reflect the fact that we do not have an infinitely precise processing chain, even when the first unit in the chain (the sensor) is perfect.

UNCLASSIFIED

Security Classification

DOCUMENT CONTROL DATA - R & D

(Security classification of title, body of abstract and indexing annotation must be entered when the overall report is classified)

1. ORIGINATING ACTIVITY *(Corporate author)*
Westinghouse Defense and Space Center
Surface Division
Baltimore, Maryland

2a. REPORT SECURITY CLASSIFICATION
UNCLASSIFIED

2b. GROUP
N/A

3. REPORT TITLE

MODELS FOR ANALYSIS OF THE CAPABILITIES OF GROUND BASED SENSORS IN DETERMINING THE MASS OF ORBITING BODIES

4. DESCRIPTIVE NOTES *(Type of report and inclusive dates)*
None

5. AUTHOR(S) *(First name, middle initial, last name)*
Walter J. Culver, et al

6. REPORT DATE	7a. TOTAL NO. OF PAGES	7b. NO. OF REFS
23 June 1967	166	50

8a. CONTRACT OR GRANT NO.	9a. ORIGINATOR'S REPORT NUMBER(S)
F19628-67-C0041	ESD-TR-68-157, Vol. I
b. PROJECT NO.	
c.	9b. OTHER REPORT NO(S) *(Any other numbers that may be assigned this report)*
d.	None

10. DISTRIBUTION STATEMENT

This document has been approved for public release and sale; its distribution is unlimited.

11. SUPPLEMENTARY NOTES	12. SPONSORING MILITARY ACTIVITY
	Space Defense Systems Program Office, Electronic Systems Division, Air Force Systems Command, USAF, L G Hanscom Fld, Bedford, Mass. 01730

13. ABSTRACT

This report contains a description of the models to be used in analyzing the capabilities of ground-based sensors in determining the mass of orbiting bodies, model coefficients, and the justification for their selection. Relations are derived for computing sensitivity coefficients and their coupling to mass variance.

DD FORM 1 NOV 65 1473

UNCLASSIFIED

Security Classification

14. KEY WORDS	LINK A		LINK B		LINK C	
	ROLE	WT	ROLE	WT	ROLE	WT
RADAR						
MASS						
ERRORS						
ANALYSIS						
SENSOR						
ORBIT						
SATELLITE						